Monitoring ecosystem health of Fynbos remnant vegetation in the City of Cape Town using remote sensing

Kim Knauer

Julius-Maximilians-Universität Würzburg
Institut für Geographie
Lehrstuhl für Fernerkundung

Monitoring ecosystem health of Fynbos remnant vegetation in the City of Cape Town using remote sensing

Diplomarbeit im Fach Geographie

Kim Knauer

Würzburg, März 2011

Gutachter:

Prof. Dr. Roland Baumhauer

Prof. Dr. Stefan Dech

Abstract

Increasing urbanisation is one of the biggest pressures to vegetation in the City of Cape Town. The growth of the city dramatically reduced the area under indigenous Fynbos vegetation, which remains in isolated fragments. These are subject to a number of threats including atmospheric deposition, atypical fire cycles and invasion by exotic plant and animal species. Especially the Port Jackson willow (*Acacia saligna*) extensively suppresses the indigenous Fynbos vegetation with its rapid growth.

The main objective of this study was to investigate indicators for a quick and early prediction of the health of the remaining Fynbos fragments in the City of Cape Town with help of remote sensing.

First, the productivity of the vegetation in response to rainfall was determined. For this purpose, the Enhanced Vegetation Index (EVI), derived from Terra MODIS data with a spatial resolution of 250m, and precipitation data of 19 rainfall stations for the period from 2000 till 2008 were used. Within the scope of a flexible regression between the EVI data and the precipitation data, different lags of the vegetation response to rainfall were analysed. Furthermore, residual trends (RESTREND) were calculated, which result from the difference between observed EVI and the one predicted by precipitation. Negative trends may suggest a degradation of the habitats. In addition, the so-called Rain-use Efficiency (RUE) was tested in this context. It is defined as the ratio between net primary production (NPP) – represented by the annual sum of EVI – and the annual rainfall sum. These indicators were analysed for their suitability to determine the health of the indigenous Fynbos vegetation.

Furthermore, the degree of dispersal of invasive species especially the *Acacia saligna* was investigated. With the specific characteristics of the tested indicators and the spectral signature of *Acacia saligna*, i.e. its unique reflectance over the course of the year, the dispersal was estimated. Since the growth of invasive species dramatically reduces the biodiversity of the fragments, their presence is an important factor for the condition of ecosystem health.

This work focused on 11 test sites with an average size of 200ha, distributed over the whole area of the City of Cape Town. Five of these fragments are under conservation and

the others shall be protected in the near future, too, which makes them of special interest. In January 2010, fieldwork was undertaken in order to investigate the state and composition of the local vegetation.

The results show promising indicators for the assessment of ecosystem health. The coefficients of determination of the EVI-rainfall regression for Fynbos are minor, because the reaction of this vegetation type to rainfall is considerably lower than the one of the invasive species. Thus, a good distinction between indigenous and alien vegetation is possible on the basis of this regression. On the other hand, the RESTREND method, for which the regression forms the basis, is only of limited use, since the significance of these trends is not given for Fynbos vegetation. Furthermore, the RUE has considerable potential for the assessment of ecosystem health in the study area. The Port Jackson willow has an explicitly higher EVI than the Fynbos vegetation and thus its RUE is more efficient for a similar amount of rainfall. However, it has to be used with caution, because local and temporal variability cannot be extinguished in the study area over the rather short MODIS time series.

These results display that the interpretation of the indicators has to be conducted differently from the literature, because the element of invasive species was not considered in most of the previous papers. An increase in productivity is not necessarily equivalent with an improvement in health of the fragment, but can indicate a dispersal of *Acacia saligna*. This shows the general problem of the term ‘degradation’ which in most publications so far is only measured by productivity and other factors like invasive species are disregarded.

On the basis of the EVI-rainfall regression and statistical measures of the EVI, the distribution of invasive species could be delineated. Generally, a strong invasion of the Port Jackson willow was discovered on the test sites. The results display that a reasoned and sustainable management of the fragments is essential in order to prevent the suppression of the indigenous Fynbos vegetation by *Acacia saligna*. For this purpose, remote sensing can give an indication which areas changed so that specific field surveys can be undertaken and subsequent management measures can be determined.

Zusammenfassung

Zunehmende Urbanisierung stellt eine der größten Bedrohungen für die Vegetation im Großraum Kapstadt dar. Durch das schnelle Wachstum der Stadt bleibt immer weniger der ursprünglichen Vegetation in isolierten Fragmenten zurück. Diese sind in ihrer Funktion als Lebensraum für Flora und Fauna unter Anderem durch Luftverschmutzung, untypische Feuerzyklen und das Eindringen fremder Arten gefährdet. Besonders die Weidenblatt-Akazie (*Acacia Saligna*) verdrängt die einheimische Fynbos-Vegetation großflächig durch ihr schnelles Wachstum.

Hauptziel dieser Arbeit war es, mit Hilfe der Fernerkundung Indikatoren zu finden, um eine schnelle und frühzeitige Aussage über die Gesundheit der verbliebenen natürlichen Vegetationsfragmente im Großraum Kapstadt zu ermöglichen.

Zunächst wurde die Produktivität der Vegetation und deren Reaktion auf Niederschlag analysiert. Zu diesem Zweck wurden der Enhanced Vegetation Index (EVI) aus Terra-MODIS-Daten mit einer räumlichen Auflösung von 250m und Niederschlagsdaten von 19 Wetterstationen aus dem Zeitraum 2000 bis 2008 verwendet. Im Rahmen einer flexiblen Regression zwischen EVI und Niederschlagsdaten wurden verschiedene Verzögerungen der Reaktion der Vegetation auf den Niederschlag getestet. Des Weiteren wurden residuale Trends (RESTREND) berechnet, die sich aus der Differenz zwischen beobachtetem EVI und dem aus dem Niederschlag vorhergesagten EVI ergeben. Zusätzlich wurde die sogenannte Rain-use Efficiency (RUE) getestet. Diese ist definiert durch das Verhältnis zwischen Nettoprimärproduktion, repräsentiert durch die Jahressumme des EVI, und der Jahressumme des Niederschlags. Die angewandten Indikatoren wurden darauf untersucht, ob sie eine Aussage über die Gesundheit der einheimischen Fynbos-Vegetation ermöglichen.

Des Weiteren wurde der Verbreitungsgrad invasiver Arten, besonders der der Weidenblatt-Akazie bestimmt. Auf Basis der spezifischen Charakteristika der getesteten Indikatoren und der spektralen Signatur von *Acacia saligna*, also ihrer besonderen Reflexion über den Jahresverlauf, wurde die Verbreitung ermittelt. Da das ungehinderte Wachstum invasiver Arten die Biodiversität der Fragmente stark verringert, ist ihre Anwesenheit ein wichtiger Faktor für die Gesundheit von Ökosystemen.

Diese Arbeit konzentrierte sich auf 11 Testflächen mit einer durchschnittlichen Größe von 200ha, die über die gesamte Fläche des Großraums Kapstadt verteilt sind. Fünf dieser Fragmente stehen bereits unter Schutz, während die anderen in absehbarer Zeit folgen sollen; dies macht sie von besonderem Interesse. Im Januar 2010 wurden Geländearbeiten durchgeführt um den Zustand und die Zusammensetzung der Vegetation vor Ort festzustellen.

Die Ergebnisse weisen aussichtsreiche Indikatoren zur Abschätzung der Ökosystemgesundheit auf. Die Werte des Bestimmtheitsmaßes der EVI-Niederschlags-Regression sind niedrig für Fynbos, da die Reaktion dieses Vegetationstyps auf Niederschlag wesentlich geringer ist als die der invasiven Arten. Daher ist auf Basis dieser Regression eine gute Unterscheidung zwischen einheimischer und invasiver Vegetation möglich. Auf der anderen Seite ist die RESTREND-Methode, für die diese Regression die Grundlage bildet, nur begrenzt von Nutzen, da die Signifikanzen dieser Trends für Fynbos-Vegetation nicht gegeben sind. Des Weiteren weist die RUE Potential für die Abschätzung von Ökosystemgesundheit im Testgebiet auf. Die Weidenblatt-Akazie hat einen wesentlichen höheren EVI als die Fynbos-Vegetation und daher ist deren RUE bei vergleichbarer Niederschlagsmenge effizienter. Dennoch muss diese mit Vorsicht angewandt werden, da die hohe lokale und temporale Variabilität der RUE im Testgebiet über die relativ kurze MODIS-Zeitserie nicht eliminiert werden kann.

Die Ergebnisse verdeutlichen zudem, dass die Interpretation der Indikatoren anders als in der Literatur durchgeführt werden muss, da das Element der invasiven Vegetation in den meisten der vorangegangenen Arbeiten nicht berücksichtigt wurde. Ein Anstieg der Produktivität ist hier nicht gleichzusetzen mit einer Verbesserung der Gesundheit eines Fragments, sondern deutet viel mehr auf eine Verbreitung der Weidenblatt-Akazie hin. Dies verdeutlicht das generelle Problem des Begriffs ‚Degradation', welche in den meisten Veröffentlichungen nur über die Produktivität der Vegetation bestimmt wird während andere Faktoren wie zum Beispiel invasive Arten unberücksichtigt bleiben.

Auf Basis der EVI-Niederschlags-Regression und der statistischen Messgrößen des EVI konnte die Verbreitung der invasiven Arten abgegrenzt werden. Generell wurde ein starker Befall der Testflächen durch die Weidenblatt-Akazie festgestellt. Die Ergebnisse machen deutlich, dass ein durchdachtes und nachhaltiges Management der Fragmente notwendig ist um die Verdrängung der einheimischen Fynbos-Vegetation durch *Acacia*

saligna zu verhindern. Die Fernerkundung kann zu diesem Zweck Hinweise liefern, welche Flächen sich verändert haben um anschließend gezielte Begehungen vorzunehmen und Maßnahmen einzuleiten.

Contents

List of Abbreviations

ASTER	Advanced Spaceborne Thermal Emission and Reflection Radiometer
AVHRR	Advanced Very High Resolution Radiometer
AVIRIS	Airborne Visible InfraRed Imaging Spectrometer
CERES	Clouds and the Earth's Radiant Energy System
CREW	Custodians of Rare and Endangered Wildflowers
CV	Coefficient of variation
DFD	Deutsches Fernerkundungsdatenzentrum
DLR	Deutsches Zentrum für Luft- und Raumfahrt
ENVI	Environment for Visualizing Images
EOS	Earth Observing System
ESH	Ecosystem Health
ESRI	Environmental Systems Research Institute
ETM+	Enhanced Thematic Mapper Plus
EVI	Enhanced Vegetation Index
FAO	Food and Agriculture Organizsation of the United Nations
GCP	Ground Control Points
GIS	Geographic Information System
GPS	Global Positioning System
GTP	Ground Truth Polygon
HDF	Hierarchical Data Format
IDL	Interactive Data Language
Lidar	Light detection and ranging
LP DAAC	Land Processes Distributed Active Archive Center
MISR	Multi-Angle Imaging Spectroradiometer
MODIS	Moderate Resolution Imaging Spectroradiometer
MOPITT	Measurement of Pollution in the Troposphere
MRT	MODIS Reprojection Tool
MS	Multispectral
NASA	National Aeronautics and Space Administration
NDVI	Normalised Difference Vegetation Index
NIR	Near-Infrared
NLC	National Land Cover

NPP	Net primary production
RESTREND	Residual Trends
RS	Remote Sensing
RUE	Rain-use Efficiency
SAEON	South African Environmental Observatory Network
SANBI	South African National Biodiversity Institute
SAWS	South African Weather Service
SWIR	Short-wave Infrared
TIFF	Tagged Image File Format
TiSeG	Time Series Generator
USGS	United States Geological Survey
UTM	Universal Transverse Mercator
UNESCO	United Nations Educational, Scientific and Cultural Organization
VI	Vegetation Index

List of Figures

List of Tables

1 Introduction and Objectives

"The United Nations declared 2010 to be the International Year of Biodiversity" (Convention on Biological Diversity, 2010). This decision emphasises the importance and the growing attention to the health of ecosystems. "Biodiversity and ecosystems deliver crucial services to humankind – from food security to keeping our waters clean, buffering against extreme weather, providing medicines to recreation and adding to the foundation of human culture" (Nellemann & Corcoran, 2010). This study goes in line with a global trend of monitoring the health of ecosystems and restoring disturbances.

The study area of this work is the City of Cape Town Metropolitan Municipality, which is part of the Cape Floristic Region. This is the smallest, but one of the most species-rich floristic regions in the world. "It represents less than 0.5% of the area of Africa but is home to nearly 20% of the continent's flora" (UNESCO, 2010). It mostly consists of Fynbos, "an evergreen, fire-prone shrubland, confined largely to sandy, infertile soils" (Cowling, Richardson, & Pierce, 2004). With its great biodiversity and high endemism of the indigenous species, the Cape Floristic Region has long been in the focus of researchers. In 2004, the UNESCO declared eight core areas, the 'Cape Floral Region Protected Areas', as a World Heritage Site (UNESCO, 2010). Nevertheless, these areas only cover about 7% (553,000 ha, acc. to UNESCO, 2010) of the whole Floristic Region, while the rest is endangered by a number of threats.

For the natural vegetation in the City of Cape Town Metropolitan Municipality urbanisation has been identified as one of the biggest pressures. While the city boundaries are constantly spreading, the vegetation only remains in fragments. These small habitats have to cope with atmospheric deposition, atypical fire cycles and invasion of exotic plant and animal species. Because of human control, fires cannot spread naturally anymore which affects the life cycle of the Fynbos vegetation (de Klerk, 2008). Furthermore, all biota are likely to be affected by fragmentation depending on their foraging ranges, seasonal habitat requirements, breeding success, and interactions with other fauna and flora which determine their success and survival, e.g. pollination or seed dispersal. The human influence on the remaining fragments by cattle grazing or other types of land use brings further disturbance to them.

The future prospects of the Fynbos biome are rather serious, too. Midgley et al. (2002) analysed the influence of climate change on the Fynbos biome as a whole, and for 330 species of the endemic family Proteaceae. Depending on the climate scenario, he estimated a loss of Fynbos biome area between 51% and 65% by the year 2050. Furthermore, about 10% of the endemic Proteaceae have ranges that are restricted to the area lost.

This short overview of the situation of Fynbos vegetation points out the need for protection and management in order to conserve the remaining vegetation fragments. The City of Cape Town's Biodiversity Management Branch has identified all natural and semi-natural fragments within the metropolitan area and has conducted baseline work to determine their conservation status. Several fragments are formally conserved by the City or other agencies.

The SAEON Fynbos Node in the South African National Biodiversity Institute (SANBI) would like to monitor the ecosystem health of these fragments in order to support management measures. Remote sensing can be used cost and time efficiently to observe the whole region without intensive field work. In the context of the collaboration between SANBI and the Department of Remote Sensing at the University of Wuerzburg (Germany) it was decided to investigate the potential of remote sensing for the local ecosystems of the City of Cape Town Metropolitan Municipality.

The aim of this study is to find remotely sensed indicators that are able to monitor ecosystem health of the local Sand Fynbos vegetation. The decision to focus on this special type of Fynbos is explained in chapter 3.4. If the results of this study prove to be suitable, they could be applied to different regions of the world.

Terra MODIS data from 2000 to 2009 are used to analyse the development of the vegetation fragments over this time. The data of this sensor is delivered as the Enhanced Vegetation Index (EVI), which measures the 'greenness' of vegetation. Furthermore, precipitation data from 19 rainfall stations are employed to analyse the reaction of the EVI to rainfall over the course of the year. The results are used to delineate degraded from intact Sand Fynbos areas.

Several researchers have worked with remote sensing to analyse the productivity of vegetation in South Africa. Wessels et al. (2007) tested three indicators, the rain-use efficiency, the correlation between EVI and rainfall, and the residual trends method in

order to distinguish between degraded and non-degraded areas. He showed that all three of them have certain potential, which is discussed in detail in chapter 5.1. Bai & Dent (2008) applied these indicators to their study about degradation in South Africa and confirmed their suitability. Since these two studies are closely related to the topic of this work, they form the basis for the methodology.

Following the introductory words of this thesis, the second chapter presents the theoretical background. The definition and parameters of ecosystem health are outlined and the fundamentals of remotely sensed data are described as far as they matter for this study. The chapter illustrates the importance of different resolutions and the scope of spectral characteristics. Furthermore, the role of remote sensing in the literature concerning the analysis of ecosystem health is delineated.

Chapter 3 gives a general overview of the study area, which is located in the City of Cape Town Metropolitan Municipality. After an introduction to the study area, local climate, geology and soil, the natural vegetation of the Western Cape lowlands is presented and it is explained why the focus lies on Sand Fynbos. Furthermore, threats that the indigenous vegetation has to cope with, especially urbanisation and invasive alien vegetation are described. Then, the common terms ‘degradation’ and ‘improvement’ are discussed on the basis of the special characteristics of the local vegetation.

Chapter 4 introduces the data used in this study and how they were pre-processed. For this purpose, the general atmospheric and geometric corrections of remotely sensed data are depicted. Thereafter, the satellite system is explained from the satellite platform, over the sensor to the used vegetation indices. The second half of this chapter presents further data used in this study, like rainfall data, GIS data, and aerial images. An important set of data described in this section is the ground truth information which was collected during five weeks of field work. The last part of this chapter summarises background information about the fragments that were gathered during the same field trip.

Chapter 5 is a compilation of the methods and indicators used in this study. The first section presents the indicators determining the productivity of vegetation. These are the rain-use efficiency, an EVI-rainfall regression, and the residual trends method. The second section describes the process of delineating the distribution of invasive species. First, the classification of the ground truth data is explained. After this, the analysis of the statistical

measures of the vegetation phenology is displayed. Then, the delineation itself with the help of the ENVI Decision Tree is illustrated.

Chapter 6 summarises and discusses the results of this study. The outcomes of the different methods and indicators are presented and their usefulness for the monitoring of ecosystem health is assessed.

The final chapter 7 summarises the study and draws conclusions for the different methods applied. The important factors for future research within this study area are outlined and further potential indicators are suggested.

2 Theoretical Background

2.1 Ecosystem Health

The beginnings of the concept of ecosystem health can be found in the writings of the American naturalist Aldo Leopold in the 1940's. He mentioned that "ecosystems can become unhealthy, if overstressed by anthropogenic activities" (Rapport, 2007). Especially since the 1990's, the subject came into the public focus with a growing awareness for the ecology of the planet and resulted in several studies (e.g. Johnson & Patil, 1998; Covington et al., 1997).

The term 'ecosystem health' is hard to define and because of several parallels, it is often compared to human health. For both, human and ecosystem health, applies that the definition is rather imprecise and in many cases health is only recognised in its absence (Costanza, Norton, & Haskell, 1992). Parameters such as species richness and quantity of the individuals living in the habitats are easy to collect, but key data for a 'well-functioning' of the ecosystem are hard to identify. Those parameters cannot just be adopted from other studies, because each ecosystem has its own key factors which have to be found and defined individually. In order to find these, one should first look for signs which differentiate unstressed from stressed ecosystems. One of these could be the loss of biodiversity, declining primary productivity or increases of invasive plant species (Rapport, 2007).

Another problem occurs if the conditions of the ecosystem change, e.g. due to human influence: The ecosystem will change too and this will affect the parameters. Thus, they have to be sufficiently dynamic in order to change accordingly with the developing ecosystem.

Rapport, Costanza & McMichael (1998) defined three general measures for assessment of ecosystem health. The first one is 'vigour' or 'vitality', which can be measured in terms of metabolism or primary productivity. The second one is 'organisation', which can be assessed "as the diversity and number of interactions between system components" (Rapport, Costanza, & McMichael, 1998). The third measure is 'resilience', "the degree to which ecosystems can „buffer perturbations and maintain their basic structure and

function" (Rapport, Costanza, & McMichael, 1998). An example for these three measures can be given by a case study about ecosystem health indicators in the Great Lakes Basin in North America (Shear, Stadler-Salt, Bertram, & Horvatin, 2003). With the European settlement in the 19th century, intensive agriculture, commercial forestry and fishery established in a region, that was formerly known to have a high abundance and diversity in fish, forests and mammals. Overfishing and the intensive use of the soil for farming lead to a reduced *vitality*, i.e. a decline in fish abundance and infertility of agricultural soils. The *organisation* or community structure of the ecosystem changed with the introduction of exotic fish species. Together with overfishing and decline in water quality this caused the local extinction of native fish species and a reorganisation from nearshore benthic fish associations to offshore pelagic associations. The extinction of the native fish species for wide areas and a flip to eutrophic conditions implied a loss of *resilience* as the ecosystem would not be able to regenerate from these stresses anymore (Shear, Stadler-Salt, Bertram, & Horvatin, 2003).

These three established measures have to be analysed for each single ecosystem in order to find indicators that give evidence about the state of health of the ecosystem (Rapport, 2007).

2.2 Principles of Remote Sensing

Remote sensing sensors have various characteristics and are consequently used for different approaches. These basic properties are presented in the following chapter and can help during the decision progress about which remote sensing system should be used. With unique characteristics, two different sensors can provide completely different information about the same study area; hence the choice of remotely sensed data is very important.

2.2.1 Scale and Resolution

The extent of the study area and the resolution of the sensor are two almost antagonistic factors, which define the information content that can be extracted from the data. With an increasing extent, the amount of retrieved data increases too, which can also result in higher costs and time involved. In this case, it is advisable to reduce the level of detail in

order to maintain the effort on an acceptable level. Remote sensing has four different types of resolution, which are described in the following.

Spatial Resolution is defined as "a measure of the smallest angular or linear separation between two objects that can be resolved by the remote sensing system" (Jensen, 2005). Each remote sensing sensor has a certain spatial resolution, usually defined by the pixel size, i.e. the length and width of the smallest unit of an image. For example, the Landsat 7 Enhanced Thematic Mapper Plus (ETM+) has a spatial resolution of 30 x 30 m² for its six multispectral bands, 60 x 60 m² for its thermal band and 15 x 15 m² for its panchromatic band. The smaller the spatial resolution, the greater is the level of detail and the easier to discriminate between certain objects. On the other hand, smaller spatial resolution also means more pixels per image and thus higher amount of data that has to be stored (Jensen, 2005).

Temporal Resolution is the inherent repeating coverage of the same area on the earth (Schowengerdt, 2007). Multiple records of the same area for different points in time are useful to map the changes that this area is subject to. "Ideally, the sensor obtains data repetitively to capture unique discriminating characteristics of the object under investigation" (Jensen, 2005). Vegetation, for example, has unique *phenological cycles* in different geographic regions and depending on its composition. The phenology of vegetation is discussed in section 2.2.3.

Radiometric Resolution is defined as "the sensitivity of a remote sensing detector to differences in signal strength" (Jensen, 2005). Some remote sensing systems have a higher precision in measuring electromagnetic radiation than other systems. It is measured as the number of gray-scale levels and typically recorded in bits (binary digits). For example, Landsat 1 MS, launched in 1972, recorded reflected energy with a precision of 6 bit (values 0 - 63), Landsat 4 and 5 recorded already in 8 bit (values 0 - 255) and several new sensor systems like MODIS use 12 bit radiometric resolution (values 0 – 4,095).

Spectral Resolution is the number and dimension of specific wavelength intervals (called *bands* or *channels*) in the electromagnetic spectrum to which a remote sensing instrument is sensitive (Jensen, 2005). The higher the number of bands and the smaller the band width, the higher is the spectral resolution of the sensor. In general, a sensor is called *multispectral* if it has about 10 bands and *hyperspectral* if it acquires data in hundreds of spectral bands (Jensen, 2005). The measurements of all spectral bands combined for one location point on the earth are called *spectral signature*. A land cover type can have a typical or at least similar spectral signature in different regions of the earth (Lillesand, Kiefer, & Chipman, 2004). In the following section, spectral signatures of typical land cover types are described.

2.2.2 Spectral Signatures

If the spatial resolution of a sensor is too low, the colours of the image seem blurry and objects cannot be identified by their shape or spatial detail. In this case, it is often useful to extract the full spectrum of brightness of that area or object to identify it with the help of its *spectral signature* (also referred to as *spectral profile*). Although it is often possible to distinguish different types of materials, the distinction is sometimes foiled by factors like natural variability for a given material type, coarse spectral quantisation or modification of signatures by the atmosphere (Schowengerdt, 2007).
Averaged spectral signatures for three basic land cover types are shown in figure 2.1. The x-axis identifies the wavelength or in some other illustrations the number of the individual bands; the y-axis documents the percent reflectance if the data have been calibrated (otherwise the total brightness value) (Jensen, 2005).

Water is probably the easiest land cover type to deduce from its spectral signature. The most distinctive characteristic of water is the energy absorption at near-infrared wavelengths and beyond (Lillesand, Kiefer, & Chipman, 2004). Depending on the turbidity of the water, changes in spectral signature can be dramatic. Chlorophyll concentration or suspended sediment content are the major factors of influence on its spectral profile (Lillesand, Kiefer, & Chipman, 2004).

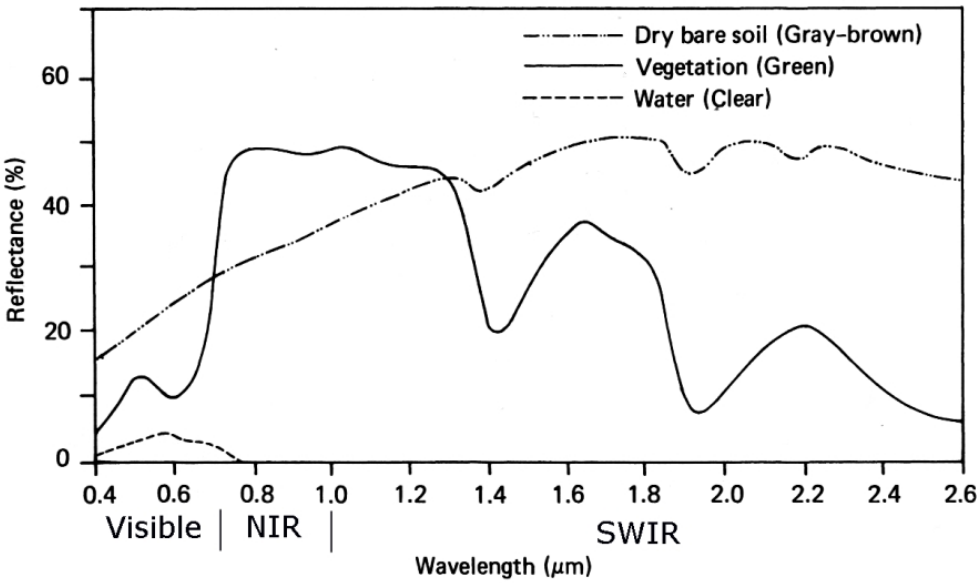

Figure 2.1: Typical spectral reflectance curves for vegetation, soil, and water (Lillesand, Kiefer, & Chipman, 2004).

Bare Soils commonly have spectral signatures that increase quite steady up to 1.8 µm with wavelength. (compare figure 2.1), because the factors that influence soil reflectance act over less specific spectral bands (Lillesand, Kiefer, & Chipman, 2004). The major factors affecting its reflectance are moisture content, soil texture, surface roughness, presence of iron oxide, and organic matter content. For example, soil moisture or the presence of iron oxide decrease the reflectance of the soil while a coarse texturing of a soil increases its reflectance (Lillesand, Kiefer, & Chipman, 2004).

The chlorophyll in green vegetation strongly absorbs energy in the blue and red wavelength bands (referred to as *chlorophyll absorption bands*) but reflects green radiation and near-infrared. Hence, our eyes perceive healthy vegetation as green in colour (Lillesand, Kiefer, & Chipman, 2004). If the plant is subject to some sort of stress disturbing its normal productivity, the chlorophyll absorption bands are less distinctive. As a result, we see the plant yellow combining green and red reflectance. Going further from the visible to the near-infrared portion of the spectrum at about 0.7 µm, the reflectance of green vegetation increases dramatically. This significant change is called *red edge* and occurs slightly shifted in stressed vegetation towards shorter wavelengths (Jensen, 2005). Dips in reflectance occur at 1.4, 1.9, and 2.7 µm because water in the leaves strongly

absorbs radiation at these wavelengths. These spectral regions are called *water absorption bands* (Lillesand, Kiefer, & Chipman, 2004).

2.2.3 Vegetation Phenology

Another possibility besides spectral signatures to distinguish different land cover types, especially different types of vegetation, is the phenology. This is defined as the temporal development of the vegetations' spectral information over the course of the year. Vegetation grows according to relatively predictable seasonal and annual phenological cycles (Jensen, 2005). During winter or the dry season, it is often easy to distinguish annual from perennial species (compare figure 2.2). Especially if the analyst does not have remotely sensed data with a high temporal resolution for plotting the whole phenological cycle, it is necessary to know the biophysical characteristics of the vegetation in order to choose the right time of the year for the investigation (Jensen, 2005).

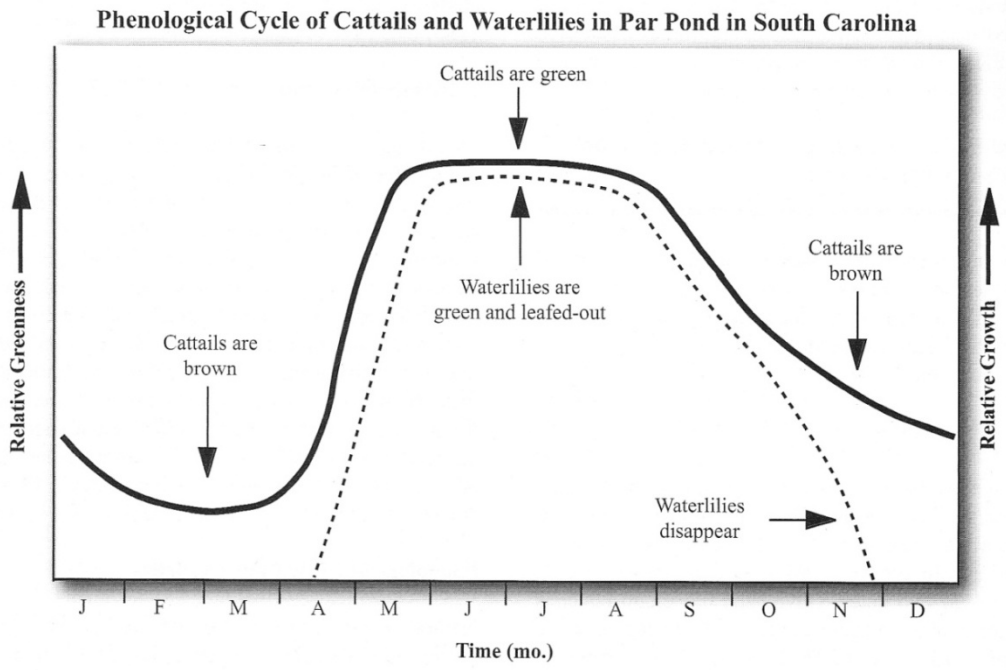

Figure 2.2: Yearly phenological cycle of Cattails and Waterlilies in Par Pond, South Carolina. (Jensen, 2005).

In addition to the distinction between different vegetation species, it is also possible to detect changes in annual productivity of a certain species with the help of phenological cycles. For this purpose, correlations between the vegetation phenology and factors that

affect the phenology, usually precipitation, are calculated. If differences in annual productivity cannot be explained by rainfall, this might indicate anthropogenic influence, fires etc. (Fabricante, Oesterheld, & Paruelo, 2009). In order to draw the right conclusions, one has to have certain background information about the study area.

2.3 Ecosystem Characterisation using Remote Sensing

Since the launch of the first satellite carrying a multispectral sensor, Landsat 1 in 1972, vegetation dynamics has been one of the primary tasks of remote sensing. Several sensors were only developed to display the unique characteristics of vegetation with channels for e.g. the red edge or the water absorption bands (Jensen, 2007).

Especially the analysis of the productivity of vegetation has led to many publications (e.g. Curran, 1981; Holm, Cridland, & Roderick, 2003; Li, Lewis, Rowland, Tappan, & Tiszen, 2004). Holm, Cridland, & Roderick (2003) compared biomass production with the remotely sensed Normalized Difference Vegetation Index (NDVI) in Western Australia and determined that the NDVI can be a good surrogate for ground measuring. They also analysed the relationship between NDVI and rainfall. For this purpose, Holm calculated the rain-use efficiency (RUE), the ratio between annual NDVI and annual rainfall. Today, this is a commonly known indicator and has also been used in Argentina (Guevara, Estevez, & Torres, 1996), the West African Sahel (Nicholson, Tucker, & Ba, 1998), South Africa (Bai & Dent, 2008; Wessels et al., 2007) and many other regions of the world. Another possibility to analyse the vegetation-rainfall relationship is the correlation or regression of these two variables. Fabricante, Oesterheld, & Paruelo (2009) used NDVI data from the AVHRR sensor in North Patagonia and correlated it with precipitation data from rainfall stations. They observed high correlations of NDVI with precipitation accumulated during a few months of the previous growing season. Li et al. (2004) came to similar conclusions for different vegetation types and discovered several degraded areas in the Senegal.

A further indicator for the analysis of productivity is the residual trends method which was introduced by Evans & Geerken (2004) and became more and more popular in recent years (Herrmann, Anyamba, & Tucker, 2005; Wessels et al., 2007; Bai & Dent, 2008). This method is based on a regression between NDVI and rainfall and negative trends may

indicate a degradation of the land. Evans & Geerken (2004) applied the residual trends method in Syria with AVHRR data and found it a useful indicator for human influences although the direction of the trend has to be analysed carefully. Wessels et al. (2007) and Bai & Dent (2008) also utilised this indicator but since this work is based on their research, chapter 5.1 presents a more detailed view on their analysis.

This short review displays that the productivity of vegetation seems to be a suitable measure of ecosystem health that can be analysed by remote sensing. Thus, an application in this work assessing the general measure 'vitality' by Rapport, Costanza, & McMichael (1998) was intended.

Furthermore, remote sensing has received considerable interest in the field of biological invasion in the recent years. Invasive plants may rapidly decrease the biodiversity of an ecosystem and thus there is a need for large-scale monitoring of endangered areas. Between 1990 and 2000 the number of publications on this topic has grown from about 20 to 80 publications per year (Joshi, Leeuw, & Duren, 2004). The detection and delineation of invasive alien species can be based on their unique spectral or phenological properties, structural characteristics, or the spatial patterns of infestations (Strand et al., 2007). Asner, Jones, Martin, Knapp, & Hughes (2008) studied the discrimination between native and invasive species in Hawaiian forests on the basis of their spectral characteristics. They used an Airborne Visible and Infrared Imaging Spectrometer (AVIRIS) and discovered differences in leaf and canopy properties like water content and pigment-related absorption features. Thus, they were able to differentiate between 7 native and 24 introduced tree species, the latter group containing some highly invasive species.

Another application of remote sensing in California focuses on the delineation of the invasive weed yellow starthistle with hyperspectral imagery (Miao et al., 2006). Knowing the unique phenology of the plant, the starthistle was delineated in the earlier growing season because it becomes greener more quickly.

Focusing on the structural characteristics, Rosso, Ustin, & Hastings (2006) used lidar to delineate the distribution of *Spartina* species in the San Francisco Bay marshes. Lidar is related to radar using a laser beam instead of radio waves and can detect small differences in the height of vegetation. The study displayed the expansion patterns of *Spartina* and indicated the great potential of lidar for the analysis of wetland topography.

As the following chapter 3.5 presents, the delineation of invasive alien species is an important task in the study area. High densities of alien species dramatically reduce the biodiversity of an area. Thus it is analysed in this study addressing the second of the three general measures ‘organisation’ by Rapport, Costanza, & McMichael (1998).

3 Study Area: City of Cape Town, South Africa

3.1 Study Area

The study area is situated in South Africa's Western Cape Province, in and adjacent to the City of Cape Town Metropolitan Municipality. It ranges from 33°25'50'' S to 34°08'00'' S and from 18°21'44'' E to 18°58'50'' E (compare figure 3.1). The general elevation of the area is very low and varies from about 0 to 230 m above sea level with smaller hills in between. The whole study area covers about 4842 km² and is confined by the sea in the west and south and parts of the Cape Fold Belt in the east.

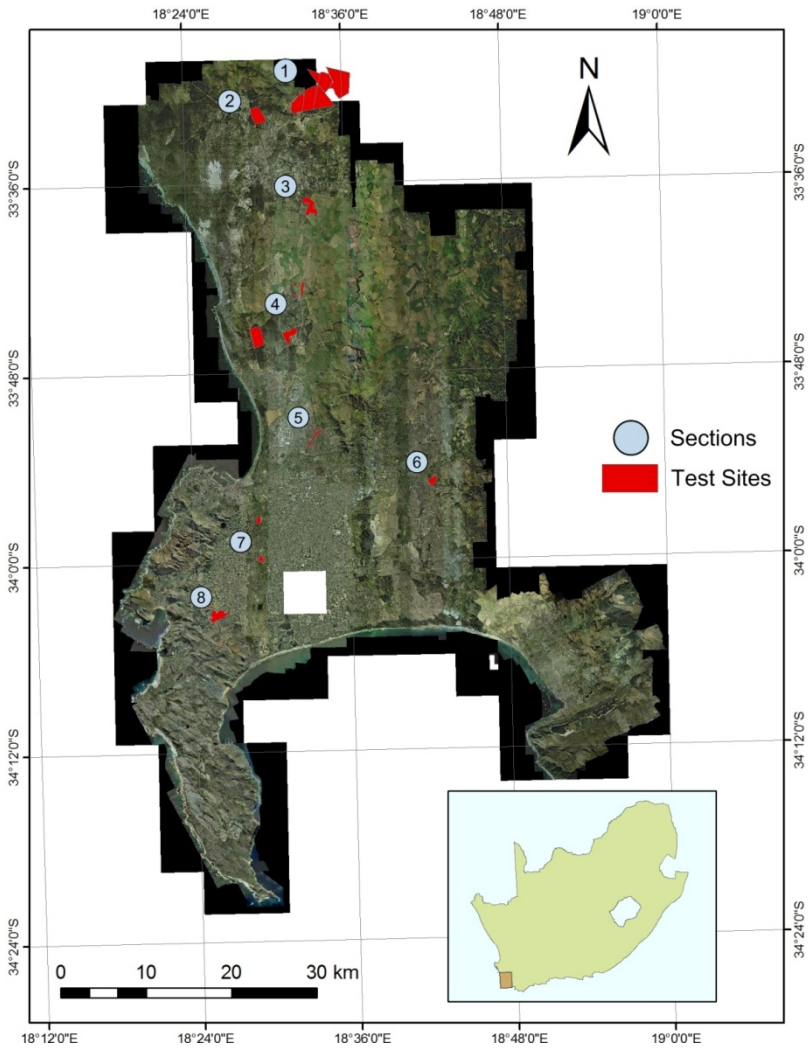

Figure 3.1: Aerial images from June 2008 showing the study area. 8 sections contain 16 test sites depicted in red. For focus maps of the sections see appendix A.1.

Eight sections with sixteen test sites (depicted in red in figure 3.1) were selected from the study area. These were specified by SANBI being the major Sand Fynbos fragments. Table 3.1 gives an overview of the different fragments with their size, protection status and in which section they are located. The boundaries and the protection status were derived from the shape file about the biodiversity network (for more information see chapter 4.7). Eight of the fragments are formally protected and the others are intended to follow.

Table 3.1: Basic Information about the vegetation fragments (adapted from the Environmental Resource Management Department, City of Cape Town).

Section	Name	Area (ha)	Protection Status
1	Riverlands Floodland	261.24	Protected
1	Riverlands Plain	613.63	Protected
1	Pella	235.5	Protected
1	Riverlands, other	808.88	Protected
1	Mamre	232.03	Protected
2	Schoongezicht	192.18	Irreplaceable Core Flora Site
3	Blaauwberg Conservation Area (East)	275.61	Partially Protected
3	Kohler Bricks	146.9	Irreplaceable High & Medium Site
3	Baasariesfontein	70.18	Irreplaceable High & Medium Site
4	Plattekloof	60.1	Core Flora Site & Natural Heritage Site
5	Haasendal	70.87	Irreplaceable High & Medium Site
6	Rondebosch Common	38.77	Protected
6	Kenilworth Race Course	56.86	Irreplaceable Core Flora Site
7	Tokai State Forest	177.18	Protected

The fragments called ‘Riverlands Floodland’, ‘Riverlands Plain’, ‘Pella’ and ‘Riverlands, other’ are part of the Riverlands Nature Reserve. For a better identification, the reserve was split into the mentioned fragments and named individually. While ‘Riverlands, other’ actually consists of three fragments, they were not sampled during the field trip and hence summarised without unique names. The Blaauwberg Conservation Area (BCA) is actually a bigger fragment, but since only the eastern part was said to contain Sand Fynbos, the rest was omitted.

Detailed descriptions of the fragments are found in chapter 4.6 containing the information gathered during the field trip.

3.2 Climate

According to the Koeppen-Geiger Climate Classification, Cape Town has a Mediterranean climate (Csb) with mild, wet winters and dry, hot summers (Kottek, Grieser, Beck, Rudolf, & Rubel, 2006). This is unique in Southern Africa and is caused by the pole-ward migration of the Hadley Cells. During the hot summers, from November to March, frequent trade-winds occur. These are strong winds, named Southeaster after their main wind direction. In winter, north-westerly winds bring most of the annual rain to the Cape Flats with an annual average of about 500 mm rainfall. Due to the mountainous landscape of Cape Town with the Table Mountain and the Cape Fold Belt, orographic rainfall occurs in these areas, especially in spring and autumn, which causes high local differences in the mean annual rainfall (Cowling, Richardson, & Pierce, 2004).

The mean annual temperature is 16.2 °C for the predominant Cape Flats Sand Fynbos (compare figure 3.2).

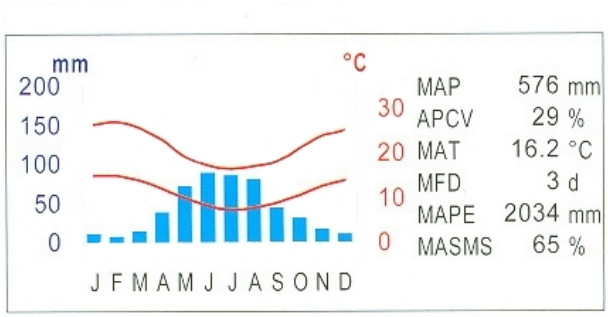

Figure 3.2: Climate diagram of Cape Flats Sand Fynbos (Mucina & Rutherford, 2006).

3.3 Geology and Soil

To understand the geomorphology, today visible at the Cape Peninsula and Cape Flats, it requires a little background. About 450 million years ago, the region was a large coastal plain with several river deltas. During this time, the Table Mountain Group sandstones were sedimented and lithified by pressure. When the continents collided to form the supercontinent Pangaea about 250 million years ago, these sediments were folded and raised to create the Cape Fold Belt. This mountain range was much higher than it is today, visible as a dashed line in figure 3.3 (Compton, 2004).

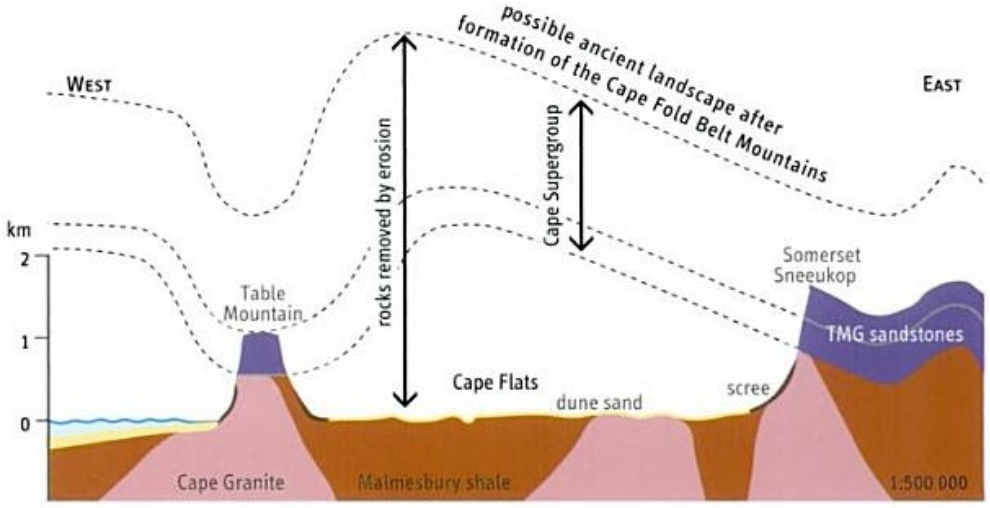

Figure 3.3: Geology of the Cape Flats and surrounding mountains (Compton, 2004).

Theory says that today's landscape might be an inverted version of the past. The Cape Flats were once a mountain ridge of the Cape Fold Belt and the visible remnants of the Table Mountain Group sandstones, which are the Table Mountain itself and the Hottentots Holland Mountains in the east, were troughs. Because of the exposure of that large mountain, those sandstones were eroded a lot faster by wind and rainfall than the ones in the troughs. Due to this erosion, the Malmesbury Shale and the Cape Granite Suite, which are of older origin, were uncovered (compare figure 3.3).

Since the Tertiary, the sea level fluctuated -120 to +200m from the present mean sea level. Thus, the Cape Flats got flooded several times and marine sediments accumulated on the Flats (Compton, 2004).

The soils of the study area are commonly nutrient-poor sandy soils. These sands can be aeolian or fluvial deposits and depending on location and lime content, they can be acidic or neutral. In some parts of the area, the underlying Malmesbury Shale or the Cape Granite leads to a clay-rich soil.

The geologic diversity and the resulting soils are an important factor for the evolution of the botanic diversity in the study area (Mucina & Rutherford, 2006).

3.4 Natural Vegetation

There are three major vegetation types in the study area: Fynbos, Renosterveld and Strandveld. In this work, the focus lies on one type of Fynbos vegetation, Sand Fynbos. This special vegetation type is due to its rarity of high conservation interest. Furthermore, the decision to focus on Sand Fynbos was made in order to eliminate as many variables as possible since it was expected that the other vegetation types of the study area have different phenologies. However, in the following will be given a short introduction to all three vegetation types in order to understand the differences.

"Fynbos (derived from the Dutch 'fijn-bosch' and pronounced 'feinbos') means 'fine bush', with a Dutch connotation for 'kindling' – as opposed to fire-wood. It is an evergreen, fire-prone shrubland characterised by the presence of restios (wiry, evergreen graminoids of the Restionaceae), a high cover of ericoid shrubs (fine-leaved, principally in the families Ericaceae, Asteraceae, Rhamnaceae, Thymelaeaceae, Rutaceae), and the common presence of proteoid shrubs (exclusively Proteaceae)" (Mucina & Rutherford, 2006). Proteoid shrubs are usually bigger than ericoid shrubs and have thicker stems and broader leaves (compare figure 3.4). Grass is a minor component in the cover of intact Fynbos vegetation. Fynbos is characterised by the recurrence of summer fires appearing at intervals of 10-30 years and fuelled by the fine-leaved shrubs and the Restionaceae. Many of the Proteaceae are adapted to fire and only release their seeds after burning, when the general vegetation cover is low and the soil is well fertilised (Mucina & Rutherford, 2006).

The major type of Fynbos in the study area is Sand Fynbos, which occurs on "acidic tertiary, grey regic [≙ undeveloped soil] sands" (Mucina & Rutherford, 2006). It is dominated by dense ericoid shrubland with emergent proteoid shrubs and restios. The latter are the prevailing type in areas that are seasonally waterlogged.

This work focuses on Sand Fynbos vegetation which divides into Atlantis Sand Fynbos and Cape Flats Sand Fynbos in the study area. The northern part of the study area is usually Atlantis Sand Fynbos, while the southern part is Cape Flats Sand Fynbos. Since the differences are rather minor in the study area, these are not explained any further (Mucina & Rutherford, 2006).

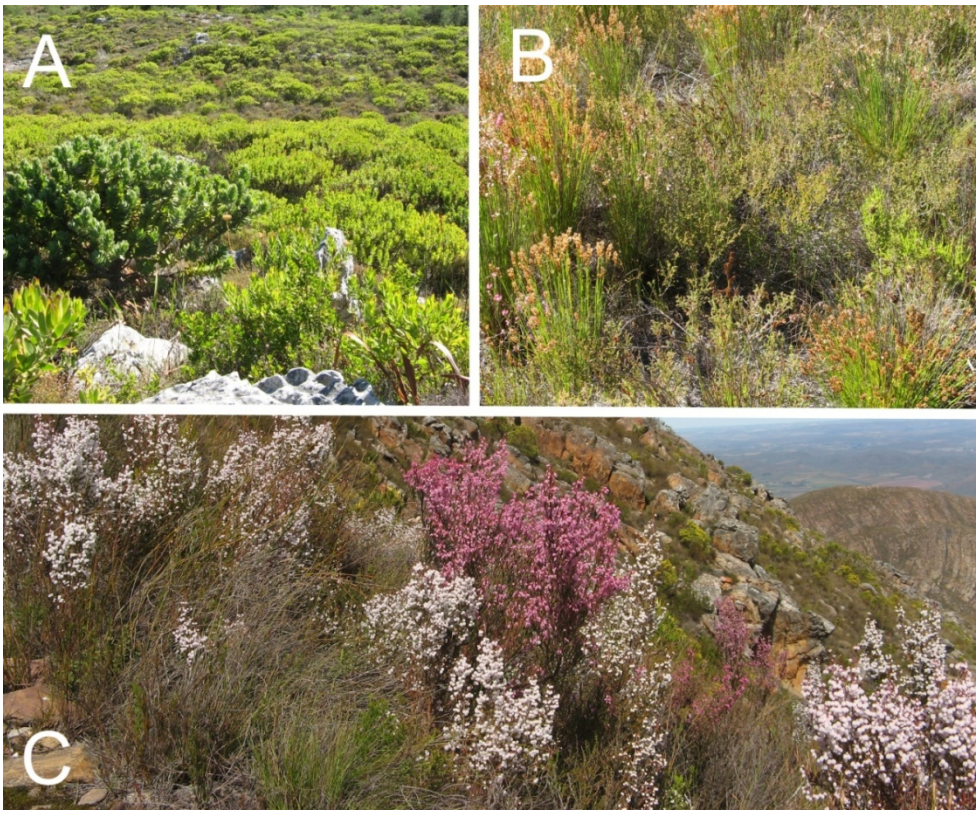

Figure 3.4: Exemplary photographs of the three major plant families in Fynbos: Proteaceae (A), Restios (B) and Ericoid Shrubs (C). Taken by Dr. Nicky Allsopp.

Renosterveld occurs on the clay-rich soils derived from shale and granite. It is an "evergreen, fire-prone shrubland or grassland dominated by small cupressoid-leaved evergreen asteraceous shrubs (principally renosterbos) with an understorey of grasses (Poaeceae) and a high biomass and diversity of geophytes" (Mucina & Rutherford, 2006). In comparison to Fynbos, it is lacking Proteaceae and Ericaceae and should have less than 5-10% cover of Restionaceae. Because of the dominance of fine, fast-growing grasses, the fire frequency (3-5 years) is higher than it is in Fynbos. Renosterveld may transform to Fynbos, where annual rainfall increases and leaching leads to a nutrient-poor soil.

Strandveld consists of medium dense to closed shrubland with a succulent character in the arid areas. It occurs on mineral-rich soils usually close to the sea, but never under direct influence of sea spray. "Unlike in Fynbos or Renosterveld, fire plays a lesser role in the Strandveld communities" (Mucina & Rutherford, 2006). The main reason is the succulent nature of the Strandveld vegetation, impeding the spread of fire (Mucina & Rutherford, 2006).

In the following chapters, the term 'Fynbos' is used as an abbreviation for 'Sand Fynbos'.

3.5 Threats for the local Ecosystems

The natural vegetation of the study area has faced and is still facing many threats – most of them are man-made. Some of them directly affect the Fynbos vegetation like urban sprawl or invasive vegetation and some of them are more subtle like climate change.
In the following, the two major threats to Fynbos vegetation in the study area besides climate change are presented.

3.5.1 Urbanisation of Cape Town

In the past half century, Cape Town has undergone some major changes. In 1950, the southern half of the study area was more or less uninhabited, but during the following apartheid era it got populated by the black community being forced out of the city centre by the government. In the following years, the townships and existing villages, today known as the Southern Suburbs, expanded and grew together to cover most of the southern Cape Flats (Wilkinson, 2000).
The northern half of the study area is only populated with some smaller villages, but agriculture plays a major role here. During the last century, the growing demand for food led to a massive extension of the agricultural area and thus to a shrinking of the natural vegetation. Grain and wine are the major cultivation products and stock farming is quite common (Wilkinson, 2000).
Between 1985 and 2005, the physical extent of Cape Town grew by 40%. The rate at which the city is developing almost doubled in the last thirty years and is now increasing at an average rate of 1232 hectares per year (Spatial Planning and Urban Design Department, 2009).

3.5.2 Invasive Vegetation

Beside the rapid decrease of the area with potential natural vegetation due to agriculture and urbanisation, the remaining vegetation fragments are under heavy pressure by the invasion of alien vegetation.
In the early nineteenth century, colonists introduced a wide variety of plants to South Africa. At first, these were predominantly agricultural crops. With the spread of the settlement an increasing need for firewood and building materials occurred. The local

Fynbos vegetation, which lacks trees and grows slowly, could not fill this role. For this reason, tree species were brought to the country, especially from Australia and South America (Cowling, Richardson, & Pierce, 2004).

"The drift-sands on the Cape Flats [...] posed an especially vexing problem. They had for years resisted attempts at control and made travel across them hazardous and unpleasant" (Day, Siegfried, Louw, & Jarman, 1979). In order to stabilise the dunes and for the production of firewood, *Acacia saligna* (compare figure 3.5) and *Acacia cyclops* were introduced in the 1830s from Australia. For the need of building materials, different pine species were brought to South Africa. To date, 113 naturalized alien grass species, especially from Europe were introduced to South Africa; some of them on purpose, e.g. for pasture or as ornamental grasses and some by accident with imported seeds or wool (Milton, 2004). Musil, Milton, & Davis (2005) hold that the invasion by alien grasses is still underestimated compared to other invaders.

Figure 3.5: Photograph of dense *Acacia saligna.*

However, a lot of different plant species were brought to the country, but no other species affected the natural vegetation of the study area till today like the two mentioned acacia species (Day, Siegfried, Louw, & Jarman, 1979).

Acacia cyclops and *Acacia saligna* have been the most extensive invaders of Fynbos reserves. According to a survey (1983-1985) documented by Cowling, Richardson, &

Pierce (2004), *Acacia cyclops* covered 52.6 % and *Acacia saligna* 37 % of all grid cells tested. Today, especially *Acacia saligna* is regarded as "the most important invasive weed in the Cape Floristic Region" (Maslin & McDonald, 2004). It is well adapted to the dry and nutrient-poor soils of the Cape Flats. The main root may grow to 16 m deep (Maslin & McDonald, 2004) and it is able to fix atmospheric nitrogen (Marsudi, 1999). This nitrogen-fixing attribute can change the whole soil regime. Yelenik, Stock & Richardson (2004) have shown that long-term invasions and as a consequence the enrichment of the soils not only hinder the recovery of Fynbos after a clearing, but also lead to higher growth rates of a weedy grass species. This may cause serious problems for restoration of the native vegetation.

In order to control the invasion of *Acacia saligna*, different approaches were applied. The most obvious one is to cut down the trees or burn them. Depending on the size of the area, there are three general ways to do this: 'burn standing', 'fell and burn' and 'fell, remove and burn'. Holmes, Richardson, Wilgen & Gelderblom (2000) suggest that 'burn standing' is the best treatment to promote Fynbos recovery, since it causes the least change to vegetation variables.

Another approach is the introduction of biological control agents, i.e. natural enemies of the invaders. 73 species of herbivorous natural enemies have been introduced to South Africa to control the dispersal of all kinds of alien plants (Cowling, Richardson, & Pierce, 2004). In 1987, the rust fungus *Uromycladium tepperianum* was introduced to control the *Acacia saligna* and established throughout the stands of the weed. The fungus releases hormones causing the tree to rapidly produce galls with an average diameter of 1-2 cm (Serdani, 2001). The infection with *U. tepperianum* itself does not kill the tree, but the high gall production stresses it to such an extent that it cannot cope with other environmental stresses like droughts and dies or shows reduced vigour especially in seed production (Wood & Morris, 2007).

The seed-feeding beetle *Melanterius compactus* has been introduced in 2001 to increase the pressure on the acacia populations (Wood & Morris, 2007). Statistics about the success of the beetle are outstanding to this date.

Despite great successes with these biological control agents, it is still necessary to cut down and/or burn the acacia to completely clear invaded areas. This requires good management over several years.

3.6 Monitoring 'Degradation' and 'Improvement' in the Context of the Study Area

Land degradation is one of the most common topics in ecological research (e.g. Blaikie & Brookefield, 1987; Meadows & Hoffman, 2003; Pickup, Bastin, & Chewings, 1998). It is generally defined by the FAO as the "temporary or permanent decline in the productive capacity of the land" (Stocking & Murnaghan, 2001). Most of these definitions refer to land as an economic resource and link degradation with the term 'land use'. Thus, land degradation is usually indirectly measured as the value for human use. For example Bai & Dent (2008) primarily define land degradation "as a long-term decline in ecosystem function" and then cut it down on the measurement of net primary productivity (NPP) with degradation as a decline of NPP and improvement as an increase in NPP. This might be appropriate for a nationwide or global approach but chapter 2.1 already depicted that this may not be appropriate for the analysis of complex ecosystems.

After an analysis of the conditions of the study area in combination with the general behaviour of EVI it becomes apparent that the general approach of Wessels et al. (2007) and Bai & Dent (2008), which form the basis for this study, have to be modified. Since the focus is on areas with natural or semi-natural vegetation and rangelands are excluded, it is not reasonable to look at these from an economic point of view. Measuring the value of a natural area for human benefit is rather vague and not part of this study.

As mentioned in the previous chapter, a main problem of the study area is the invasion of alien vegetation, especially of *Acacia saligna* and alien grasses. Because degradation through direct anthropogenic influences is rather minor on the fragments, the invasion of alien species is the main problem and thus the first indicator for degradation of Fynbos vegetation. In this context, alien plants as well as an exceedingly high cover of grasses indicate degradation, since the grass fraction of pristine Fynbos vegetation is rather minor.

4 Data and Data Pre-Processing

In this work, a combination of remotely sensed data, GIS data and precipitation data was used for the analysis. In addition, ground truth data was collected during field work in January – February 2010. The data and the way it was processed are presented in the following section.

4.1 Satellite Data

The remotely sensed data used in this study is described in the following. The basis for this remote sensing approach is the data of the MODIS sensor on the platform Terra. This data is pre-processed by NASA and different vegetation indices are calculated and provided online.

4.1.1 Terra - Satellite

The satellite Terra, also known as EOS AM-1, was launched in December, 1999 by the American NASA and started to collect data in February, 2000 (NASA Science, 2010). It is flying in a 705-km (on the equator) high sun-synchronous orbit and crosses the equator each day at 10.30 a.m. from north to south at an inclination of 98° (Lillesand, Kiefer, & Chipman, 2004). Table 4.1 gives an overview of Terra's characteristics.

Table 4.1: Characteristics of the Terra satellite (adapted from ERSDAC, 2010).

Orbit	Sun-synchronous, polar orbit
Equatorial pass time	Descending node at 10:30 a.m.
Altitude	700-737 km (705 km on the equator)
Inclination	98.2°
Repetition cycle	16 days
Inter-orbit distance	172 km
Revolution time	98.88 min.

The so-called flagship satellite of NASA's earth observing systems provides global data on the state of the atmosphere, land, and oceans. It carries five instruments with different specifications on board: CERES, MISR, MODIS, MOPITT, ASTER (NASA Science, 2010).

The design of Terra and its complementary satellite *Aqua* is intended to provide different instruments with a synergetic effect. Aqua was launched in May, 2002; following the same orbit as Terra, it is possible to monitor the same region on the earth during different times of the day. Measurements of one instrument can be used to atmospherically correct the data of another instrument. In addition, the results of the different instruments can be composed for a number of interrelated scientific objectives like vegetation structure and dynamics or atmospheric radiative balance (Lillesand, Kiefer, & Chipman, 2004).

4.1.2 MODIS - Sensor

The **MOD**erate Resolution **I**maging **S**pectrometer MODIS is installed on both Terra and Aqua satellites. It provides long-term observations to derive an enhanced knowledge of global dynamics and processes of land-cover, ocean and the lower atmosphere (Jensen, 2005). With its one to two days global repetition rate, it is eminently suited for questions about the phenological cycle of vegetation. Thus, this sensor was chosen for the study in order to correlate its data with constant rainfall data.

MODIS is a whiskbroom scanner, collecting signals with a rotating mirror along scan lines at right angles to the flight line. Thus, it has a wide field of view of ±55° off-nadir (the base point opposite to the zenith) and reaches a swath width of 2,330 km. As mentioned in the theoretical background, it has a high radiometric resolution of 12 bit. Collecting data in 36 spectral bands, it also offers a good spectral resolution (compare table 4.2). 20 of these bands detect solar radiation in the range of 0.4 to 3 µm and the other 16 bands collect thermal signals from 3 to 15 µm (Jensen, 2005).

Table 4.2: Characteristics of the MODIS sensor (adapted from Jensen, 2005).

Band	Spectral Resolution (µm)	Spatial Resolution	Band Utility
1	0.620 - 0.670	250 x 250 m	Land-cover classification, chlorophyll absorption, leaf-area index mapping
2	0.841 - 0.876	250 x 250 m	
3	0.459 - 0.479	500 x 500 m	
4	0.545 - 0.565	500 x 500 m	
5	1.230 - 1.250	500 x 500 m	
6	1.628 - 1.652	500 x 500 m	
7	2.105 - 2.155	1 x 1 km	Ocean colour, phytoplankton, biogeochemistry
8	0.405 - 0.420	1 x 1 km	
9	0.438 - 0.448	1 x 1 km	
10	0.483 - 0.493	1 x 1 km	
11	0.526 - 0.536	1 x 1 km	
12	0.546 - 0.556	1 x 1 km	
13	0.662 - 0.672	1 x 1 km	
14	0.673 - 0.683	1 x 1 km	
15	0.743 - 0.753	1 x 1 km	
16	0.862 - 0.877	1 x 1 km	
17	0.890 - 0.920	1 x 1 km	Atmospheric water vapour
18	0.931 - 0.941	1 x 1 km	
19	0.915 - 0.965	1 x 1 km	
20	3.600 - 3.840	1 x 1 km	Surface-cloud temperature
21	3.929 - 3.989	1 x 1 km	
22	3.929 - 3.989	1 x 1 km	
23	4.020 - 4.080	1 x 1 km	
24	4.433 - 4.4498	1 x 1 km	Atmospheric temperature
25	4.482 - 4.549	1 x 1 km	
26	1.360 - 1.390	1 x 1 km	Cirrus Clouds
27	6.535 - 6.895	1 x 1 km	Water vapor
28	7.175 - 7.475	1 x 1 km	
29	8.400 - 8.700	1 x 1 km	
30	9.580 - 9.880	1 x 1 km	Ozone
31	10.780 - 11.280	1 x 1 km	Surface-cloud temperature
32	11.770 - 12.270	1 x 1 km	
33	13.185 - 13.485	1 x 1 km	Cloud-top altitude
34	13.485 - 13.785	1 x 1 km	
35	13.785 - 14.085	1 x 1 km	
36	14.085 - 14-385	1 x 1 km	

Depending on the band, MODIS' coarse spatial resolution ranges from 250 x 250 m² for the bands 1 and 2 to 500 x 500 m² for the bands 3 through 7 and 1 x1 km² for the other bands from 8 to 36. The MODIS data have one of the most comprehensive calibration settings and are characterized by improved geometric rectification and radiometric calibration (Lillesand, Kiefer, & Chipman, 2004). Furthermore, the products about the land

surface are already atmospherically corrected. With these stringent calibration standards, a large variety of data products is derived from this sensor with the following main application areas (after Lillesand, Kiefer, & Chipman, 2004):

- **Cloud masks** for the assessment of climate and potential climate change.
- **Aerosol concentration and optical properties.**
- **Cloud properties** like optical thickness and effective particle radius.
- **Vegetation and land surface cover**, several kinds of atmospherically corrected vegetation indices like net primary productivity, leaf area index, normalised difference vegetation index and enhanced vegetation index.
- **Snow and sea-ice cover and reflectance.**
- **Surface temperature** with an absolute accuracy goal of 0.3 to 0.5 °C over oceans and 1 °C over land.
- **Ocean colour**, spectral radiance (visible and near-infrared bands) leaving the ocean.
- **Concentration and fluorescence of chlorophyll** in surface water.

These products are available online at no charge, e.g. at the USGS Global Visualization Viewer (USGS, 2010).

4.1.3 Vegetation Indices

In this study, the Enhanced Vegetation Index (EVI) is used to determine the relationship between primary production and rainfall. The EVI is part of the MODIS product *MOD13Q1*, which also contains a second vegetation index, the so-called Normalised Difference Vegetation Index (NDVI). Both indices are in a 250 x 250 m² spatial resolution and are delivered as a 16-days composite, which means there are 23 composites, so-called *time steps* per year. As mentioned in the previous chapter, MODIS actually has a global repetition rate of one to two days, but because of effects like cloud cover and viewing geometry these data are not always useful. Thus, the observations are collected over 16 days and composited by the MODIS VI algorithm applying a filter based on quality, cloud, and viewing geometry (Huete et al., 2002).
Since the NDVI forms the basis for the EVI, it is described in the following, too.

NDVI The NDVI is commonly known as a remotely sensed surrogate for net primary production (NPP) and has been used in numerous studies (e.g. Wessels et al., 2007; Bai & Dent, 2008; Fabricante, Oesterheld, & Paruelo, 2009). It is one of the most important vegetation indices because it is able to monitor "seasonal and inter-annual changes in vegetation growth and activity" (Jensen, 2005). Taking advantage of the red edge in vegetation signatures (compare chapter 2.2), the NDVI is calculated as follows (Jensen, 2005):

$$\text{NDVI} = \frac{\rho_{nir} - \rho_{red}}{\rho_{nir} + \rho_{red}} \tag{4.1}$$

where:

ρ_{nir} = near-infrared band

ρ_{red} = red band

The possible range of values for the NDVI goes from -1 to 1. Areas with a high vegetation cover will generally yield high values for the index having high near-infrared reflectance and low reflectance in the red band. With a larger reflectance in the visible bands than in the near-infrared band, clouds, water, and snow yield negative index values. Areas with open ground and rocks tend to have similar reflectances in both bands and result in an NDVI near zero (Lillesand, Kiefer, & Chipman, 2004).

However useful the NDVI is, it should be pointed out that it has certain disadvantages. This ratio-based index is nonlinear and can be affected by certain noise effects such as atmospheric scattering. Another problem is the saturation effect in high-biomass regions like forests. The NDVI dynamic range is compressed for these high-biomass regions and rather stretched under low-biomass conditions. The third disadvantage of the NDVI is its sensitivity to canopy background such as visible soil. The NDVI values seem particularly higher with darker canopy backgrounds (Jensen, 2005). This also makes it a rather "poor indicator of vegetation biomass if the ground cover is low, as in arid and semi-arid regions" (Schowengerdt, 2007).

EVI The EVI was developed by the MODIS Land Discipline Group especially for the use with MODIS data. As the name suggests, the EVI is an enhanced version of the NDVI and is calculated as follows (Schowengerdt, 2007):

$$\text{EVI} = G\left(\frac{\rho_{nir} - \rho_{red}}{L + \rho_{nir} + C_1\rho_{red} - C_2\rho_{blue}}\right) \quad (4.2)$$

where:

G = 2.5

L = 1

C_1 = 6

C_2 = 7.5

The bands ρ_{NIR}, ρ_{red} and ρ_{blue} are atmospherically corrected or partially corrected (Rayleigh and ozone absorption) surface reflectances. L is the soil adjustment factor, G is a gain factor and the two coefficients C_1 and C_2 describe an atmospheric correction using the blue band to correct the red band. Huete et al. (2002) has shown that the EVI has an improved sensitivity to high biomass and does not saturate as easy as the NDVI. Furthermore, atmospheric influences are reduced for the EVI and the monitoring of vegetation is improved through a decoupling of the canopy background signal (Jensen, 2005; Huete et al., 2002). Because of these advantages over the NDVI, the EVI was chosen for this study. The whole times series from the start of the data collection in February 2000 till the end of 2009 was used.

4.2 Pre-Processing of Remotely Sensed Data

Depending on the remote sensing system, the data is usually not delivered 'ready-for-use'. Several pre-processing steps like atmospheric correction or georectification have to be done in order to use it for further applications. In some cases, these pre-processings are already calculated by the provider, in some not, but they always have to be done first.

4.2.1 Atmospheric Correction

While travelling through the atmosphere from the earth's surface to the sensor, the electromagnetic radiation signals are modified by scattering and absorption by gases and aerosols (Song, Woodstock, Seto, Pax Lenney, & Macomber, 2001).

The total radiation at the sensor consists of three components shown in figure 4.1:

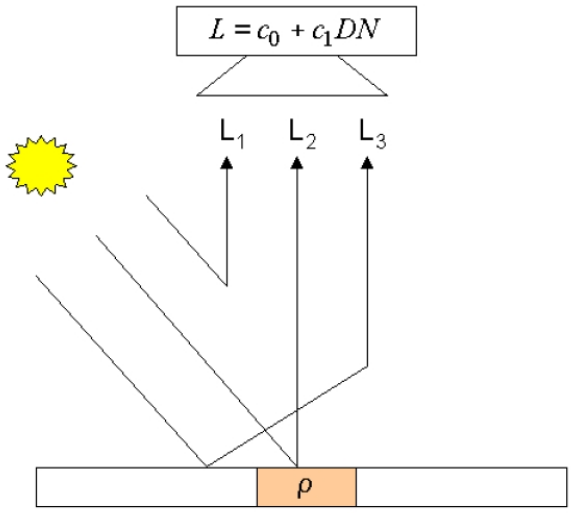

Figure 4.1: Solar radiation components (Richter, 2010): path radiance (*L1*), reflected radiation (*L2*) and adjacency radiance (*L3*).

1. **Path radiance** (*L1*). This is light scattered from the atmosphere and received by the sensor without having made ground-contact.
2. **Reflected radiation** (*L2*). Direct and diffuse solar radiation is reflected by the pixel i.e. the earth's surface and transmitted to the sensor. The diffuse solar radiation is light scattered in the atmosphere so that it is redirected to the pixel and reflected towards the sensor.
3. **Adjacency radiance** (*L3*). Solar radiation is reflected by neighbouring pixels and scattered by the atmosphere right in the direction of the sensor.

The task of atmospheric correction is to remove the effects of the path radiance, the adjacency radiance and the diffuse solar radiation in order to retrieve the information from the currently viewed pixel contained in *L2* (Richter, 2010).

Atmospheric correction is not always necessary, depending on the type of analytical method used. For certain classifications, which only use a single date, it is unnecessary to

atmospherically correct them as long as the training data and the data to be classified are in the same relative scale (Jensen, 2005).

4.2.2 Geometric Correction

Geometric Correction is the second important type of correction and is usually necessary because the remotely sensed data are not in their proper geometric *x, y* location (Jensen, 2005). The remotely sensed data typically exhibits *internal* and *external geometric errors*, i.e. distortions of the image (Jensen, 2005). Internal geometric errors are mostly systematic distortions and can be caused by the earth's rotation or the scanning system itself. Those distortions are usually identified and corrected rather easy. On the other side, external geometric errors are caused by changes in altitude or attitude of the sensor. If the remote sensing platform, i.e. the aircraft or spacecraft gradually changes its altitude or if the elevation of the ground changes, the scale of the imagery changes, too (Jensen, 2005). While satellite platforms are not affected by atmospheric effects, aircraft platforms constantly contend with atmospheric turbulence or wind and thus change their attitude, i.e. axial position or pitch up and down (Jensen, 2005). These geometric distortions can be corrected using *ground control points* (GCP) and appropriate mathematical models (Jensen, 2005).

4.2.3 MODIS Processing

Since the MODIS EVI data is calculated with an atmospheric correction, it is not necessary to correct them any further. However, some processing steps have to be done in order to use and correlate them with the rainfall data. At first, MODIS data always have to be reprojected from the sinusoidal projection to the projection of one's choice, in this case the Universal Transverse Mercator UTM Zone 34 S, which was used for all data in this study. This was done using the *MODIS Reprojection Tool* (MRT) (LP DAAC User Services, 2010). Further functions of this program are the subsetting and resampling of the data. Subsetting was used to reduce the size of the MODIS data to the area of interest, i.e. the study area. Resampling changes the spatial resolution (pixel size) of the data. The exact pixel size of the MODIS EVI 250m product is 232m, so the data was resampled to this size. Because these MRT processings have to be done for each single file, two small IDL (Interactive data Language) scripts were used in order to automate these functions.

Furthermore, it is essential to analyse the quality of the whole time series used in this study and correct errors if necessary. For this purpose, Colditz et al. (2008) developed a tool called *Time Series Generator (TiSeG)*, which uses the quality-assurance science data set included in the MOD13Q1 product. The time series is analysed for outliers, which can still be contained in the data despite the corrections during the pre-processing of the provider. These outliers or as they are called in the tool 'invalid pixels' may result from insufficient atmospheric correction and prevail during the rainy season (approximately April – September for Cape Town), while the cloud cover is dense. The invalid pixels are temporally interpolated after certain rules that have to be set by the user. For detailed information on the tool and its parameters see Colditz et al. (2008). In general, the interpolation rules for the rainy season are set a bit more flexible so that bigger gaps of invalid values can be filled. The whole EVI time series used in this study was processed with this tool.

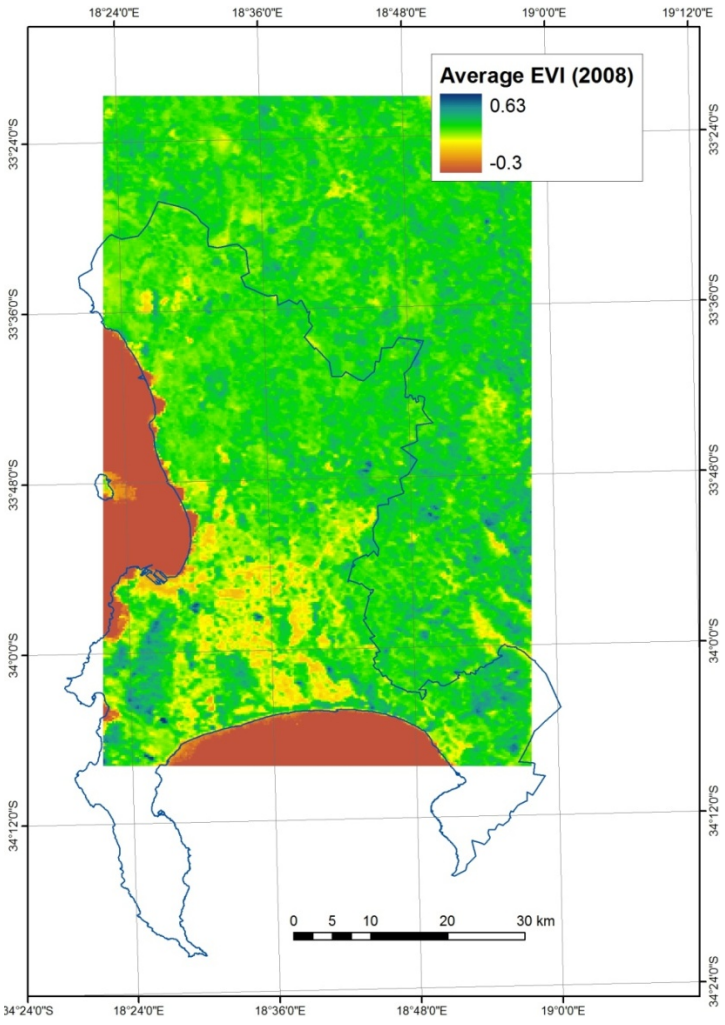

Figure 4.2: Annual average of EVI in the study area (year 2008).

Finally, the data format has to be converted to a more practicable format. The MODIS data are delivered in the so called Hierarchical Data Format (.hdf). Since most of the remote sensing programs have their problems with this format, the data were converted to the common GeoTIFF format. Figure 4.2 shows an example for a readily processed EVI scene for the year 2008.

4.3 Rainfall Data

The rainfall data were provided by the South African Weather Service (SAWS) from 19 rainfall stations. These data were delivered in Excel-format for the years 1999 to 2008. Each rainfall station was listed in annual sheets containing daily precipitation records with rows for the days and columns for the months. In order to integrate these into a *Geographic Information System* (GIS), the data had to be modified. These modifications were implemented by me in an *IDL* (Interactive Data Language) script (compare appendix A.2). First, the script reads in the precipitation data from the Excel file and then the annual sheets are converted so that the daily records of the whole time series are lined up in a column for each rainfall station. Furthermore, the daily records are aggregated to 16-days sums in order to match the MODIS data. Finally, the script exports the converted data to a text file. Afterwards, a point shape file was generated manually with the software *ESRI ArcGIS 9.3* using the coordinates of the climate stations. The rainfall records were imported from the text file to the GIS and linked with the shape file. Finally, each 16-days sum was interpolated to a raster in ArcGIS using the *Natural Neighbour* method. 232m, the same cell size as for the EVI data was chosen and the output files were snapped to the EVI data so that they perfectly match them. Furthermore, the 16-days sums were aggregated to annual sums of rainfall for the processing of the rain-use efficiency. Figure 4.3 shows the readily processed annual rainfall sum of 2008.

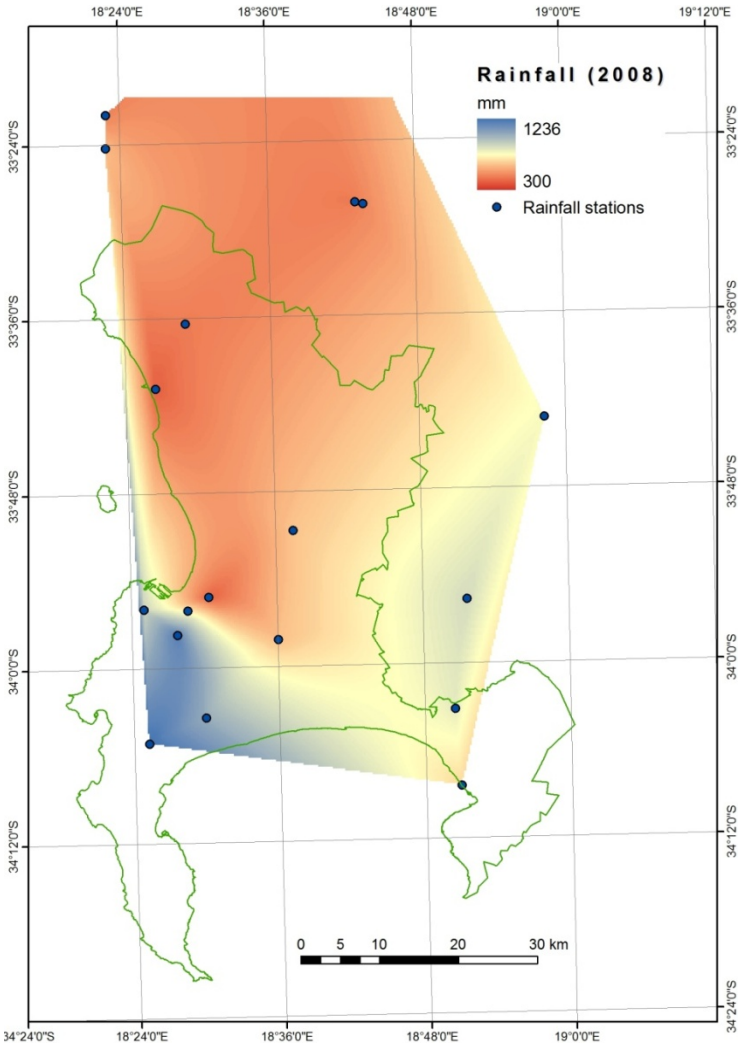

Figure 4.3: Annual sum of rainfall and 19 rainfall stations (year 2008).

4.4 Aerial Images

The aerial images were provided by the City of Cape Town's Environmental Resource Management Department. Two data sets from April 2000 and June 2008 were used in this study, primarily to get a first impression of the fragments. Unfortunately, the images do not cover all of the fragments (compare figure 3.1 or appendix A.1). The Riverlands Nature Reserve is displayed only partially on both data sets and the Blaauwberg Conservation Area, Baasariesfontein, the Rondebosch Common and the Kenilworth Race Course are not covered by the 2000 data set.

The images were interpreted visually and used to select the pixels for ground truthing.

4.5 Ground Truth Data

The ground truth data acquisition was performed between 11th January and 14th February 2010, which is towards the end of the dry season.

After some consultations with the local botanists at the SANBI office, a pre-selection of the fragments had to be done. Because of diverse reasons, not all sites could be visited. It turned out that for Tokai State Forest, the area under potential Fynbos vegetation is too small for a serious remote sensing analysis. Furthermore, it was recommended not to visit the Haasendal fragment due to safety issues in the area. The fragments Plattekloof and Kenilworth Race Course were also eliminated from the schedule because of time and size issues. In addition, the Plattekloof fragment with its long and narrow shape is not even covering the width of one MODIS pixel and thus its signal must be influenced by neighbouring effects of the surrounding built-up area.

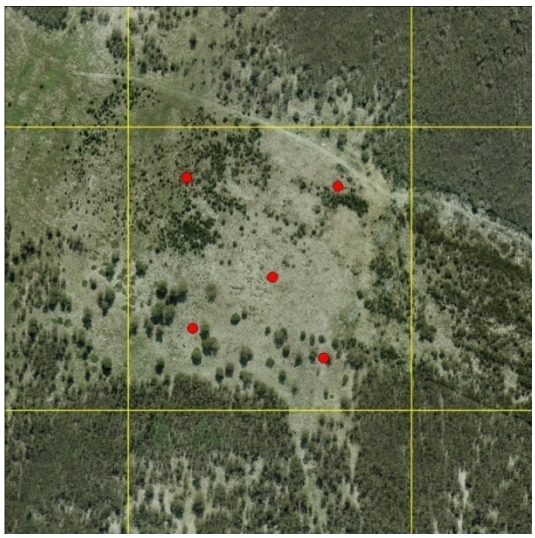

Figure 4.4: Sampling scheme of the ground truth polygons consisting of five sampling points. Yellow lines mark the pixel boundaries of the EVI pixels.

In order to get a broad spectrum of vegetation types, a visual interpretation of the aerial images was done before entering the fragments. On the basis of these interpretations, certain areas, always in the centre of a MODIS pixel have been chosen for ground truthing. Each one of these 'ground truth polygons' (GTP) was sampled at five locations, always in the same scheme (red points in figure 4.4). The middle point of the polygon was taken and then additional points towards all four corners of the polygon. The distance between the points and the offset from the border of the surrounding pixel was

measured with a Garmin GPS device. For a better orientation, a grid of the pixel boundaries (yellow lines in figure 4.4) was uploaded on the GPS device before the field trip. Due to a certain inaccuracy during the measuring progress, the sampling points do not always form a perfect square.

Around each sampling point, an imaginary 20 x 20 m² area was defined. The percentage cover of vegetation and bare soil of this area was visually estimated and digital photographs in four different directions (North, East, South, and West) were taken (compare figure 4.5).

Figure 4.5: Photographs of all directions (North, East, South and West) taken at an exemplary sampling point during the ground truthing.

In order to improve the estimation, the sampling area was divided into four 10 x 10 m² squares. The vegetation types were documented in detail, so they could be aggregated to more coarse vegetation groups during the appraisal. Afterwards, the percentage cover of the four 10 x 10 m² sub-squares and then the cover of the five 20 x 20 m² squares were aggregated to one percentage cover for each GTP.

With this procedure, it was intended to get a representative vegetation cover of the surrounding area. Although, the centre of a pixel was always chosen for the sampling of the GTP, it was considered that the pixel may have a certain shift due to geo-correction

issues. Therefore, pixels in homogenous areas of the fragment were preferred for the GTP in order to cope with a possible shift.

For the rather homogenous fragment Riverlands Plain, the sampling procedure was simplified and a transect of nine pixel middle points was collected.

This way, 21 GTPs were sampled and a total number of 126 sample points were collected (compare table 4.3).

Table 4.3: Overview of the fragments and the sampled ground truth polygons (GTPs).

Name	GTPs	Points
Blaauwberg Conservation Area	2	10
Baasariesfontein	2	10
Mamre	6	30
Rondebosch Common	3	15
Kohler Bricks	2	10
Pella	2	11
Riverlands Floodland	3	15
Riverlands Plain	0	transect of 9 points
Riverlands, other	1	5
Haasendal	-	-
Kenilworth Race Course	-	-
Plattekloof	-	-
Schoongezicht	-	-
Tokai State Forest	-	-

After the field work trips, the GPS coordinates of the sample points were downloaded from the GPS device and saved in a shape file. The notations of the vegetation cover were entered into Excel and joined in ArcGIS with their particular point in the shape file. Of course, not all the different vegetation cover types can be detected by a remote sensing system as coarse as MODIS. Thus, the types had to be aggregated to more coarse vegetation groups.

4.6 Additional Information about the Fragments

A second aim during the field work was the acquisition of background information about the different vegetation fragments. This could be protection status, date of protection, management measures, fire events or information about the utilisation of the fragments in the past, e.g. grazing. This information is very important for the analysis of the time series. Since the general scale and area used in this work is very small, any disturbance of the fragment caused by fires or other factors could have serious impacts on the EVI.
Unfortunately, the records of the different vegetation fragments that could be gathered are rather sparse and most of the time not accurate enough. In the following, the information gathered about the fragments during the field trips and during email contact with different institutions is presented.
For focus maps of the fragments see appendix A.1.

1. The **Riverlands Nature Reserve** is the northernmost and biggest of the fragments with a total area of about 1920 ha. As mentioned in chapter 3.1, it is divided into six sub-fragments of different condition and management measures taken:
    a. **Pella** is the westernmost sub-fragment, probably the oldest part of the reserve and its Fynbos vegetation is in a very good condition. The northern half seems a couple of years older than the southern half.
    b. **Riverlands Plain** is the easternmost sub-fragment and named by the author of this work due to its flat grassy appearance. Some sparse, young acacia stands can be found, but they are obviously cut down on a regularly basis.
    c. **Riverlands Floodland** is also named by the author. Some parts of this sub-fragment are temporarily flooded, which is visible by the prevailing Restios and missing shrubs. In general, it contains intact Fynbos vegetation.
    d. There are three more sub-fragments, summarized as **'Riverlands, other'** in chapter 3.1, on the Riverlands Nature Reserve, but they are of less importance and have not been sampled during the field work. These un-sampled fragments are formally conserved, but have not been managed yet. Agricultural structures are still visible in some parts of them.

Since the management of the Riverlands Nature Reserve is rather strict, some background information could be acquired. The CapeNature, a public institution for biodiversity conservation in the Western Cape, provided a shape file that contained information about where and when invasive species were cleared. This data goes back to 2004, the year of the first clearings. Unfortunately the shape file contains no fire records and there is no information about the years 2000 to 2003.

2. The fragment **Mamre** is, as mentioned in chapter 3.1, formally protected but still a common for the residents. The general vegetation cover is very mixed with some dense stands of *Acacia saligna* in the north and some very young and open Fynbos vegetation in the east. According to an interview with Mr. Ismail Ebrahim (compare appendix A.4), employee of the CREW programme at SANBI, the area is used for the collection of firewood and grazing, especially for sheep, goats and pigs. Furthermore, he affirmed that parts of the Mamre common burned in 2009. During the field trips to Mamre, a burned area in the north eastern dense acacia stands was detected, but it could not be assured if this was caused by the mentioned fire or if this is the only area burned during that event. Exact records about fires or amount of livestock units are missing for the Mamre common.
3. Generally, the **Blaauwberg Conservation Area** (BCA) is a protected and managed vegetation fragment directly at the coast. Only the eastern part is potential Fynbos vegetation and of interest for this study. This section of the BCA is only formally conserved but no management measures have been taken so far. It was owned by Garden Cities, a development company, but not used for any certain purpose and thus no records exist. However, according to the Friends of BCA, a non profit organisation for the health of the BCA, the area has not been burnt the last ten years. A spot in the northeast of the actual study area was cleared by the friends of the BCA in 2005 and seems to be covered with intact Fynbos vegetation to date. Unfortunately, the area is too small to include it in the analysis.
4. **Rondebosch Common** is a conservation area in the middle of the city area. This fragment is protected for a long time but since it is surrounded by dense city area, it is still used as a local recreation site and for walking dogs etc. It is mainly covered with grasses, herbaceous plants and a few shrubs. Joanne Eastman, a member of the Friends of the Rondebosch Common, assured in an interview that the last clearings of

acacia happened in the 1990s (compare appendix A.5). At that time infestations of alien grasses were also cleared and some more during the last ten years but not as severe as it was in the 1990s. The last fire was in 1999 but did not burn the whole common. All in all, the Rondebosch Common should not have changed a lot between 2000 and 2009.

5. **Baasariesfontein** is with ca. 70 ha one of the smallest test sites. It is surrounded by farmland and not protected yet. Because of its small size and long shape, neighboring effects to the wheat fields could occur.
6. **Kohler Bricks** is named after the bricks company which owns this fragment. The northern part of the adjacent bricks company is used as a waste dumb. The test site is not under protection and the vegetation cover is basically *Acacia saligna*.
7. As the name implies, **Kenilworth Race Course** is used for horse-racing, but the centre of the race track is left natural. According to the Gold Circle Racing and Gaming Group (2010), which owns the property, the approximately 52 ha are conserved and managed since 2006. Since the fragment is almost too small for the analysis and due to time constraints, it was not visited during the field trip.
8. **Haasendal** is a fragment in the southeast of the study area. It is not protected and since it is said to have illegal housing lately, this site was not visited during the field trip.
9. **Tokai State Forest** is a plantation that has been harvested on a cyclical basis for a long time. Since 2005, Tokai is part of the Table Mountain National Park but the harvesting continues for another 20 years till all matured trees are felled. This way, the fragment will be renaturalised bit by bit. Up to now the area under potential Fynbos is too small for the analysis with remote sensing and was thus omitted from the study.
10. **Schoongezicht** is a family-owned farm and is said to have some intact Fynbos vegetation in the northern part. Since this fragment was recommended by the City's Environmental Management Branch after the field work was undertaken, it could not be sampled.

In general, the background information about the fragments is very sparse which makes an interpretation of the indicators for the whole time series difficult. Thus, this work

focuses in the following chapters on the analysis of the most recent data and the time series became secondary.

4.7 Additional GIS Data

In addition to the self-made shape files for the ground truth data and the rainfall stations, several other datasets have been used in this study.

The City of Cape Town's Environmental Resource Management Department (Biodiversity Management Branch) provided a shape file that contained information about the biodiversity network of the city. This file displays all the remnant vegetation fragments for 2008 in the City of Cape Town and contains information about their actual conservation status. The shape file of the test sites (compare figure 4.6) was extracted from this dataset. According to this shape file, the test sites cover three different conservation categories:

- **Protected**, sites that are currently being managed as part of existing reserves
- **Irreplaceable Core Flora Site**, sites that are irreplaceable, of historical significance and very high priority
- **Irreplaceable High & Medium Site**, sites that contain critically endangered vegetation of high and medium quality

Another shape file provided by this department illustrates the potential natural vegetation of the City of Cape Town, i.e. the vegetation type that would prevail if the area is still natural. The intersection between the biodiversity network data and the potential natural vegetation was used to decide which Sand Fynbos fragments are chosen for this work.

An updated version of the National Land Cover project (NLC) was provided by SANBI (compare figure 4.6). This classification is based on different datasets from the CAPE project of 2000 to 2005 with a 30 x 30 m² resolution to update the NLC 2000 version. In this work, the dataset was used to understand the distribution of the different land cover types in the study area and to compare the land cover with the results.

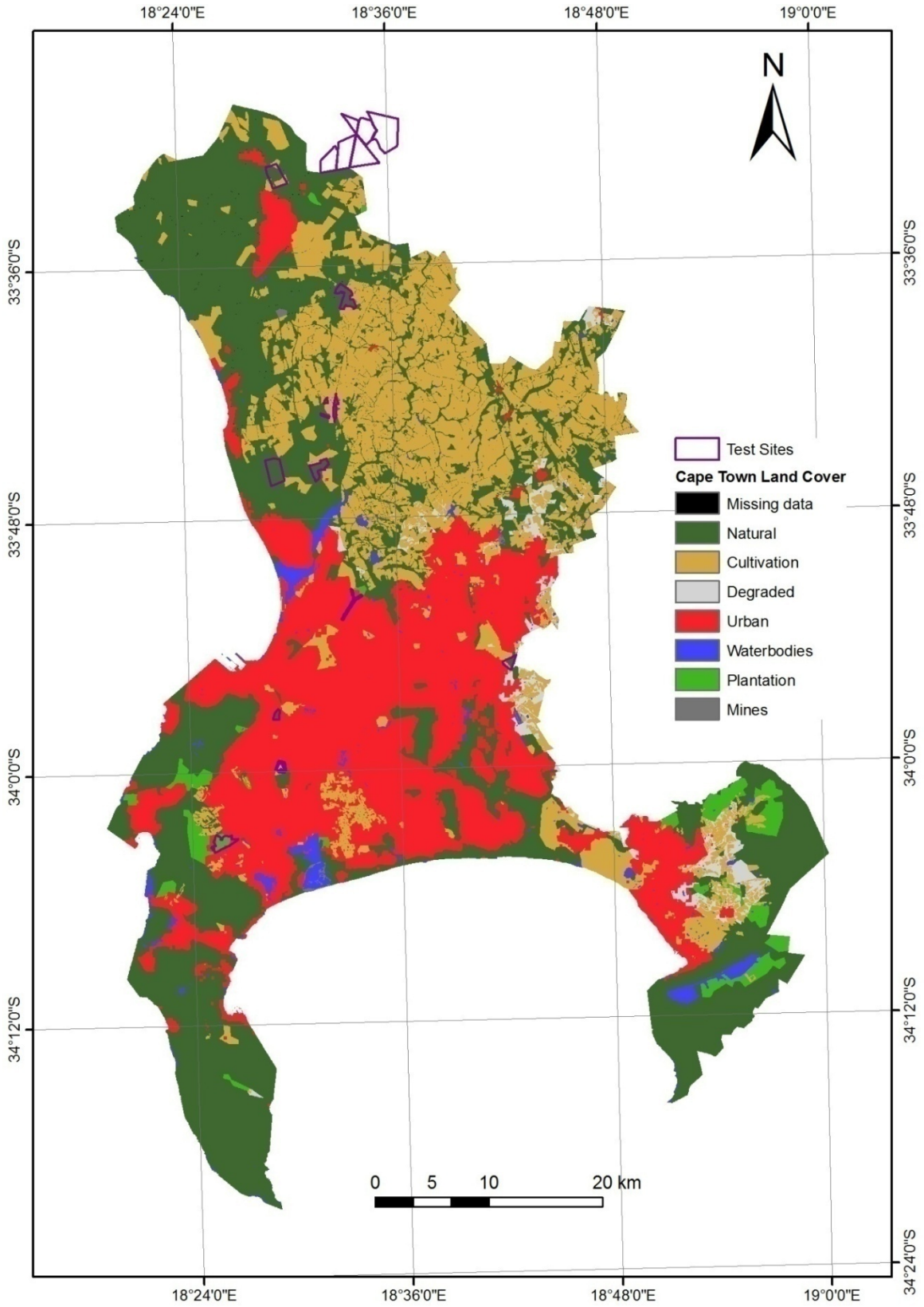

Figure 4.6: Land cover of the City of Cape Town derived from different datasets (period 2000-2005) created by the National Land Cover project (NLC).

5 Methodology

As mentioned in chapter 2.1, ecosystem health is a very complex issue and indicators have to be found separately for each area of interest. Rapport (2007) described three general measures: vitality, organisation and resilience, which have to be analysed in order to find indicators for ecosystem health. Since this work is not able to cover all aspects of ecosystem health, it focuses on indicators of two of the three measures: vitality and organisation. Vitality is basically measured in terms of primary productivity for which remote sensing is a generally known instrument. In this work, it is the primary goal to analyse the reaction of the local vegetation to rainfall as a measure of vitality.

Furthermore, the organisation of an ecosystem, the second measure, is estimated by its biotic diversity. Since this diversity dramatically decreases with the introduction of dominant alien species (e.g. Van Der Wal et al., 2008; Alvarez & Cushman, 2002), the distribution of invasive species is delineated in this study. For the City of Cape Town, the *Acacia saligna* is regarded as the most important invasive weed (Maslin & McDonald, 2004).

5.1 Productivity of Vegetation

Since the methodology of this study is based on the papers by Wessels et al. (2007) and Bai & Dent (2008), three common methods were used to analyse the productivity of the vegetation: the rain-use efficiency, a regression between rainfall and EVI and the residual trends method (RESTREND).

5.1.1 Rain-use Efficiency

The rain-use efficiency has been used in numerous studies as an index of degradation (Nicholson, Tucker, & Ba, 1998; Wessels et al., 2007; Bai & Dent, 2008; Symeonakis & Drake, 2004). The RUE is the ratio between annual NPP and annual rainfall. Since NPP is not easy to obtain, the NDVI is commonly used as a surrogate and has been proven comparable in several studies (e.g. Bai & Dent, 2008). It has been proposed that the RUE is able to normalize the inter-annual variability in the NPP which is caused by rainfall

variability and consequently provides an index of degradation that is almost independent of the effects of precipitation (Nicholson, Tucker, & Ba, 1998).

For the north-eastern part of South Africa, Wessels et al. (2007) employed the rain-use efficiency to compare degraded and non-degraded areas. These areas have been selected on the basis of the National Land Cover (NLC) project (Fairbanks, Thompson, Vink, Newby, & Van Den Berg, HM, Everard, 2000). In order to isolate effects of degradation from local variations in soil, terrain etc., he selected comparable degraded and non-degraded test sites on the basis of *Land Capability Units* (for further information see Klingebiel & Montgomery, 1961). For the calculation of the RUE, Wessels worked with the ∑NDVI and rainfall data for the region's growth season. His results show that degraded areas have significantly lower RUE than the non-degraded areas. However, he also pointed out that the RUE strongly correlated with rainfall and cannot be expected to be independent of the effects of precipitation. Thus, RUE had a rather high variability over time and space.

Bai & Dent (2008) based their RUE analysis for South Africa on Wessels' paper and judged that long-term trends of RUE should distinguish between rainfall variability and land degradation. To get around the correlation of RUE and rainfall, they developed a so-called *RUE-adjusted NDVI* which basically masked out the areas where productivity was not determined by rainfall.

In this study, RUE was used as a first indicator for the state and development of the fragments and not for the final conclusion whether a fragment degraded over time or not. Thus and because the whole study area is rather small, further regional selections like Bai & Dent employed have not been used here.

As mentioned before, the EVI was used instead of the NDVI in this study. As Wessels et al. (2007) suggested, not the whole annual sum of the NPP surrogate and annual sum rainfall were used to calculate the RUE, but only the sum of time steps for the growth season. On the basis of the EVI's course of the year, this period was estimated for the City of Cape Town to be between April and September (time steps 8 to 18). The calculation of the RUE was implemented in a program using the Interactive Data Language (IDL). The complete source code of the program can be seen in appendix A.3. Single files for the years 2000 to 2008 of the growth season ∑EVI and the interpolated growth season ∑rainfall were imported from GeoTIFF-Format with the same spatial extent and the same pixel size of 232m. Then the EVI data was rescaled by the factor 0.0001 to get the original values as

described on the web site of the LP DAAC (LP DAAC, 2010). In the results section, the values of the RUE were multiplied again by 100 for a better visualisation, because the original values are very small (around 0.007). Afterwards, the ratio between imported EVI and rainfall was calculated for each year and the result was exported into a GeoTIFF-stack of the nine years. By using a pixel-based approach for the RUE, each pixel can be analysed separately over time and can be compared with others.

Subsequently, the values for the ground truth polygons (GTP) were extracted from the output annual stack, imported into Excel and grouped after the main vegetation type of the polygons. Afterwards, a diagram of the RUE for 2008 comparing the different GTPs was compiled. Since 2008 is the most recent year of the analysis, it is best suited for the comparison with the GTP data from January, 2010. The growth season ∑rainfall was added to the diagram in order to comprise the influence of the rainfall on the interpretation of the RUE.

For the temporal development of the RUE in the study area, the test polygons have been combined after their predominant vegetation type and mean RUE values of these groups have been calculated for each year. Again, the growth season ∑rainfall values were added to the resulting diagram.

Furthermore, statistics about the RUE of 2008 for each fragment were calculated using the function *zonal statistics as table* in ArcGIS. This way, the average RUE of the fragments can be compared among each other.

In a second approach, the difference between each year and its subsequent year was calculated and stacked to an 8-layer 'tendency stack'. This one was averaged for each pixel to get a single mean layer showing the general tendencies over time. At this point, it must be mentioned that I am aware of the fact that analysing a time period of nine years is too short to speak of the term 'trend'. Thus, I did not use the term 'trend' and the term 'tendency' was employed in this study. The tendencies were intended to give an indication of potential developments in the study area, but since the background information about the fragments are rather sparse, they only play a minor role in this study.

Furthermore, the values of the RUE mean tendency were extracted for the GTPs and normalised by the mean RUE of the time series. The results are displayed in a diagram with the mean percentage increase or decrease for the ground truth polygons.

5.1.2 EVI-rainfall Regression

The relationship between biomass and rainfall is an important indicator for the vitality of vegetation and has been analysed with remote sensing (e.g. Fabricante, Oesterheld, & Paruelo, 2009; Li, Lewis, Rowland, Tappan, & Tiszen, 2004). In this work, a linear regression was calculated in order to determine the response of the vegetation to precipitation.

The regression analysis is one of the most flexible and commonly used statistical analysis techniques. It is used to analyse the relationship between a dependent variable and one or more independent variables (Backhaus, Erichson, Plinke, & Weiber, 2008). The regression is especially employed to quantitatively describe and explain relationships and to estimate values of the dependent variable. In this work, the dependant variable will be represented by the EVI data and the independent variable by the rainfall data.

A simple regression for the estimation of the dependent variable is defined as follows (Backhaus, Erichson, Plinke, & Weiber, 2008):

$$\hat{Y} = b_0 + b_1 X \tag{5.1}$$

where:

$\hat{Y}$ = estimation of the dependent variable *Y*

b_0 = constant

b_1 = regression coefficient

X = independent variable

The factors b_0 and b_1 are determined by the method of least squares. Basically, this method assesses a curve in the data scatter plot which minimises the sum of errors in the explanation of the observed points. For detailed information on the method of least squares see Backhaus, Erichson, Plinke, & Weiber (2008).

For the purpose of a linear regression, an IDL program developed by Ursula Geßner (2011) was employed. The linear regression was calculated between the 16-days composites of rainfall as the independent variable and the 16-days EVI composites as the dependent variable (compare figure 5.1). Since the vegetation might need some time to respond with increased growth to the rainfall, different time lags between 0 and 7 time steps (= 16-days composites) were used as well as different rainfall sums. These sums

vary from the concurrent time step up to 7 preceding time steps. The maximum number of lags and sums was chosen on the basis of a past approach by Klein & Roehrig (2006) and due to calculation constraints. Klein & Roehrig (2006) discovered maximum correlations with lags of 1-2 and sums of 5-6 decades (= 10-days composites) for their two test regions in Benin and Kenya. Since Fynbos vegetation predominantly consists of evergreen sclerophyll plants, it cannot be excluded that there might be an annual lag of reaction, e.g. after several dry years, but this was not tested here because the time series is too short for this approach.

The calculations were done for the whole time series from 2000 to 2008 with additional rainfall time steps from 1999 for the sums and lags. In addition, the regression analysis was done for two-year periods with their respective preceding time steps. This way, I wanted to minimise the effect that possible fires or other disturbances could have on the results of the regression of the whole time series, since there are not enough background information to date such events. Thus, particular attention was paid to the most recent time period 2007-2008, to compare it with the ground truth polygons. The output of the used IDL program is a TIFF-file for the coefficient of determination and one for the significance of the regression for each lag and sum combination. Afterwards, the coefficient of determination layers were stacked and their maximum was retrieved for each pixel.

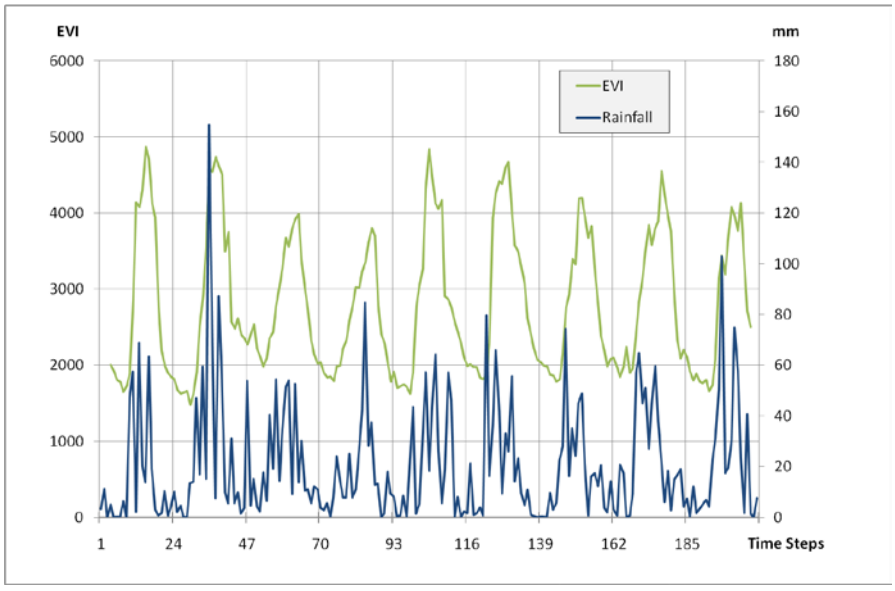

Figure 5.1: Exemplary EVI and rainfall time steps of the used time series (period 2000-2008).

5.1.3 Residual Trends (RESTREND)

Evans & Geerken (2004) developed a method to monitor degradation or improvement of vegetated areas which is independent of the effects of rainfall variability. This method, the so-called residual trends was adopted by Wessels et al. (2007) and Bai & Dent (2008) and shall be used in this work, too. In order to remove the effects of rainfall, the difference between the observed EVI and the linear regression predicted EVI is calculated. These differences between observed and predicted EVI are referred to as residuals (Evans & Geerken, 2004). In order to get trends, the residuals are correlated over time. Wessels et al. (2007) used the paired areas again for the RESTREND method to show the different behaviour for degraded and non-degraded areas. Wessels and also Bai & Dent (2008) found the RESTRENDs to be independent of the effects of rainfall and showed that it can be a good indicator for the monitoring of 'degradation' or more commonly for monitoring changes decoupled from rainfall. According to their results, negative trends indicate 'degradation'; positive trends indicate an 'improvement' of the vegetated area.

In order to calculate the RESTREND in this work, the linear regression from the previous section was used. The IDL program used for the regression also contained a function to compute the residuals and to correlate them over time. The residual trends were only calculated for the whole time series and not for 2-year periods to show trends over the longest period possible. At this point it must be mentioned again that a 9-year period is often not enough to monitor long-term effects and the results have to be treated with caution. However, since remote sensing so far has no longer time series with such a good combination of temporal and spatial resolution, MODIS is often used for the monitoring of phenological trends (e.g. Fensholt, Rasmussen, Nielsen, & Mbow, 2009; He, J. Zhang, & Q. Zhang, 2009). The IDL program also delivers a layer of significance for the residuals of each tested lag and sum combination. Again, this method is pixel based in order to compare local variations which can be aggregated later on.

5.2 Distribution of Invasive Species

The second focus of this work is the distribution of invasive species into Fynbos, in particular the *Acacia saligna* and different Grass species. While these invasive species suppress the local Fynbos vegetation, they have the potential to reduce the biodiversity of the region and consequently degrade the ecosystem health (compare Van Der Wal et al., 2008). Therefore, it is important to establish an early warning system which is able to indicate areas that have been infested with alien vegetation to initiate appropriate measures. The results of this work shall be the basis for such a monitoring system and will give a first overview of the condition of the Fynbos fragments.

In order to delineate the distribution, a knowledge-based threshold method, the ENVI decision tree has been used. Basic statistical measures derived from the vegetation phenology as well as the methods from the previous sections establish the basis for this analysis.

5.2.1 Classification Scheme

The first step towards a suitable classification is a good aggregation of the sampling data. Since the data collected during the field trips is too detailed for a suitable remote sensing classification, it has to be grouped to more appropriate classes. As mentioned above, this part of the study focuses on the delineation of invasive species in order to form the basis for an early warning system for the dispersal of these invasive species within the fragments. Thus, it is sufficient to define three different classes: 'Acacia', 'Fynbos' and 'Grass'. The ground truth polygons (GTP) were distributed manually to these classes according to their predominant vegetation cover (compare appendix A.6). In order to be classified as Acacia, a polygon must have at least 70 % acacia cover. The same applies for Grass with the exception of three polygons where the total vegetation cover was generally low and Grass still the dominant class with only a minor portion of Fynbos or *Acacia saligna* (less than 12.5 %) on it. For the Fynbos class, a fixed threshold was not chosen at all, because intact Fynbos vegetation has a rather high cover of open ground in between. The GTP classified as Fynbos, had a Fynbos cover of at least 34 %, less than 5 % acacia cover and less or equal than 10 % grass cover on them. Polygons that did not

match any of these criteria were marked as 'Mixed' and not taken into account for the classification.

5.2.2 Statistical Measures of the Phenology

Land cover classifications based on satellite imagery utilise the spectral or phenological characteristics to assign a certain class to a pixel. In this approach, these characteristics are derived from the phenological cycle of the vegetation. Figure 5.2 shows an example for a phenological cycle of three GTPs with the corresponding rainfall for the year 2008. Obviously there seem to be some general differences between the three classes concerning the general amount of EVI and the reaction to rainfall. The polygon classified as Acacia seems to have a generally higher EVI with rather strong reactions to the two rainfall peaks while the Fynbos GTP only reacts to the first higher amount of rainfall and then stays on its rather low level of EVI.

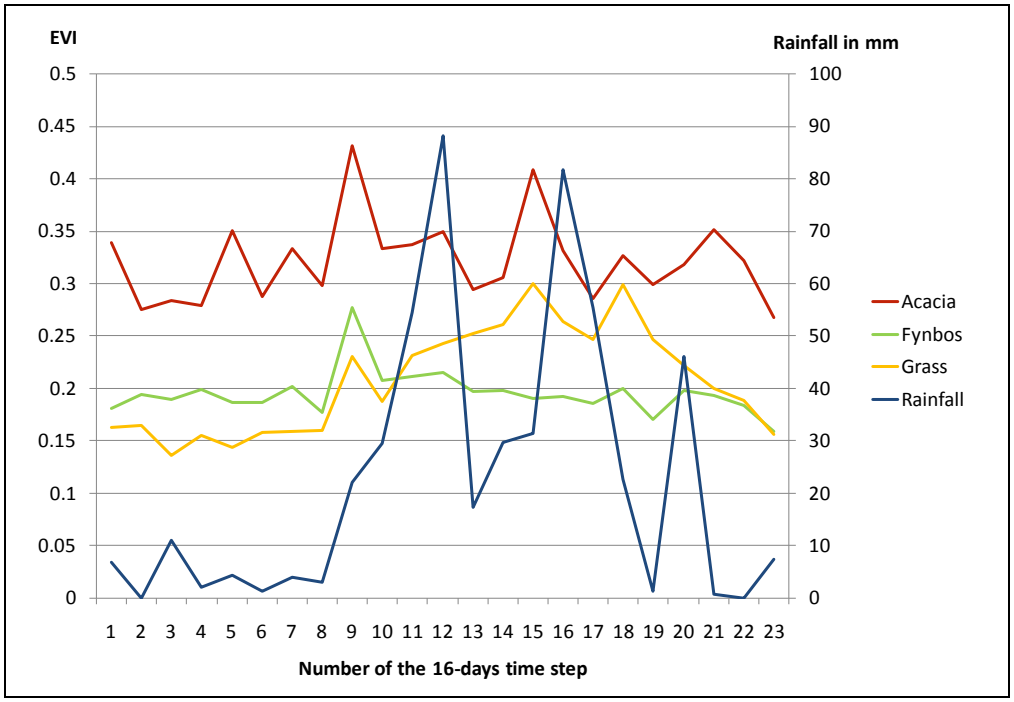

Figure 5.2: EVI phenology of three exemplary ground truth polygons and the corresponding rainfall graph (year 2008).

These differences in the phenological cycle of EVI were analysed for the different classes on the basis of common statistical measures. Using an IDL program compiled by Dr. Doris

Klein, these measures were calculated for each pixel of the study area and each year of the time series:

- Mean annual EVI
- Median of the annual EVI
- Standard deviation of the annual EVI
- Variance of the annual EVI
- Annual sum of EVI
- Minimum of the annual EVI
- Maximum of the annual EVI
- Range of the annual EVI

The statistical measures of the classified GTP were tested for their separability and the best measures were chosen for the delineation of invasive species.

5.2.3 Delineation using the ENVI Decision Tree

The Decision Tree is a tool of the image processing software *ENVI* by ITT. This tool performs a classification based on a series of binary decisions to place pixels into classes (ITT, 2008). Each decision divides the concerned pixels into two new classes using a Boolean expression (compare figure 5.3). It is possible, to split the classes into subclasses as often as necessary. The defined decisions can be simple expression, e.g. “EVI greater 0” or more complex one. After a suitable decision tree is assembled, you can execute it and automatically classify a dataset with the defined expression. The result will be a classified image of the area of interest.

The decision tree developed in this work was based on the statistical measures and the EVI-rainfall regression from the previous sections. The indicators and thresholds were selected on the basis of the values of the ground truth polygons. Afterwards, the indicators with distinct gaps between the classes were chosen for the classification. The indicators used for the decision tree are presented in chapter 6.2.

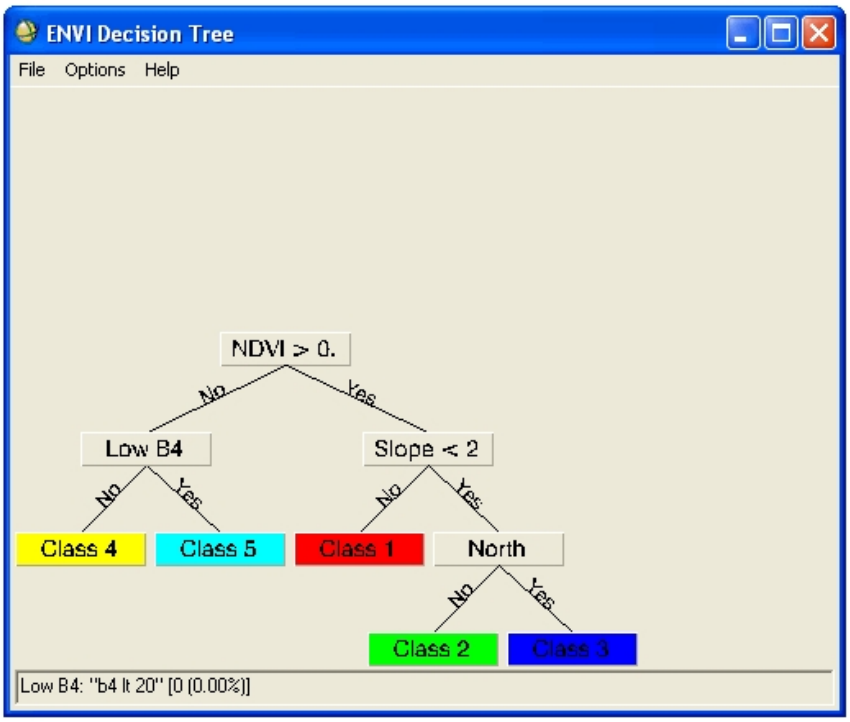

Figure 5.3: Example for an ENVI Decision Tree (ITT, 2008).

6 Results and Discussion

After the presentation of the adopted methods in the previous section, this chapter summarises the results. Furthermore, the results and the suitability of the indicators are displayed.

6.1 Productivity of Vegetation

The methodology for the productivity of vegetation was described in chapter 5.1. The following section presents the results and the corresponding discussion about the usefulness of the indicators.

6.1.1 Rain-use Efficiency

Figure 6.1 shows a general overview of the rain-use efficiency in the study area for the year 2008. The northern part seems to have a generally higher RUE than the southern part, although it has to be considered that the southern part is predominantly city area. Focusing on the northern half, the areas under cultivation (compare figure 4.6) have the highest values with RUEs around 1 and higher (rescaled as mentioned in section 5.1.1 by 100). The vegetated areas, occupy the medium values around 0.6, displayed in lighter colours.

Furthermore, a general comparison of the RUE, 2008 and the precipitation, 2008 (compare figure 4.3) suggests a relation between high (orographic) rainfall and low RUE values. The rainfall values at the foot of the Table Mountain and close to the Cape Fold Belt are very high with low values for the EVI.

The analysis of the RUE of the ground truth polygons (GTP) is shown in figure 6.2 for the year 2008. The diagram only shows the homogenous polygons that are either classified as Acacia, Fynbos or Grass (for the whole list of GTP RUE see appendix A.7). The rainfall values for these polygons were added to the diagram in order to display the relation to local variations of precipitation. A distinct difference in RUE between Fynbos and Acacia can be seen. While the GTPs with Acacia have RUE values over 0.6, Fynbos' values are under 0.6 and range around 0.5 for the same amount of rainfall around 420 mm.

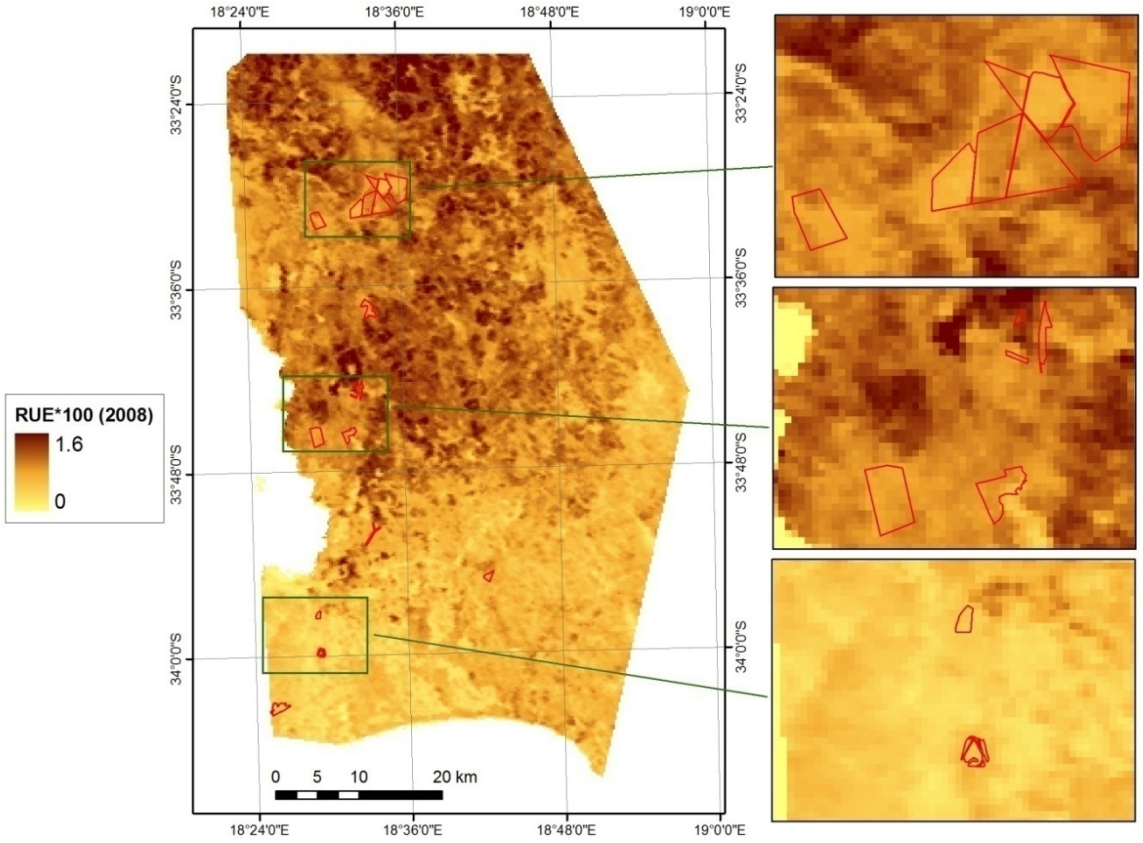

Figure 6.1: Mean annual rain-use efficiency multiplied by 100 (year 2008).

The RUE values for the Grass polygons roC03, roC04 and roC05 are distinctly lower than the three others. Compared with the rainfall graph, it becomes obvious that the rainfall is almost double as much for these Grass GTPs than the rainfall of the other polygons. The Grass GTPs baA08, RLpl08 and RLpl09 have a RUE of about 0.7, which is on the level of Acacia. While the three Grass GTPs with low RUE values lie all on the Rondebosch Common, which is in the southern, dense city area, the other GTPs are all in the northern part of the study area. This discrepancy might indicate that the local variations of rainfall play a major role in the creation of the RUE, although it has to be considered that the northern polygons might still stand under the influence of residual fertiliser or other factors from previous land use.

The temporal development of the RUE in the study area is depicted in figure 6.3. For this purpose, the test polygons have been combined after their predominant vegetation type and mean RUE values of these groups have been calculated for each year. The Grass polygons have been split into the polygons of the north and the ones of the Rondebosch Common in the south in order to show the different influence of precipitation. Thus, two rainfall lines for the north and south have been integrated.

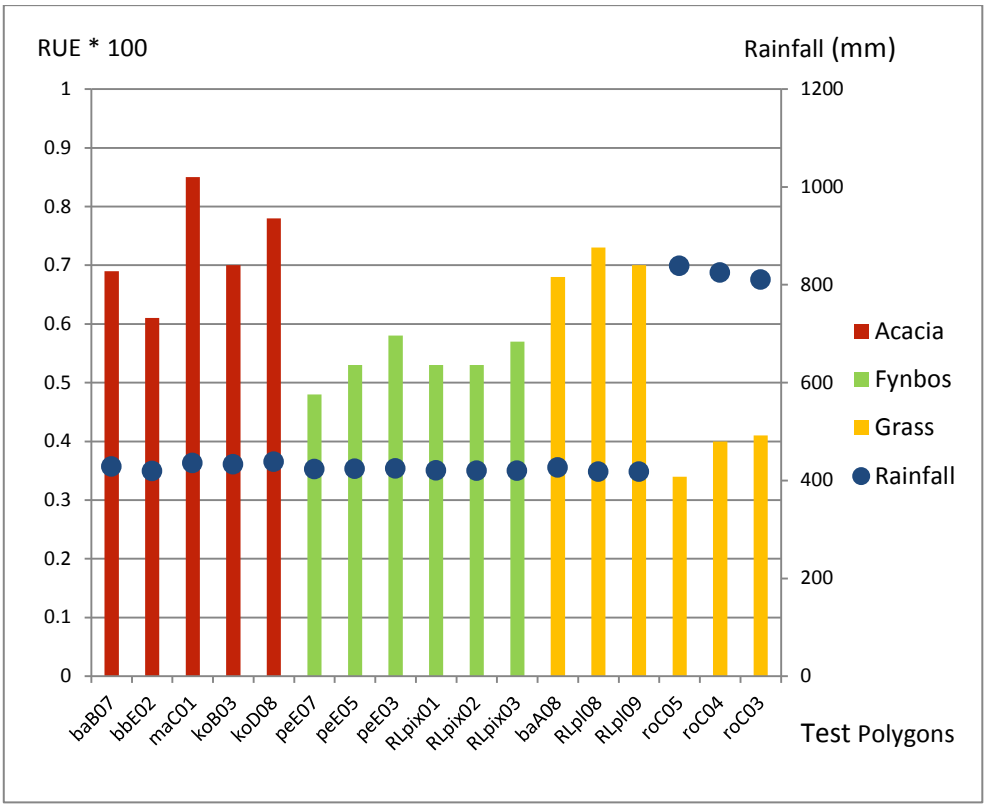

Figure 6.2: Mean annual RUE and rainfall of 17 ground truth polygons (year 2008).

In order to analyse these graphs, one has to assume a certain consistency in the vegetation cover. The RUE of Fynbos seems to be constantly lower than the one of Acacia, which confirms the interpretation of figure 6.2. Only for the first two years, the RUE values are quite similar for these two classes and even a bit higher for Fynbos in 2000. This might indicate a change in vegetation cover of the Fynbos fragments towards the following years. Since 2002, the Fynbos polygons seem distinctly different from the other classes. This could be caused by an initiated management of the Riverlands Nature Reserve, where these polygons are situated. Unfortunately, the obtained management records of these fragments do not go further back than 2004 and thus this hypothesis cannot be confirmed.

The Grass polygons of the north and the ones of the Rondebosch Common in the south display distinct differences. The RUE values for the south are constantly lower. Again, the rainfall seems to play a major role for this difference since the values are significantly higher in the south. Comparing the value of the northern Grass polygons from 2001 and the value from the southern polygons from 2003, where the rainfall was almost the same, the RUE values are similar, too. This confirms the hypothesis that the rainfall is the major reason for the different RUE of the Grass polygons.

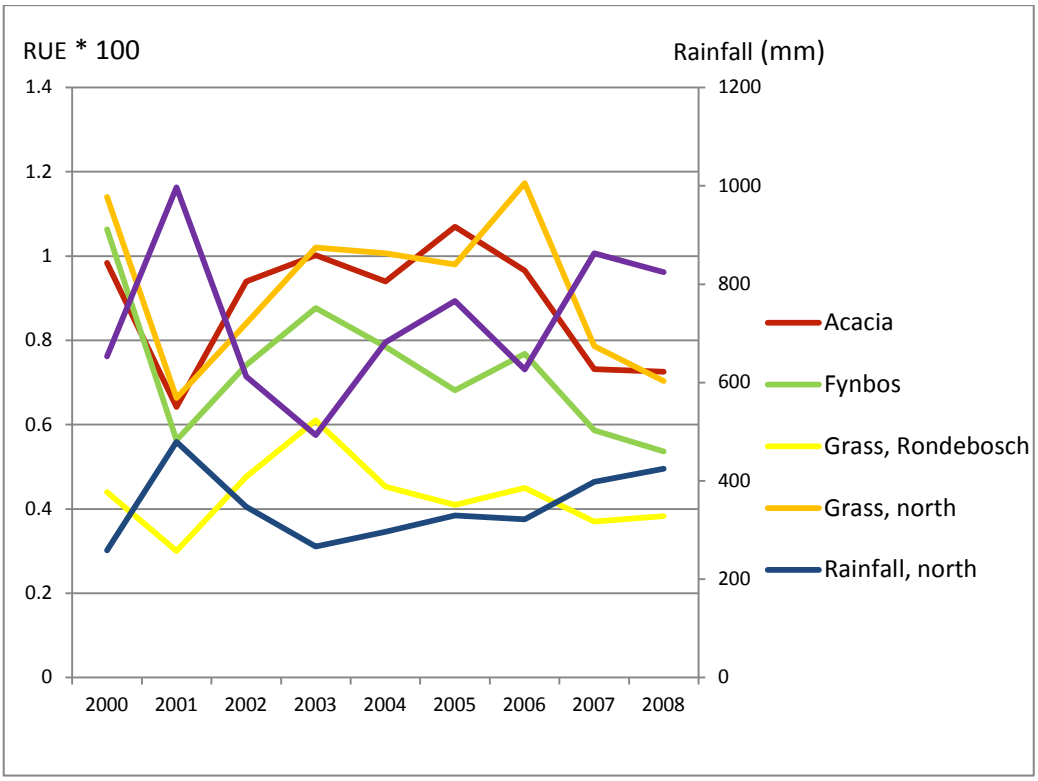

Figure 6.3: Mean annual RUE of combined test polygons over the time series (period 2000-2008).

Focusing on the fragments, zonal statistics of the RUE 2008 were calculated in ArcGIS and can be seen in table 6.1. The fragments are classified after their main vegetation type as far as one predominant type could be assigned from the field trips. The trends are in line with the ones determined with the diagrams of the GTPs. Baasariesfontein and Kohler Bricks were classified as highly infested by *Acacia saligna* and consequently have high mean values of RUE for 2008. On the other hand, the fragments Pella and Riverlands Floodland were defined as Fynbos fragments and occupy rather low mean values of RUE. Again, the grass covered Rondebosch Common has the lowest values of RUE, but as mentioned before has very high precipitation values. In contrast, Riverlands Plain, which is in the northern part of the study area with similar rainfall amounts as the Fynbos and Acacia fragments, has a high RUE value. This discrepancy can be compared to the one between the Rondebosch polygons and the northern grass covered polygons mentioned above. Thus, it seems that in years with sufficient rainfall, grass is as rain-use efficient as the acacia.

Figure 6.4 shows the mean tendencies of the RUE over the whole time series from 2000 to 2008. In general, almost the whole study area has positive tendencies, while the ones

Table 6.1: Zonal RUE statistics of the fragments (year 2008).

Fragment Name	Predominant Vegetation Type	Mean RUE * 100	Stdv. of RUE*100
Baasariesfontein	Acacia Saligna	0.7963	0.1278
Kohler Bricks	Acacia Saligna	0.6499	0.0868
Pella	Fynbos	0.5577	0.0515
Riverlands Floodland	Fynbos	0.5907	0.1147
Rondebosch Common	Grass	0.3450	0.0328
Riverlands Plain	Grass	0.6829	0.0970
Mamre	None	0.6633	0.0723
East Blaauwberg Conservation Area	None	0.6591	0.0412
Tokai State Forest	Pine Forest	0.4047	0.0261
Kenilworth Race Course	None	0.4128	0.0253
Plattekloof	None	0.5892	0.0434
Haasendal	None	0.6334	0.0583
Schoongezicht Farm	None	0.7273	0.1071
Riverlands 4	None	0.7439	0.0653
Riverlands 5	None	0.7411	0.0892
Riverlands 6	None	0.6790	0.0659

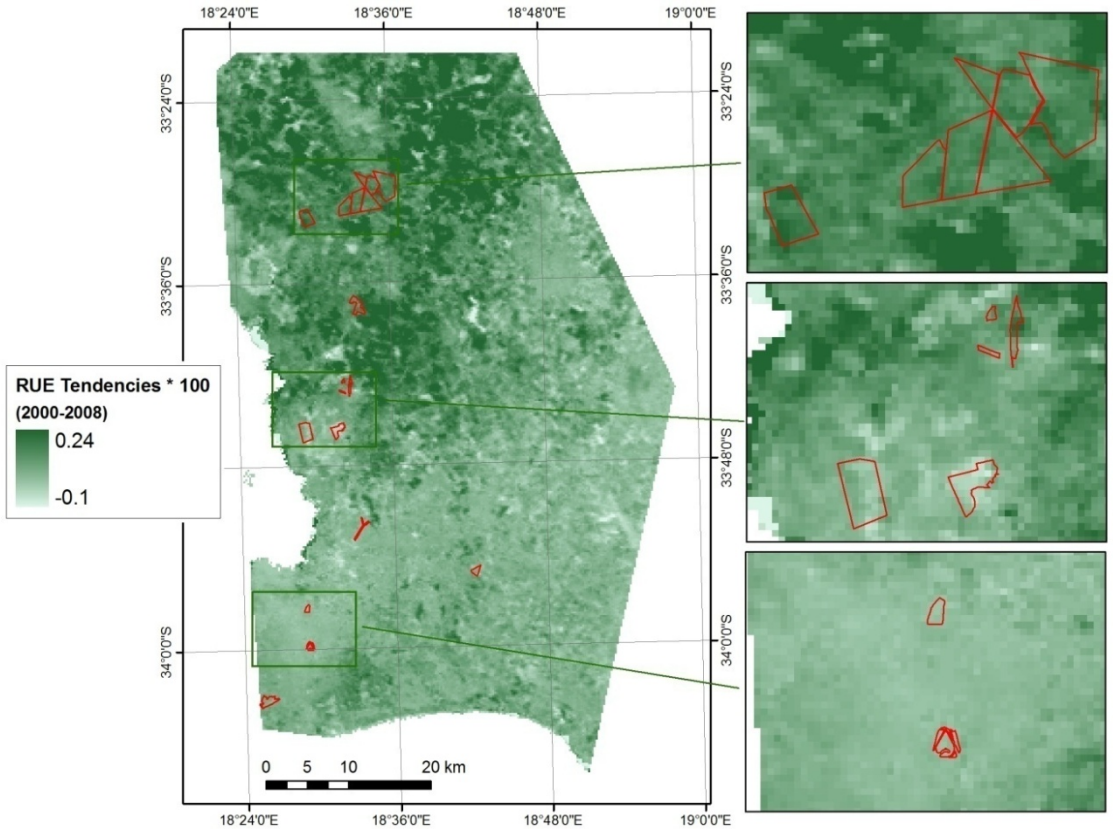

Figure 6.4: RUE tendencies multiplied by 100 (period 2000-2008).

in the north are higher than the ones in the south. The common distribution of the values strongly resembles the distribution of the RUE values in figure 6.1. Thus, cultivated areas have the highest values with tendencies of about +0.1 and naturally vegetated areas occupy medium values of around +0.07. Furthermore, the fragments in the north display higher values than the ones in the south.

The mean tendencies of the GTPs can be seen in figure 6.5 as percentage increase or decrease, relative to their mean RUE over the time series. The Fynbos classified GTPs show a similar trend with at least 8 % increase of RUE. RLpix03, a polygon of the Riverlands Floodland, even has a mean tendency of 10.7 %. The Acacia polygons do not show any general trend. While the Kohler Bricks polygon koD08 has a small decrease, the Mamre polygon maC01 has a strong increase of 10.5 %. The three Grass polygons of the southern Rondebosch Common with its generally high rainfall values exhibit rather low positive tendencies and the three Grass GTPs of the north have values around 6.0 %.

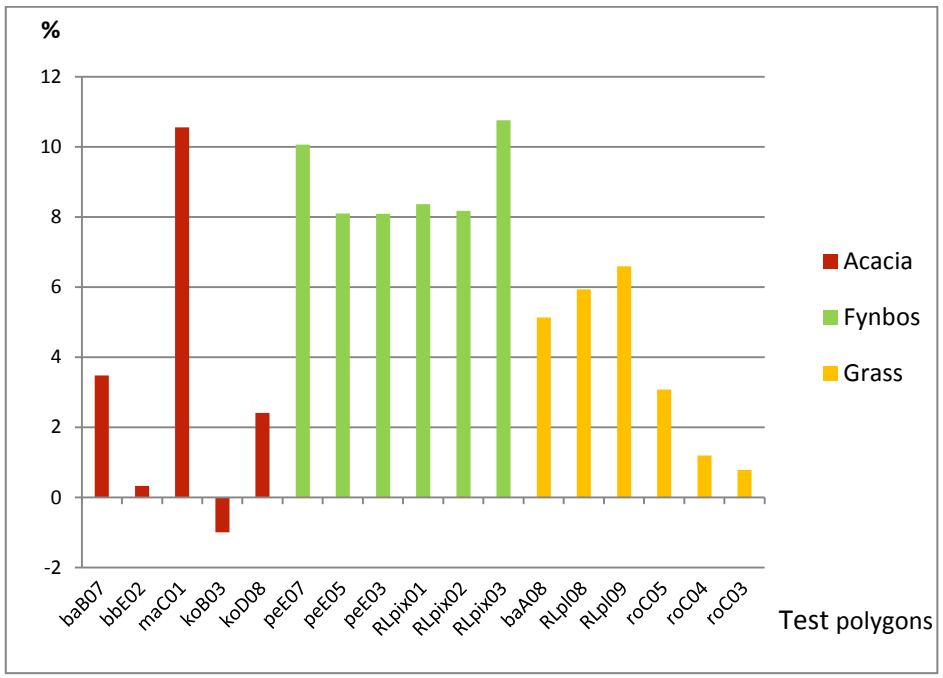

Figure 6.5: RUE tendencies for 17 ground truth polygons (period 2000-2008).

Like Wessels et al. (2007) suggested, the rain-use efficiency is still highly influenced by local and temporal variability of rainfall. Thus, the interpretation is difficult.

Despite the fact that local variations of the RUE occur in the study area, the analysis of the ground truth polygons showed differences between invasive vegetation and the

inherent Fynbos vegetation. The Fynbos vegetation has constantly lower values than acacia and grass covered areas. It seems as if Fynbos cannot express a higher availability of water in higher values of EVI, i.e. in a higher biomass production. This might result from the adaption of Fynbos to the generally dry conditions of the study area.

The different RUEs for the Grass polygons of the north and south, i.e. the Rondebosch Common indicate that grass has a certain water saturation threshold over which more rainfall does not lead to any more biomass production. It must be mentioned that this difference could also result from different states of the fragments caused by different land use in the past. However, the fairly similar RUE values of the compared regions for the years 2001 and 2003 in figure 6.3 and the generally good condition of the protected Rondebosch Common support this hypothesis.

The analysis of the vegetation fragments shows the same trends as the one of the ground truth polygons. Because of the high local precipitation variability in the study area due to the surrounding mountains, only fragments of the same region within the study area can be compared. For those, the same rule applies namely that acacia and grass covered fragments in 2008 with a normal amount of rainfall have higher RUE than the fragments with an intact Fynbos cover.

Thus, the analysis of the RUE implies, that an increased RUE for years with average rainfall indicates a degradation, i.e. an invasion of the Fynbos fragments by *Acacia saligna*.

The interpretation of the RUE tendencies is rather difficult. Since information about the general development of the fragments or management measures is insufficient, there are too many variables that influence the RUE tendencies, also including the rainfall variability.

The GTPs with intact Fynbos exhibited a quite homogenous positive tendency but it would be too vague to conclude that these polygons improved over the time series since the RUE of Fynbos strongly depends on the amount of rainfall. Furthermore, the GTP of Mamre with a currently high acacia cover had a high positive tendency too, which does not allow the establishing of a general rule.

6.1.2 EVI-rainfall Regression

As mentioned in section 6.1.2, the EVI-rainfall regression was conducted over the whole time from 2000 to 2008 and for 2-year periods. Figure 6.6 shows a general overview of the maximum coefficient of determination detected in the study area for the period 2007 - 2008. As expected, the urban area in the south has commonly rather low R^2 values, while the agricultural areas of the north give very high values of over 0.7 (displayed in dark blue). At first glance, the potentially natural areas, exhibit low values of R^2 with almost no correlation of EVI with rainfall in some parts in the north and east of the study area.

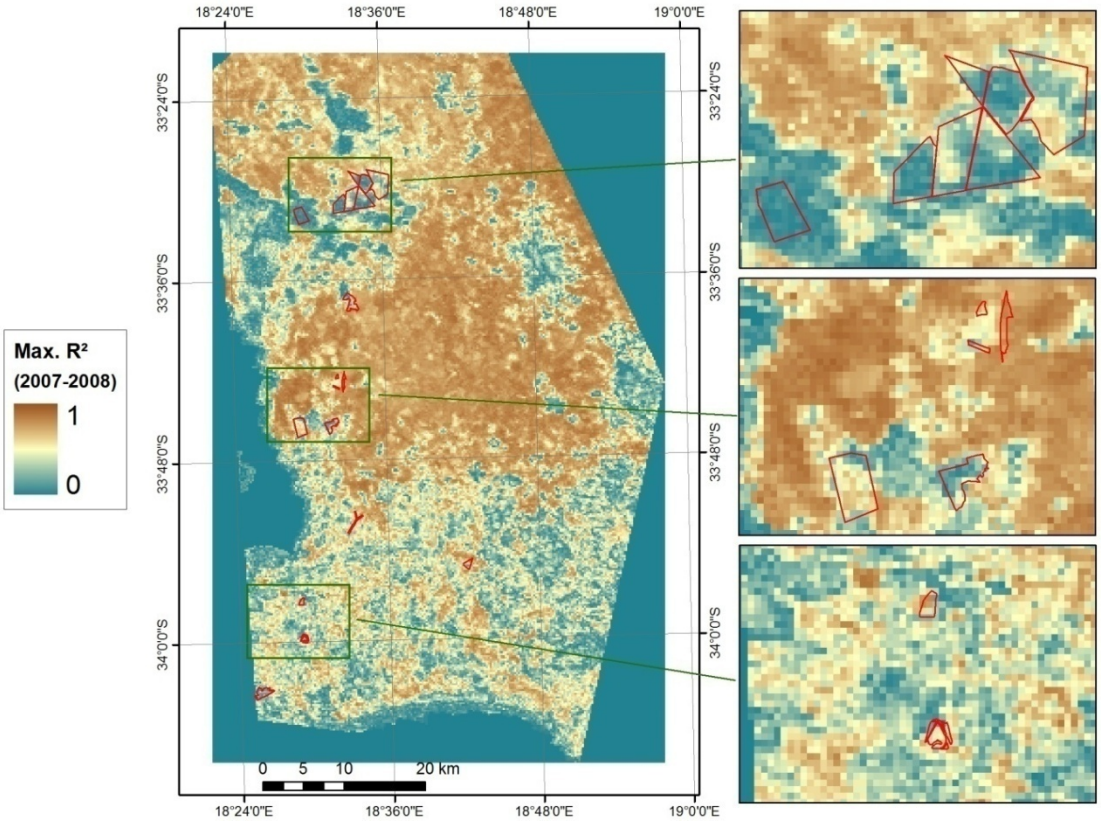

Figure 6.6: Maximum R^2 of the EVI-rainfall regression (period 2007-2008).

The ground truth polygons extracted from the regression of 2007 to 2008 are not as homogenous within the classes as the RUE of 2008 (compare figure 6.7). The Acacia exhibits medium values of 0.49 and 0.39 for the polygons of Baasariesfontein and the one of Kohler Bricks while the second polygon of Kohler Bricks and the two from Mamre and Blaauwberg show R^2 values lower than 0.2. The polygons from Pella and Riverlands

Floodland classified as Fynbos display uniformly very low values around 0.1 R^2. Only the third polygon of Riverlands Floodland has a value of about 0.2. Altogether, these values indicate no significant correlation for Fynbos between rainfall and EVI. The Grass polygons reach the highest values of the naturally vegetated areas. The Rondebosch Common has two polygons with values over 0.75 and one polygon of about 0.42. The Grass polygon situated on Baasariesfontein displays a medium value of 0.39 R^2 while the two polygons from Riverlands Plains show rather high values around 0.65 R^2. The coefficients of determination for the Grass polygons are high enough to identify a close connection between rainfall and the EVI as it could be expected from the results of the RUE.

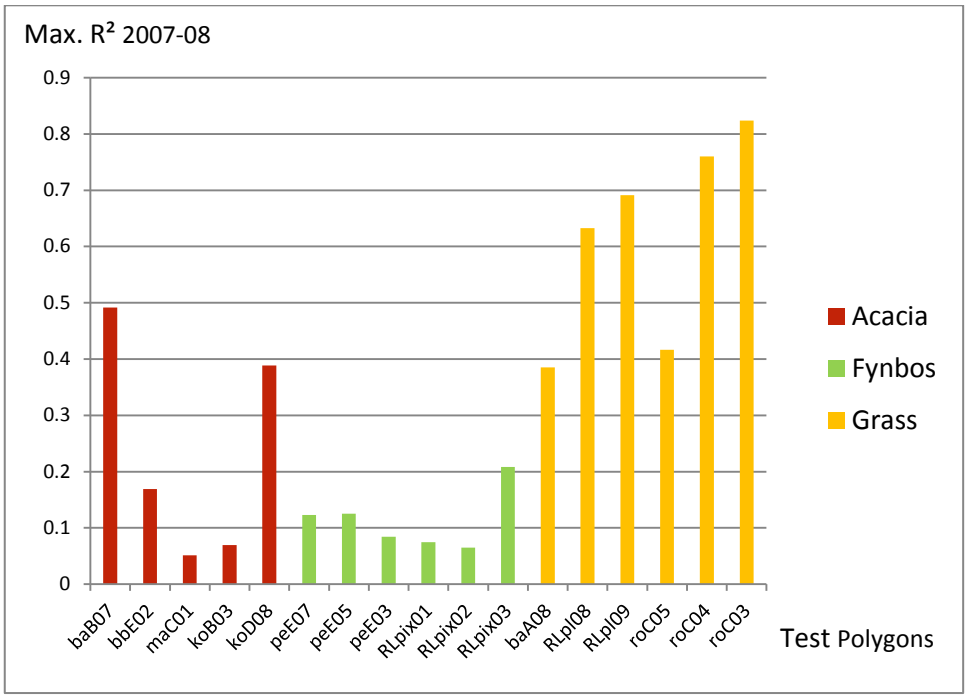

Figure 6.7: Maximum R^2 of the EVI-rainfall regression of the 17 ground truth polygons (period 2007-2008).

The aggregation of the polygon values into zonal statistics of maximum coefficient of determination is displayed in table 6.2 for the fragments. The areas classified as Acacia again show a major inconsistency. While Baasariesfontein has a high average R^2 value of 0.7, Kohler Bricks obtains a rather low value of about 0.25. On the other hand, the two Fynbos fragments Pella and Riverlands Floodland hold low average values of 0.13 and 0.16. The two fragments classified as Grass, Rondebosch Common and Riverlands Plain, show medium R^2 values of 0.39 and 0.38. Furthermore, the Mamre fragment has a very

low coefficient of determination with a very low standard deviation, indicating a homogenous appearance. Mamre actually has a diverse vegetation cover with regions of high acacia percentage but also regions with intact Fynbos vegetation. An aggregation of the vegetation cover and its associated values for this fragment obscures the infestation with *Acacia saligna*.

Table 6.2: Zonal statistics of R^2 of the vegetation fragments (period 2007-2008).

Fragment Name	Predominant Vegetation Type	Mean R^2	Stdv. of R^2
Baasariesfontein	Acacia Saligna	0.70	0.14
Kohler Bricks	Acacia Saligna	0.25	0.15
Pella	Fynbos	0.13	0.11
Riverlands Floodland	Fynbos	0.16	0.12
Rondebosch Common	Grass	0.39	0.23
Riverlands Plain	Grass	0.38	0.17
Mamre	-	0.05	0.03
East Blaauwberg Conservation Area	-	0.48	0.17
Tokai State Forest	Pine Forest	0.17	0.09
Kenilworth Race Course	-	0.42	0.20
Plattekloof	-	0.51	0.20
Haasendal	-	0.44	0.24
Schoongezicht Farm	-	0.46	0.26
Riverlands 4	-	0.29	0.14
Riverlands 5	-	0.19	0.16
Riverlands 6	-	0.19	0.16

The second step was to apply the regression between EVI and rainfall to the whole time series in order to display changes between 2000 and 2008. The general overview of the maximum coefficient of determination for this time period does not show major differences from the one of 2007 to 2008, although the values seem commonly a bit lower (compare figure 6.8).

The ground truth polygons for 2000 to 2008, visible in figure 6.9, present the same trend as the first overview indicated: a generally lower R^2, but with more or less the same appearance for the different vegetation types. The GTPs of acacia differ from 0.09 R^2 for the Mamre polygon to 0.38 R^2 for the southern polygon of Kohler Bricks. The Fynbos polygons again have a commonly low coefficient of determination, although the polygon peE03 from Pella and not RLpix03 has the highest value with 0.19 R^2 for the whole time series. The appearance of the Grass polygons is the same as for the 2007 – 2008 period

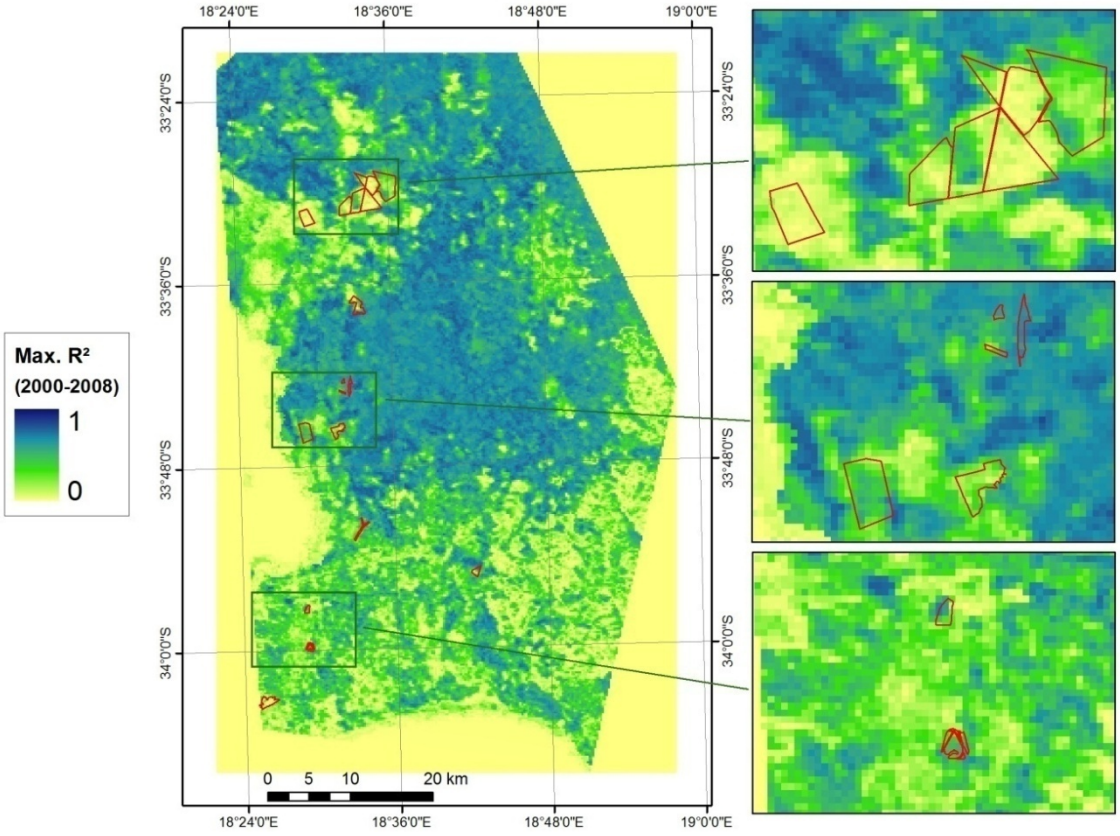

Figure 6.8: Maximum R^2 of the EVI-rainfall regression (period 2000-2008).

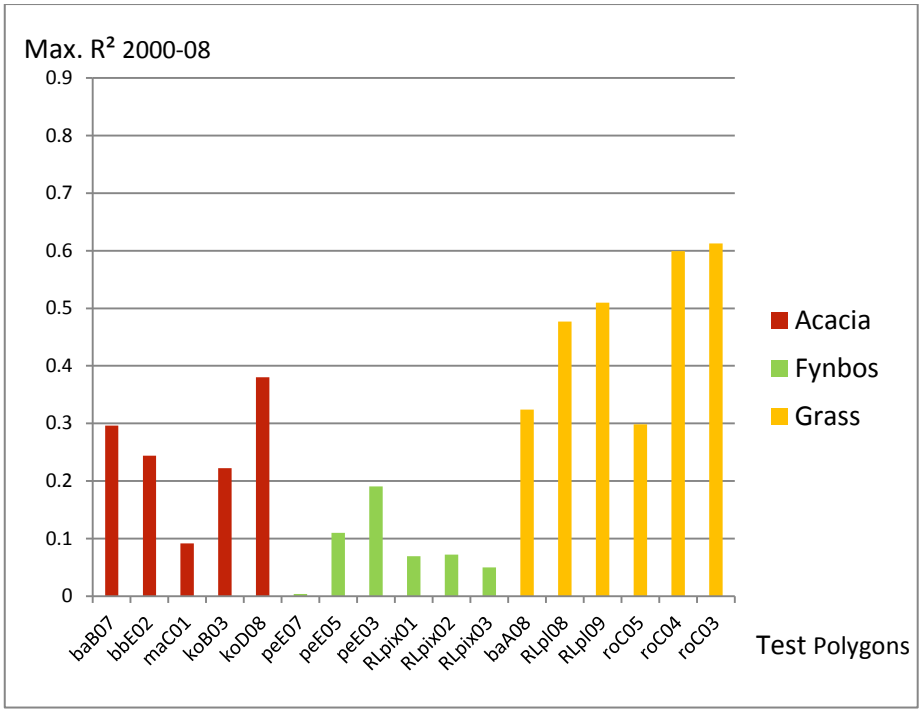

Figure 6.9: Maximum R^2 of the EVI-rainfall regression of the 17 ground truth polygons (period 2000-2008).

with high values for the Rondebosch and the Riverlands Plains polygons roC04, roC03, RLpl08 and RLpl09 and medium values for roC05 and the polygon baA08 from Baasariesfontein.

The zonal statistics of the fragments for the whole time series from 2000 to 2008 are presented in table 6.3. The R^2 values for the two Acacia fragments are very similar to the ones of the 2007 -2008 time period with a comparatively high coefficient of determination for Baasariesfontein and a lower one of 0.25 R^2 for Kohler Bricks. In contrast, the Fynbos fragments differ a bit from the 2-year period: Pella has a higher value of 0.2 R^2 while the one from Riverlands Floodland is slightly lower with 0.09 R^2. The fragments covered with grassy vegetation show slightly lower values than for the 2-year period, but both over 0.3 R^2. The diverse fragment of Mamre again has a very low R^2 value with a very low standard deviation.

Table 6.3: Zonal statistics of R^2 of the vegetation fragments (period 2000-2008).

Fragment Name	Predominant Vegetation Type	Mean R^2	Stdv. of R^2
Baasariesfontein	Acacia Saligna	0.62	0.08
Kohler Bricks	Acacia Saligna	0.25	0.11
Pella	Fynbos	0.20	0.13
Riverlands Floodland	Fynbos	0.09	0.10
Rondebosch Common	Grass	0.32	0.17
Riverlands Plain	Grass	0.31	0.14
Mamre	-	0.05	0.02
East Blaauwberg Conservation Area	-	0.43	0.12
Tokai State Forest	Pine Forest	0.10	0.06
Kenilworth Race Course	-	0.44	0.12
Plattekloof	-	0.43	0.17
Haasendal	-	0.38	0.24
Schoongezicht Farm	-	0.41	0.22
Riverlands 4	-	0.27	0.18
Riverlands 5	-	0.09	0.11
Riverlands 6	-	0.20	0.15

The EVI-rainfall regression confirms what the results of the RUE already indicated: The photosynthetic activity of undisturbed Fynbos vegetation seems not particularly dependant on annual rainfall. Due to its adaption to the low nutrient conditions, Fynbos vegetation is unable to respond to higher rainfall with more growth since nutrients are not available to support additional growth of photosynthetic material. On the other hand,

the grassy vegetation strongly depends on rainfall, which takes shape in the highest R^2 values of the fragments. The Acacia polygons do not present a homogenous trend for the interpretation. While some of them highly correlate with rainfall, others have rather low coefficients of determination. In order to explain these characteristics, one has to analyse them separately. The polygon from Baasariesfontein (baB07) has a rather high R^2 value of 0.49 for the 2-year period from 2007 to 2008 and a relatively high value for the whole time series with 0.3 R^2. Since the shape of the fragment is rather long and narrow (at some points less than 250m) and it is surrounded by intensive agriculture, neighbouring effects could occur for this fragment. This means that the high EVI and thus the high EVI-rainfall regression of the surrounding farmland affect the signal of the polygons of Baasariesfontein. The relatively high correlation of the southern polygon from Kohler Bricks (koB03) in comparison to the northern one (koD08), could be caused by a certain grass fraction of 18 % on the fragment. But since the information about the management measures and development of the fragments is insufficient, it is not assured what the 'normal' characteristics of *Acacia saligna* would be concerning the EVI-rainfall regression. Most likely, the correlation of *Acacia saligna* with rainfall (uninfluenced by e.g. neighbouring effects) lies somewhere between the one of Fynbos and Grass.

The very low homogenous correlation of the Mamre GTP and the corresponding fragment seems rather confusing at first glance since its vegetation cover has high local differences with dense areas of *Acacia saligna* and young but intact Fynbos areas. The explanation could be the heavy grazing that takes place on this fragment. The reportedly high number of livestock, especially pigs, sheep and goats on the Mamre fragment indicate an overgrazing of the fragment. During the rainy season, this would cause an uncoupling between EVI and rainfall in the measuring progress. Furthermore a fire in 2009 was recorded for the fragment, but no exact extent or location on the fragment (compare appendix A.4).

The interpretation of the whole time series is difficult once again since detailed background information is missing. The changes within the Fynbos polygons for the 2-year period compared to the whole time series seem major, but considering that all these values lie at 0.2 R^2 or underneath, there is just no real relationship between rainfall and productivity for both periods and hence the analysis of the differences is difficult but also unnecessary.

The analysis of the regression indicated that a higher coefficient of determination is closely connected with a change in vegetation cover from indigenous to invasive species, although certain issues that affect the signal of the polygons have to be considered. Thus, the regression can be a good indicator for the delineation of degraded, i.e. invaded areas.

6.1.3 RESTREND

As mentioned in section 5.1.3, the residual trends were only calculated on the basis of the regression for the whole time series and not for shorter time periods like the regression itself. Figure 6.10 shows the mean significance of the residual trends computed by the IDL program. The RESTREND is significant only for small areas, which could be expected after the results of the regression. Some parts of Kohler Bricks and Blaauwberg have significant RESTREND values, but altogether the residual trends are not consistent enough for an interpretation. In addition, some agricultural areas show high enough significance to work with but they are not of interest in this study.

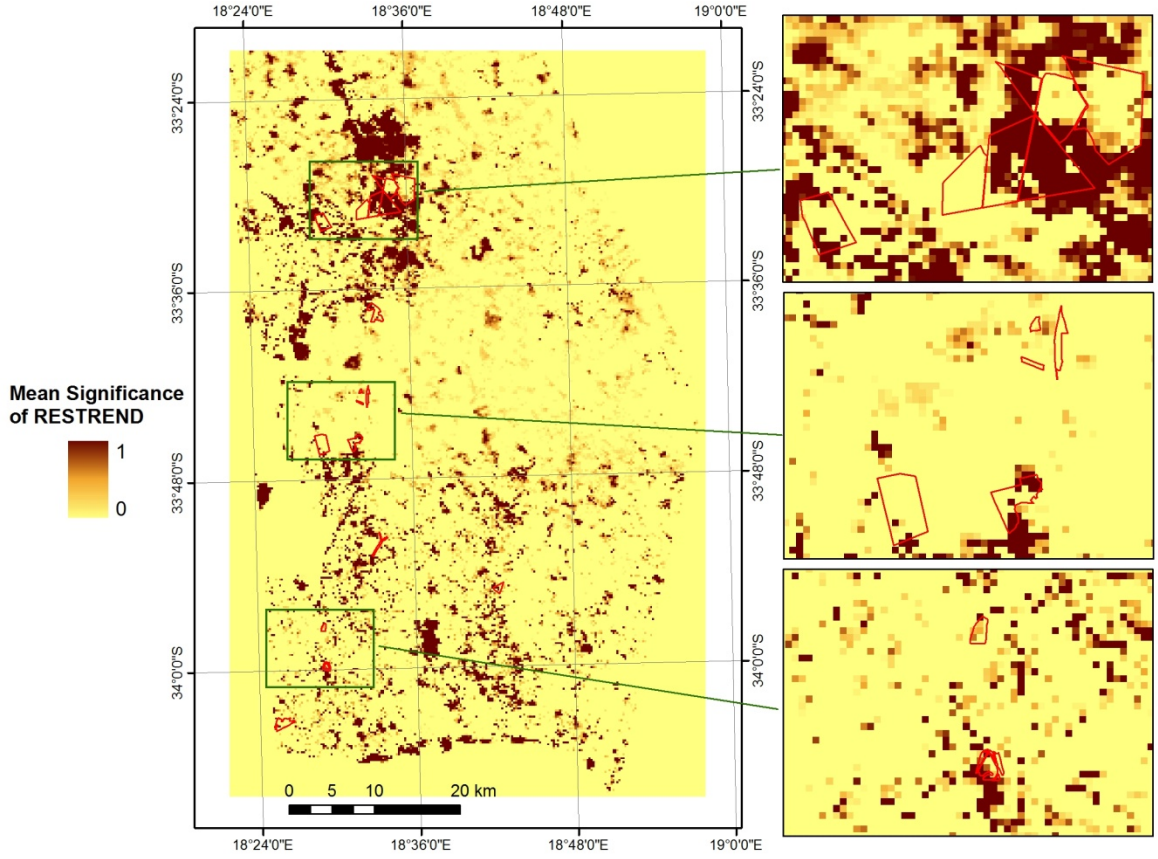

Figure 6.10: Mean significance of the residual trends (period 2007-2008).

Although it proved to be a useful indicator for degradation of rangelands for Wessels et al. (2007), the results of the RESTREND display that this is not a suitable method for Fynbos vegetation. With very low correlations, the Fynbos vegetation cannot show any significant trends for the RESTREND method. It could be more useful to analyse the annual regression and the resulting residual trends instead of the seasonal regression but the time series of nine years is too short for this approach. This might be a possibility in some years, when the MODIS time series has reached a reasonable length, provided that the sensor is working long enough.

However, the different indicators of productivity presented in this chapter all point to the same conclusion: high biomass production of the tested fragments does not stand for Fynbos vegetation but rather for the infestation with invasive species such as *Acacia saligna* or different grass species. Thus, their distribution shall be delineated in the following chapter.

6.2 Distribution of Invasive Species

As mentioned during the methodology in chapter 5.2, the second aim of this work is to determine the distribution of invasive species, especially *Acacia saligna* and different Grass species. These species are one of the most important factors regarding ecosystem health in this region and have to be analysed.
In the following, the results of the different statistical measures of the vegetation phenology are presented and discussed and subsequently the delineation of the invasive species using the ENVI Decision Tree.

6.2.1 Statistical Measures of the Phenology

The statistical measures of the EVI have been calculated for every year and the values for the ground truth polygons (GTP) were extracted afterwards. Because of the temporal proximity to the ground truth data, the focus lies on the EVI of the year 2009. Figure 6.11 till 6.14 show the statistical EVI values of the different classified GTPs for the year 2009.

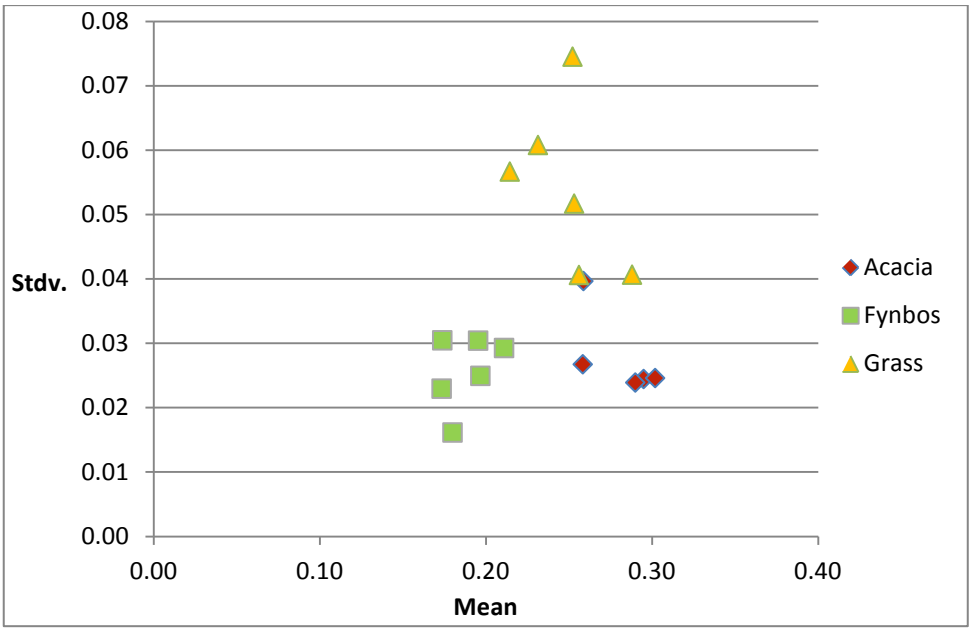

Figure 6.11: Standard deviation and mean EVI of 17 ground truth polygons (year 2009).

Figure 6.11 depicts the mean EVI and its standard deviation of 2009 for the 17 GTPs. At first glance, the separability of Fynbos vegetation is obvious with a quite homogenous appearance. Its mean EVI values lie around 0.19 and thus Fynbos has the lowest values of the GTPs. The standard deviation for Fynbos is also rather low with values from 0.016 to 0.034, the 6 GTPs lie close together. The Acacia classified polygons exhibit generally higher mean EVI values between 0.25 and 0.3. The standard deviation of this class is quite homogenously low at 0.025 except for one outlier at 0.04 stdv. from Kohler Bricks. The grass covered polygons obtain medium values of mean EVI around 0.25 in a wider range than Acacia or Fynbos. The standard deviation of Grass is very high with at least 0.04 and the values even range up to 0.075 which indicates a high seasonal variability of EVI for grass.

Figure 6.12 shows the median and coefficient of variation (CV) of the EVI for 2009. Again, the Fynbos polygons are clearly separated from the other two classes. As expected, the median of EVI is similar to the mean and thus it is not discussed any further. Acacia shows the lowest CV values with about 0.08 with a rather low range up to 0.15. The polygons classified as Grass obtain quite high values but with a relatively wide range from 0.2 to 0.29. The CV for Grass also ranges widely from medium values around 0.14 up to the top value for the GTPs at 0.295.

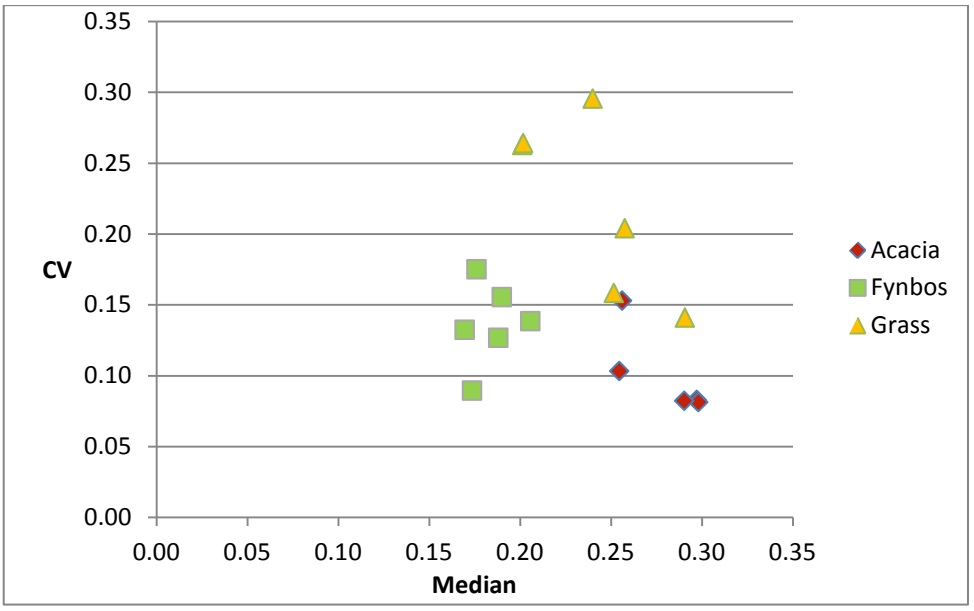

Figure 6.12: Coefficient of variation and median EVI of 17 ground truth polygons (year 2009).

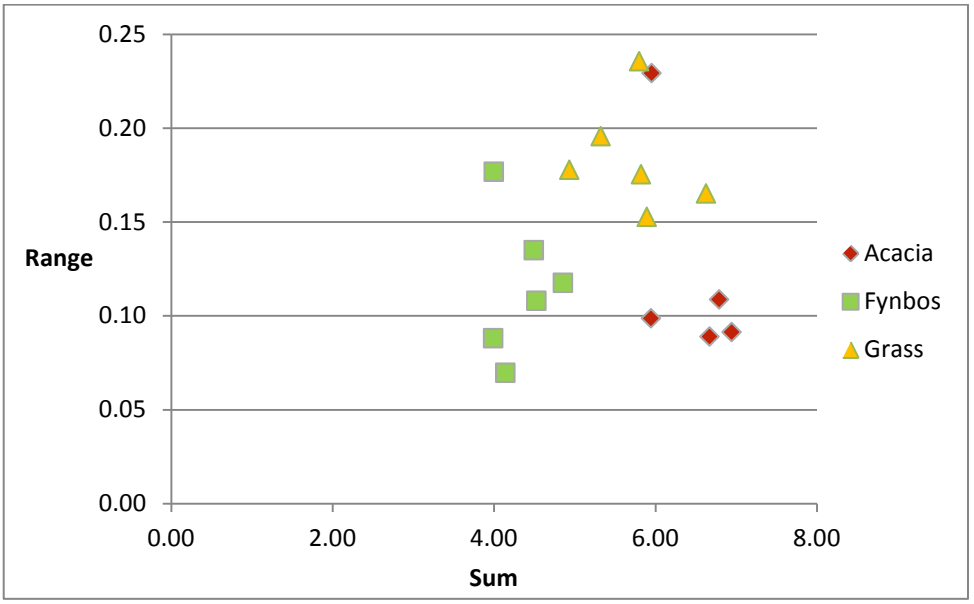

Figure 6.13: Range and sum EVI of 17 ground truth polygons (year 2009).

In figure 6.13, the relation between the annual sum of EVI and the range of EVI values over the course of the year can be seen for 2009. The sum of EVI is directly comparable to the mean EVI, since the basis for the mean is constantly 23 time steps. For this reason the relations between the GTPs are the same and it is not discussed any further from this point. The range of possible EVI values differs rather widely for Fynbos. While the polygon RLpix02 from Riverlands Floodland has a very low range of 0.07, the polygon from the same fragment, RLpix01 has a rather high value of 0.18. On the other hand, Acacia has a

rather low range around 0.1 with one very high outlier, the polygon from Kohler Bricks again, at 0.23. Grass exhibits a generally high range between 0.15 and the top value of 0.236 which corresponds with high values of the EVI's standard deviation.

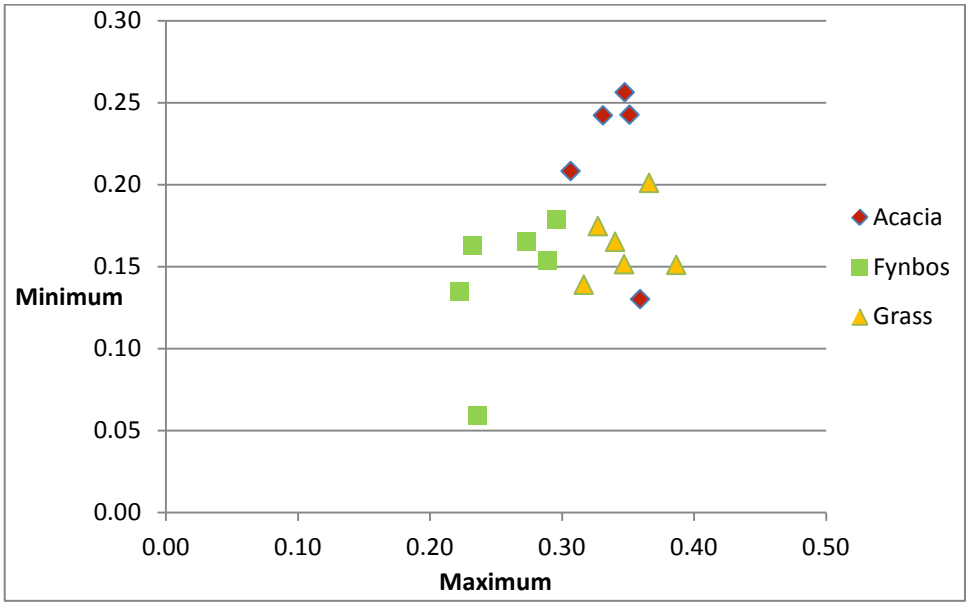

Figure 6.14: Minimum and maximum EVI of 17 ground truth polygons (year 2009).

The last of the four diagrams in figure 6.14 presents the relation between maximum EVI and minimum EVI for 2009. The maximum EVI for Fynbos vegetation is very low with values between 0.22 and 0.30. The minimum EVI is on a medium level with 0.16 for Fynbos except for one very low outlier at 0.06 which is the polygon from Riverlands Floodland RLpix01 again. The reason for such a low minimum could be something like a small local fire and would also explain the high range of EVI for this polygon. However, it seems to be an exception and is not considered any further. The maximum values for Acacia are all higher than for Fynbos and range between 0.31 and 0.36. Its minimum EVI is the highest of the three classes around 0.23, but the polygon from Kohler Bricks is an outlier again with a rather low value of 0.13. Again, a small local fire could be the explanation for this phenomenon, but cannot be verified with background information. Compared to the other two classes, the Grass polygons are rather homogenous for both indicators. The maximum values range from 0.32 to 0.39 and the minimum EVI values for Grass vary between 0.14 and 0.20.

The characteristics of the different classes become clear with the analysis of the phenology of the EVI. Since Fynbos vegetation has a rather low photosynthetic activity and is not dependent on seasonal rainfall variability, it has a very constant but low EVI. That results in low values for mean and median EVI. The more or less unchanged appearance of the plants over the course of the year causes a low standard deviation. However, the range of possible EVI values over the course of the year differs rather widely between the different Fynbos polygons, which could be caused by a different vegetation composition. The polygons from Riverlands Floodland for example have a considerably higher cover of Restionaceae than the ones from Pella. Further research would be necessary to understand the influence of the different vegetation compositions on the EVI in Fynbos vegetation.

The grass covered polygons present a high seasonal variability of EVI. Since the local grassy vegetation is not evergreen but has a strong greenness during the winter months, a high standard deviation and range of EVI is the result. This strong greenness also explains the high maxima of EVI during the year. In short, almost all of the statistical measures express the dynamic of pure grass vegetation in the study area.

In contrast to the grass vegetation, the *Acacia saligna* is an evergreen plant which results in high mean and median values. The standard deviations for the Acacia polygons are rather low and express the constant appearance over the course of the year. Similar to Fynbos, the Acacia is adapted very well to the low nutrient conditions of Fynbos soils, but has a higher biomass production and thus higher minima and maxima of EVI.

As mentioned above, certain outliers of the classes could be explained by small local fires but since the background information about these regions is rather poor, these fires cannot be confirmed and one can only conjecture about the reasons. Despite this, the statistical measures reflect typical characteristics of the different vegetation types and therefore a delineation of the invasive species should be possible on their basis.

6.2.2 Delineation using the ENVI Decision Tree

As mentioned in the previous chapter, several indicators could have been used for the delineation of invasive species. But since the Decision Tree is a simple threshold method only the ones that seemed to be the most useful were integrated in the tree. Figure 6.15 displays an overview of the statistical measures analysed in the previous chapter with the

additional maximum coefficient of determination from the period 2007 – 2008. This diagram has standardised values in order to make the different units comparable. It depicts the mean values of the different indicators and shall give a first impression which one might be more useful for the Decision Tree than others. Under consideration of the range of possible values for the different indicators and their classes, three have been chosen for the decision tree:

The maximum coefficient of determination for 2007-2008, the mean EVI of 2009 and the standard deviation of EVI for 2009.

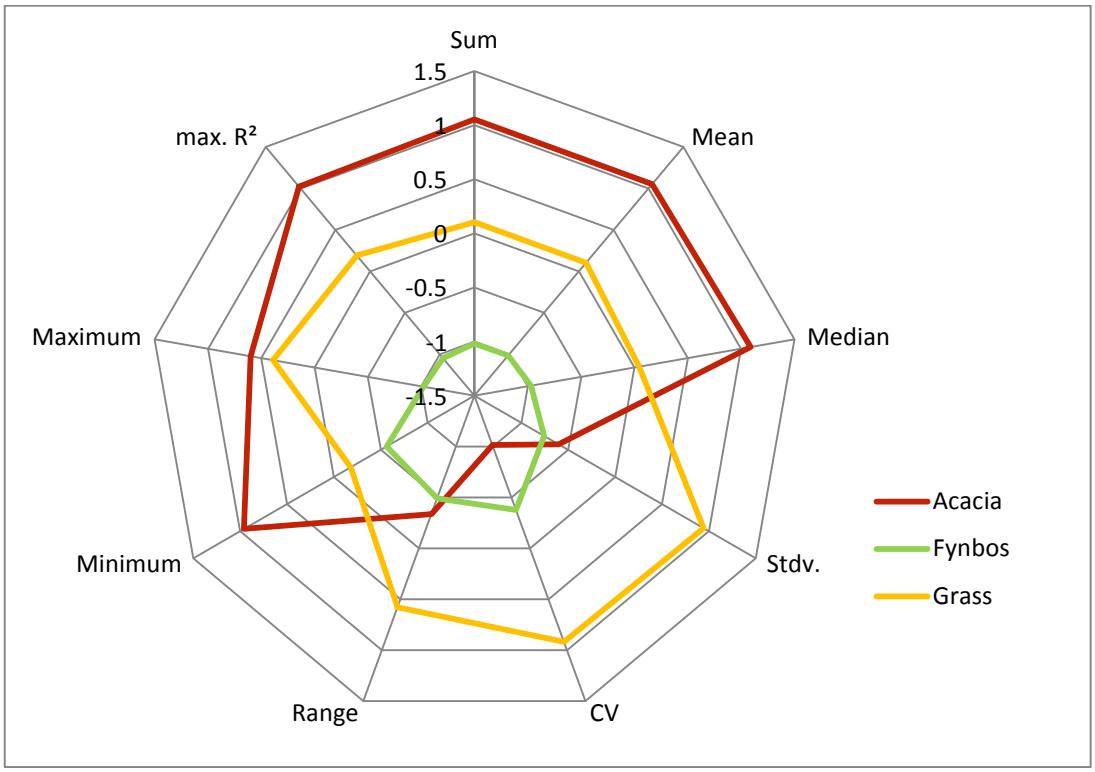

Figure 6.15: Statistical measures of EVI (year 2009) and maximum coefficient of determination of EVI (period 2007-2008).

The first decision (compare figure 6.16) separates most of the Grass pixels into the right branch. It is based on the maximum R^2 which has to be greater than 0.38 in order to fulfil the condition. Since the border between Grass and Acacia is rather narrow, a second node is inserted to eliminate the Acacia from the Grass pixels. The mean EVI is used in this case with a threshold of 0.2565; everything greater than this value is classified as Acacia. The left branch also starts with a mean EVI node in order to separate the Acacia from the rest. In this case, everything less than 0.244 mean EVI is assumed not to be Acacia. The

final decision is to delineate the remaining Grass pixels from the Fynbos. Every pixel with a standard deviation greater than 0.31 is assumed to be Grass. The remaining pixels should represent natural vegetation. At this point, it must be mentioned that Acacia classified pixels could still have a certain grass cover as well as Grass classified pixels could have a certain percentage of acacia but since the focus lies on the identification of disturbed, i.e. invaded areas in general, this is not of importance.

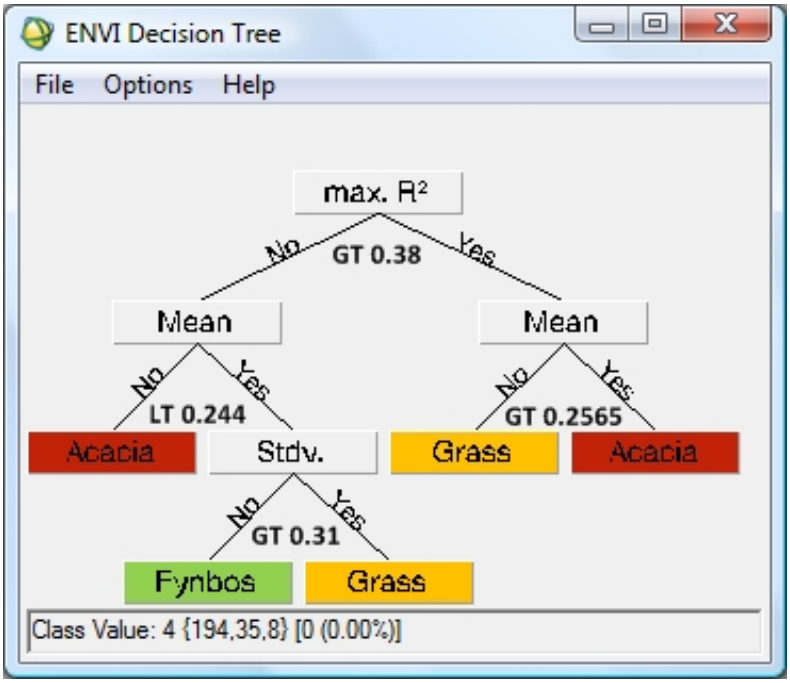

Figure 6.16: Applied ENVI Decision Tree. Separation values added underneath the nodes. GT = greater than, LT = less than.

Figure 6.17 shows the classification of the potential Sand Fynbos areas, which have been extracted from the shape file provided by the city (compare chapter 4.7), on the basis of the explained decision tree. Generally, it can be seen that most of the area is invaded and covered with *Acacia saligna*. Only the fragments in the north from Riverlands Nature Reserve and Mamre seem to have a fairly high cover of Fynbos. The one pixel classified as Fynbos on the Kohler Bricks fragment is probably wrong classified since there is a strong influence on the reflectance from the dump that the fragment partially surrounds in the south east. The fragment Baasariesfontein is generally covered *Acacia saligna*, only the small southern strip actually contains a mix of grassy Fynbos vegetation. But obviously this is just too small to be classified and in addition, the neighbouring effects to the agricultural areas are too dominant. The same could apply for the Kenilworth Race Course

which is classified as Acacia but the fragment is very small and surrounded by irrigated grass and built area. But since this fragment was not visited during the field trip, this still has to be validated. According to the classification, Riverlands Plain, the north easternmost fragment of the Riverlands Nature Reserve seems to have some considerable Fynbos vegetation. However, these areas basically consist of grassy vegetation with some restios in between and are thus more mixed pixels than Fynbos vegetation.

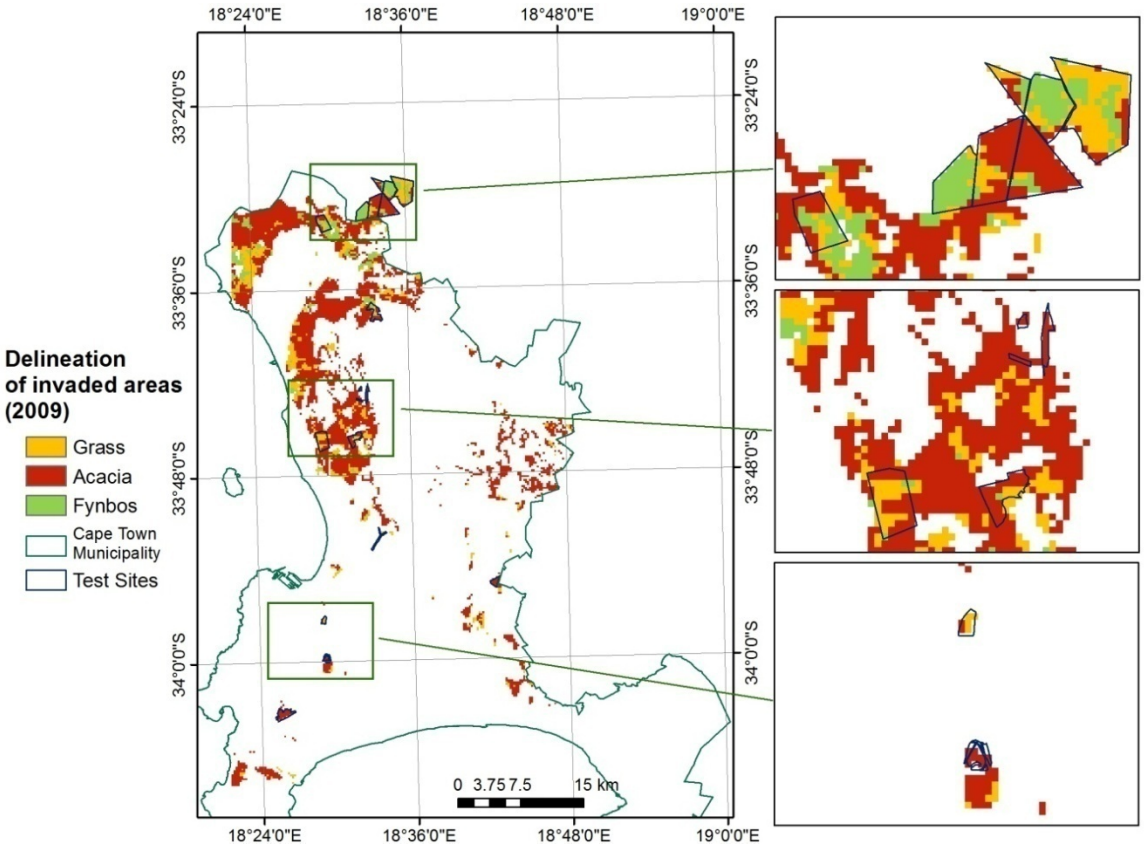

Figure 6.17: Delineation of invaded areas on potential Sand Fynbos areas (year 2009).

Focusing on three different fragments, figure 6.18 displays the comparison between the aerial images from 2008 and the classification. The left comparison shows the fragment Pella (compare figure 6.18a), which is strictly managed for several years. Almost the whole fragment is classified as Fynbos, only in the border area there are some Grass and Acacia pixels, which could result from neighbouring effects. Mamre (compare figure 6.18b) is formally protected and fenced in but still subject to heavy grazing. Its northern and south western areas are classified as Acacia with some bigger areas of Fynbos and

some Grass in between. From the aerial images and the field trips, it can be assured that the Acacia cover is quite accurately defined. Though the Fynbos vegetation in the western part of the fragment exits, it is rather mixed with grassy vegetation and some acacias. The pixels of the eastern part classified as Fynbos are also correct, but the vegetation cover is generally rather low, probably due to the heavy grazing or a fire in 2009.

The third fragment Blaauwberg (compare figure 6.18c) is also only formally protected but not fenced in and only few management measures have been taken so far. As the classification depicts, the land cover of this fragment is a mix of *Acacia saligna* and grassy areas with almost no visible Fynbos vegetation on it. However, the distribution of the two vegetation types is very patchy and the fragment basically contains mixed pixels, except for some larger acacia covered areas in the north. Thus, the delineation between the two classes seems inaccurate compared to the aerial images, but this is a matter of scale. However, the important information is that the Blaauwberg fragment is completely invaded and has to be managed.

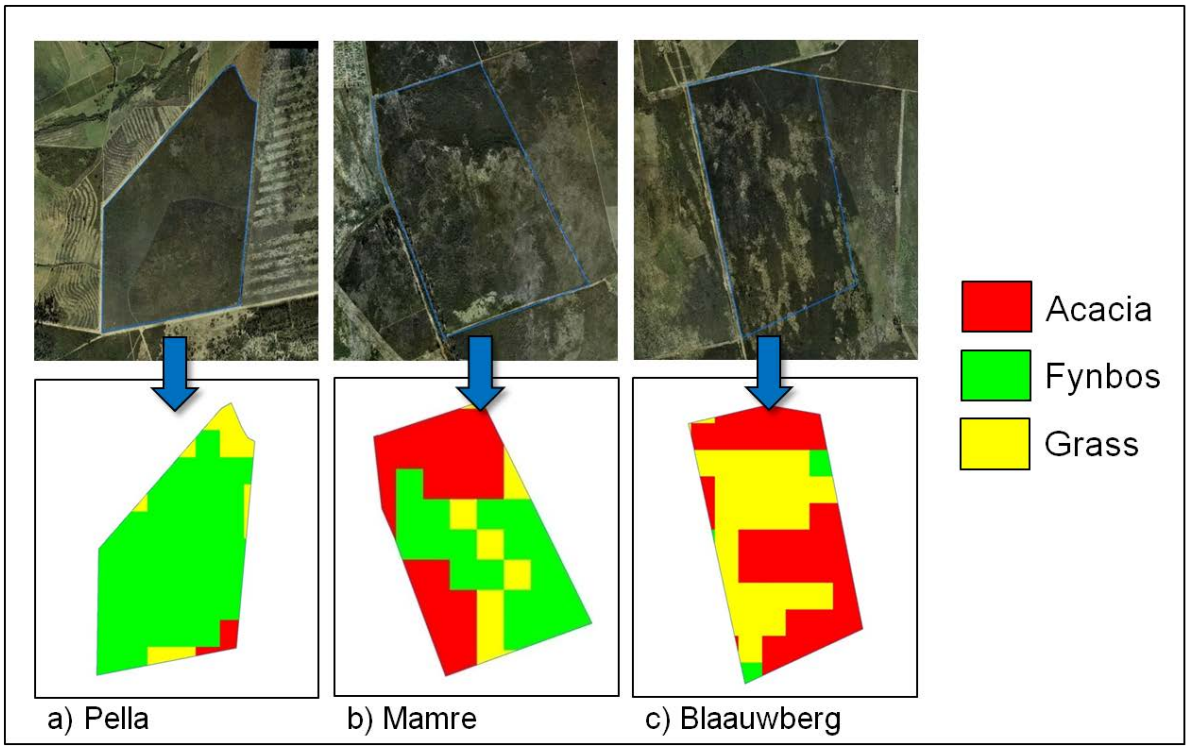

Figure 6.18: Delineation of invaded areas for three vegetation fragments (year 2009).

All in all, the delineation of invasive species worked really well for the fragments. So far, a validation could not be done since additional GTPs are not available and also due to time

constraints of this work. However, the aerial images and the overall impression of the fragments from the field trips suggest that the delineation of the alien vegetation from healthy Fynbos worked. Furthermore, a normal validation as it is common in remote sensing would not be meaningful for this small scale. As expected, the scale is a certain problem since a lot of pixels are classified as one of these three classes while they are actually rather mixed. Refining the classification and adding three transition classes could improve the delineation but again this could not be realised due to time constraints and might be part of future research.

This delineation of the invaded areas is a first step towards a monitoring of ecosystem health on the Sand Fynbos fragments. It clearly depicts that a long term management is closely related to the condition of the vegetation. There are no larger areas of Sand Fynbos vegetation in the study area that are not managed. Mamre seems to be an exception; while the grazing on the fragment not only seems to keep the Fynbos short it also hinders the dispersal of the acacia.

7 Conclusion and Perspectives

This study was intended to give a first overview of possibilities to monitor ecosystem health of remnant Sand Fynbos vegetation with the help of remote sensing. Ecosystem health is a very complex issue and indicators have to be found separately for each area of interest.

The area under intact Sand Fynbos vegetation has decreased so rapidly over the past decades that there is an urgent need today to protect and monitor the remaining fragments. Because these fragments are scattered over the whole municipality and their management is decentralised, ground monitoring is time and cost intensive. Remote sensing could be a cheap and comprehensive option for this purpose.

Since potential indicators for ecosystem health are numerous, not all of them could be covered or analysed in greater detail within the scope of this study. Thus, this topic is by far not exhausted and still has a lot of perspectives for future research.

This work focused on two of the three general measures of ecosystem health, established by Rapport, Costanza, & McMichael (1998): vitality and organisation. Vitality is basically measured in terms of primary productivity and organisation is represented by the biotic diversity of an ecosystem.

The first general measure, the vitality of vegetation was described by three indicators: the rain-use efficiency, an EVI-rainfall regression and the residual trends method.

The rain-use efficiency has been used in numerous studies as an index of degradation (e.g. Bai & Dent, 2008). If the RUE decreases over time, this area is regarded as degraded in the common literature.

Wessels et al. (2007) determined that the RUE can be a suitable indicator for degradation but he also pointed out that it is highly influenced by local and also temporal variability of rainfall. This variability could be confirmed by the results of the study, with comparably low RUE values in regions with high orographic rainfall.

Despite the fact that local variations of the RUE occur in the study area, the analysis of the ground truth polygons showed distinct differences between invasive vegetation and the inherent Fynbos vegetation. The Fynbos vegetation has constantly lower values than

acacia and grass covered areas. It seems as if Fynbos cannot express a higher availability of water in higher values of EVI, i.e. in a higher biomass production. This might result from the adaption of Fynbos to the generally dry conditions of the study area. However, this indicates that the interpretation of the RUE in the literature is not suited for this study area since degraded, i.e. invaded areas in this context have higher RUEs than the indigenous Fynbos vegetation.

The temporal development of the RUE could not be analysed properly since background information about the fragments are not consistent enough and the MODIS time series is not long enough to eliminate the effects of rainfall variability as Bai & Dent (2008) did in their study. Because of the high local variations of rainfall in the study area and subsequently of the RUE, it is not suited very well for the delineation of the different vegetation types.

Altogether, the RUE is only moderately suited as an indicator for ecosystem health of Sand Fynbos vegetation on the basis of MODIS data.

The second indicator of vitality, the regression between EVI and rainfall was employed to investigate the reaction of the local vegetation to precipitation. Generally, it reflects the results of RUE. The photosynthetic activity of Sand Fynbos is not particularly dependant on rainfall and thus its general coefficient of determination is very low. Since the degraded vegetation cover, i.e. *Acacia saligna* and grasses, correlates rather well with rainfall, a distinction on the basis of this relationship is possible. Both the 2-years time period as well as the whole time series indicate this conclusion. Thus, the EVI-rainfall regression has great potential for the discrimination between intact Fynbos vegetation and invaded areas and is considered as a suitable indicator.

The third indicator of vitality, the residual trends method (RESTREND) with its independence of rainfall variability displayed promising results in former studies (Wessels et al., 2007; Bai & Dent, 2008). For the special conditions of the study area, this method is not suited very well. Since the Sand Fynbos vegetation does not correlate with rainfall, any further developments based on this regression are not useful. Thus, the RESTREND method cannot deliver any further significant results for the application in the study area.

The analysis of the vitality displays the general problem of the term ‘degradation’. Most publications so far refer to land as an economic resource and link degradation with the

term ‘land use’. Thus, degradation is commonly measured by decreasing productivity of vegetation. This approach is not appropriate for the analysis of complex ecosystems.

The special conditions of this study area with the unique indigenous Sand Fynbos vegetation and the invasive alien species showed that degradation requires a unique definition and its detection has to be determined individually. Since the degraded areas with its invasive alien species have a higher productivity than the Sand Fynbos vegetation, the interpretation of the indicators must be conducted differently from the literature.

Table 7.1: Overview of the suitability of the tested indicators for Fynbos vegetation.

Indicator	Suitability	Reason
Rain-use efficiency	moderate	Discrimination between Fynbos and invaded areas possible, but high temporal and local variability occur
EVI-rainfall regression	good	Discrimination between Fynbos and invaded areas possible
RESTREND	unsuitable	Almost no significant results with lacking correlation for Fynbos

The second general measure by Rapport, Costanza, & McMichael (1998), the organisation of an ecosystem is represented by its biodiversity. Since this diversity dramatically decreases with the introduction of dominant alien species, like *Acacia saligna* in the study area, the distribution of these invasive species was delineated.

The vegetation phenology and the resulting statistical measures that were applied in this study display distinct characteristics of Sand Fynbos vegetation and degraded (i.e. invaded) areas. While Sand Fynbos has a constantly low EVI over the course of the year, grassy areas have a high seasonal variability with high EVI values in the winter and low EVI values in the summer. The invasive evergreen *Acacia saligna* obtains high mean values of EVI since it has a rather high biomass production and a constant appearance over the course of the year. The statistical measures derived from the vegetation phenology represent suitable indicators for the delineation of degraded areas in Sand Fynbos vegetation.

On the basis of these combined indicators, a convenient delineation of the degraded areas could be generated. First, it is advisable to analyse the EVI-rainfall regression and second the annual phenology of the vegetation. Since the resolution of the MODIS data is rather coarse and mixed pixels were not defined in this delineation, the overall accuracy is probably not very high, but the classification gives a good first impression of potentially degraded areas.

These results can be used for specific ground monitoring and planning of management measures and the developed indicators form a suitable basis for future research. This work made an important first step to display the difficulties of the study area for remote sensing, so they can be taken into account in further studies.

In order to draw the right conclusions from the interpretation of the whole time series, consistent background information about the development of the fragments are necessary. These can only be achieved by an accurate documentation of management measures, fires and other factors that influence the vegetation cover.

The following section displays improvements of the used methods and recommended approaches for further research.

The applied delineation of invasive species could be enhanced with the introduction of mixed pixels to the classification. For this purpose, the influence of different compositions of Sand Fynbos vegetation, i.e. different proportions of restioid, ericoid and proteoid Fynbos has to be investigated. Furthermore, the decision progress for the delineation could be automated by the use of the *R Regression Tree* which is based on a programming language for statistical analysis (Bates et al., 2010). However, the general accuracy of the applied delineation has to be tested in other regions of the study area.

Now that the unique characteristics of the different vegetation types are determined, the use of Landsat images with a 30m spatial resolution could be considered. Two images, one from the growing season and one from the dry season could be compared in order to distinguish between the evergreen Sand Fynbos vegetation and annual grasses.

The developed indicators could be applied to other remote sensors with higher spatial resolutions, in order to achieve a higher geometric accuracy of the delineation of invasive species and to improve the extraction of ‘pure’ spectral information. *RapidEye* would be a suitable satellite system for further research since its temporal and spectral resolution are

sufficiently high to monitor the vegetation phenology and its spatial resolution with up to 5m pixel size is significantly higher than the one of the MODIS sensor (RapidEye AG, 2010).

'Resilience', the third of the three general measures for ecosystem health by Rapport, Costanza, & McMichael (1998) could be determined on the basis of consistent background information. The recovery of vegetation after a fire or after the cutting of *Acacia saligna* could be monitored by the use of the EVI-rainfall regression or the RUE.

Another potential indicator for ecosystem health could be a fragmentation analysis (e.g. Fahrig, 2003). For this purpose, the size, surrounding land cover and connectivity between the fragments has to be investigated. Since the Sand Fynbos fragments are rather small and scattered over the whole city area, it would be important to see if the individual fragments are able to keep up their biotic diversity and if the seed exchange with other fragments is still possible.

Furthermore, the application of lidar (compare Rosso, Ustin, & Hastings, 2006) for the delineation of *Acacia saligna* seems promising for future research. Since the acacia is growing very fast and is generally taller than the Sand Fynbos vegetation, a distinction by the height of the plants should be possible and could deliver very accurate results. However, this method is rather expensive because lidar systems are only airborne and flights for certain study areas have to be ordered specifically.

Although a higher spatial resolution would have been desirable, this study shows that remote sensing can be a suitable basis for a reasoned and sustainable management of Sand Fynbos fragments. This strict management becomes essential as Fynbos vegetation cannot regenerate on its own from the infestation of alien species anymore.

References

Alvarez, M. E., & Cushman, J. H. (2002). Community-level Consequences of a Plant Invasion: Effects on Three Habitats in Coastal California. *Ecological Applications*, *12*(5), 1434-1444.

Asner, G., Jones, M., Martin, R., Knapp, D., & Hughes, R. (2008). Remote sensing of native and invasive species in Hawaiian forests. *Remote Sensing of Environment*, *112*(5), 1912-1926.

Backhaus, K., Erichson, B., Plinke, W., & Weiber, R. (2008). *Multivariate Analysemethoden - Eine anwendungsorientierte Einführung* (12nd ed., pp. 51-113). Berlin, Heidelberg: Springer-Verlag.

Bai, Z. G., & Dent, D. L. (2008). Land Degradation and Improvement in South Africa 1 . Identification by remote sensing. *GLADA Report*.

Bates, D., Chambers, J., Dalgaard, P., Falcon, S., Gentleman, R., Hornik, K., et al. (2010). The R Project. Retrieved from http://www.r-project.org/.

Blaikie, P. M., & Brookefield, H. C. (1987). *Land degradation and society* (first., pp. 1-27). London: Methuen & Co. Ltd.

Colditz, R. R., Conrad, C., Wehrmann, T., Schmidt, M., & Dech, S. (2008). TiSeG: A Flexible Software Tool for Time-Series Generation of MODIS Data Utilizing the Quality Assessment Science Data Set. *IEEE Transactions on Geoscience and Remote Sensing*, *46*(10), 3296-3308.

Compton, J. S. (2004). *The rocks and mountains of Cape Town* (p. 112). Juta and Company Ltd.

Convention on Biological Diversity (CBD). (2010). International Year of Biodiversity. Retrieved from http://www.cbd.int/2010/welcome/.

Costanza, R., Norton, B. G., & Haskell, B. D. (1992). *Ecosystem health: new goals for environmental management* (p. 269). Island Press.

Covington, B. W. W., Fule, P. Z., Moore, M. M., Hart, S. C., Kolb, T. E., Mast, J. N., et al. (1997). Restoring Ecosystem Health in Ponderosa Pine Forests of the Southwest. *Journal of Sustainable Forestry*, *95*(4), 23-29.

Cowling, R. M., Richardson, D. M., & Pierce, S. M. (2004). *Vegetation of Southern Africa* (pp. 53-208). Cambridge University Press.

Curran, P. (1981). Multispectral remote sensing for estimating vegetation biomass and productivity. In H. Smith (Ed.), *Plants and the daylight spectrum* (pp. 65-99). London: Academic Press.

Day, J., Siegfried, W. R., Louw, G. N., & Jarman, M. L. (1979). *Fynbos ecology: a preliminary synthesis* (pp. 133-150).

ERSDAC. (2010). EOS Project. Retrieved from http://www.gds.aster.ersdac.or.jp/gds_www2002/exhibition_e/e_project_e/e_project_e.html.

Evans, J., & Geerken, R. (2004). Discrimination between climate and human-induced dryland degradation. *Journal of Arid Environments, 57*(4), 535-554.

Fabricante, I., Oesterheld, M., & Paruelo, J. M. (2009). Annual and seasonal variation of NDVI explained by current and previous precipitation across Northern Patagonia. *Journal of Arid Environments, 73*(8), 745-753. Elsevier Ltd.

Fahrig, L. (2003). Effects of Habitat Fragmentation on Biodiversity. *Annual Review of Ecology, Evolution, and Systematics, 34*(1), 487-515.

Fairbanks, D., Thompson, M., Vink, D., Newby, T., & Van Den Berg, HM, Everard, D. (2000). The South African land-cover characteristics database: a synopsis of the landscape. *South African Journal of Science, 96*, 69-82.

Fensholt, R., Rasmussen, K., Nielsen, T. T., & Mbow, C. (2009). Evaluation of earth observation based long term vegetation trends — Intercomparing NDVI time series trend analysis consistency of Sahel from AVHRR GIMMS, Terra MODIS and SPOT VGT data. *Remote Sensing of Environment, 113*(9), 1886-1898. Elsevier Inc.

Geßner, U. (2011). *Erfassung raum-zeitlicher Muster der Vegetationsstruktur im südlichen Afrika mittels Fernerkundungsdaten und sozioökonomischer Informationen*.

Gold Circle Racing and Gaming Group. (2010). Kenilworth Racecourse Conservation Area. Retrieved from http://www.krca.co.za/.

Guevara, J. C., Estevez, O. R., & Torres, E. R. (1996). Utilization of the rain-use efficiency factor for determining potential cattle production in the Mendoza plain , Argentina. *Journal of Arid Environments, 33*, 347-353.

He, K., Zhang, J., & Zhang, Q. (2009). Linking variability in species composition and MODIS NDVI based on beta diversity measurements. *Acta Oecologica, 35*(1), 14-21. Elsevier Masson SAS.

Herrmann, S. M., Anyamba, A., & Tucker, C. J. (2005). Recent trends in vegetation dynamics in the African Sahel and their relationship to climate. *Global Environmental Change, 15*(4).

Holm, A., Cridland, S., & Roderick, M. (2003). The use of time-integrated NOAA NDVI data and rainfall to assess landscape degradation in the arid shrubland of Western Australia. *Remote Sensing of Environment, 85*(2), 145-158.

Holmes, P. M., Richardson, D. M., Wilgen, B. W. V., & Gelderblom, C. (2000). Recovery of South African fynbos vegetation following alien woody plant clearing and fire: implications for restoration. *Austral Ecology*, *25*(6), 631-639.

Huete, A., Didan, K., Miura, T., Rodriguez, E. P., Gao, X., & Ferreira, L. G. (2002). Overview of the radiometric and biophysical performance of the MODIS vegetation indices. *Remote Sensing of Environment*, *83*, 195 - 213.

ITT. (2008). ENVI User's Guide.

Jensen, J. R. (2005). *Introductory digital image processing: a remote sensing perspective* (p. 526). Prentice Hall.

Jensen, J. R. (2007). *Remote Sensing of the Environment: An Earth Resource Perspective*. *Perspective* (2nd ed., p. 592). Prentice Hall.

Johnson, G. D., & Patil, G. P. (1998). Quantitative Multiresolution Characterization of Landscape Patterns for Assessing the Status of Ecosystem Health in Watershed Management Areas. *Ecosystem Health*, *4*(3), 177-187.

Joshi, C., Leeuw, J. D., & Duren, I. C. V. (2004). Remote sensing and GIS applications for mapping and spatial modelling of invasive species. *Proceedings for ISPRS* (pp. 669-677). Istanbul, Turkey.

Klein, D., & Roehrig, J. (2006). How Does Vegetation Respond To Rainfall Variability In A Semi-Humid West African In Comparison To a Semi-Arid East African Environment?. *Second Workshop of the EARSeL SIG on Remote Sensing of Land Use & Land Cover* (pp. 149-156). Bonn.

Klerk, H. de. (2008). A pragmatic assessment of the usefulness of the MODIS (Terra and Aqua) 1-km active fire (MOD14A2 and MYD14A2) products for mapping fires in the fynbos biome. *International Journal of Wildland Fire*, *17*(2), 166-178.

Klingebiel, A. A., & Montgomery, P. H. (1961). Land Capability Classification. *Agriculture Handbook* (210th ed., Vol. 210). Washington, D.C.: USDA.

Kottek, M., Grieser, J., Beck, C., Rudolf, B., & Rubel, F. (2006). World Map of the Köppen-Geiger climate classification updated. *Meteorologische Zeitschrift*, *15*(3), 259-263.

Li, J., Lewis, J., Rowland, J., Tappan, G., & Tiszen, L. L. (2004). Evaluation of land performance in Senegal using multi-temporal NDVI and rainfall series. *Journal of Arid Environments*, *59*(3), 463-480.

Lillesand, T. M., Kiefer, R. W., & Chipman, J. W. (2004). *Remote sensing and image interpretation* (p. 763). Wiley.

LP DAAC. (2010). Vegetation Indices 16-Day L3 Global 250m - MOD13Q1. Retrieved from

https://lpdaac.usgs.gov/lpdaac/products/modis_products_table/vegetation_indices/16_day_l3_global_250m/mod13q1.

LP DAAC User Services. (2010). MODIS Reprojection Tool. Retrieved from https://lpdaac.usgs.gov/lpdaac/tools/modis_reprojection_tool.

Marsudi, N. (1999). Identification and characterization of fast- and slow-growing root nodule bacteria from South-Western Australian soils able to nodulate Acacia saligna. *Soil Biology and Biochemistry*, *31*(9), 1229-1238.

Maslin, B. R., & McDonald, M. W. (2004). *AcaciaSearch - Evaluation of Acacia as a woody crop option for southern Australia*. *Distribution* (pp. 204-214).

Meadows, M. E., & Hoffman, T. M. (2003). Land degradation and climate change in South Africa. *The Geographical Journal*, *169*(2), 168-177.

Miao, X., Gong, P., Swope, S., Pu, R., Carruthers, R., Anderson, G., et al. (2006). Estimation of yellow starthistle abundance through CASI-2 hyperspectral imagery using linear spectral mixture models. *Remote Sensing of Environment*, *101*(3), 329-341.

Midgley, G. F., Hannah, L., Millar, D., Rutherford, M. C., & Powrie, L. W. (2002). Assessing the vulnerability of species richness to anthropogenic climate change in a biodiversity hotspot. *Global Ecology and Biogeography*, *11*(6), 445-451.

Milton, S. (2004). Grasses as invasive alien plants in South Africa. *South African Journal Of Science*, *100*(February), 69-75.

Mucina, L., & Rutherford, M. C. (2006). *The vegetation of South Africa, Lesotho and Swaziland* (pp. 53-208). South African National Biodiversity Institute.

Musil, C. F., Milton, S., & Davis, G. W. (2005). The threat of alien invasive grasses to lowland Cape floral diversity: an empirical appraisal of the effectiveness of practical control strategies. *South African Journal Of Science*, *101*(August), 337-344.

NASA Science. (2010). Missions - Terra. Retrieved from http://science.nasa.gov/missions/terra/.

Nellemann, C., & Corcoran, E. (2010). *Dead Planet, Living Planet - Biodiversity and Ecosystem Restoration for Sustainable Development* (pp. 1-109).

Nicholson, S. E., Tucker, C. J., & Ba, M. B. (1998). Desertification, Drought and Surface Vegetation : An Example from the West African Sahel. *Bulletin of the American Meterological Society*, *79*, 815-829.

Pickup, G., Bastin, G. N., & Chewings, V. H. (1998). Identifying trends in land degradation in non-equilibrium rangelands. *Journal of Applied Ecology*, *35*(3), 365-377.

RapidEye AG. (2010). Standard Image Products. Retrieved from http://www.rapideye.de/home/products/standard-image-products/index.html.

Rapport, D. J. (2007). Chapter 32 Healthy Ecosystems : An Evolving Paradigm. *Sage Handbook of Environment and Society*, 430-441.

Rapport, D. J., Costanza, R., & McMichael, A. J. (1998). Assessing ecosystem health. *TREE, 13*(10), 397-402.

Richter, R. (2010). Atmospheric / Topographic Correction for Satellite Imagery - ATCOR-2/3 User Guide , Version 7.1.

Rosso, P., Ustin, S., & Hastings, A. (2006). Use of lidar to study changes associated with Spartina invasion in San Francisco Bay marshes. *Remote Sensing of Environment, 100*(3), 295-306.

Schowengerdt, R. A. (2007). *Remote sensing: models and methods for image processing* (p. 515). Academic Press.

Serdani, M. (2001). *The Acacia Gall Rust*.

Shear, H., Stadler-Salt, N., Bertram, P., & Horvatin, P. (2003). The Development and Implementation of Indicators of Ecosystem Health in the Great Lakes Basin. *Environmental Monitoring and Assessment, 88*(1), 119-151.

Song, C., Woodstock, C. E., Seto, K. C., Pax Lenney, M., & Macomber, S. A. (2001). Classification and Change Detection Using Landsat TM Data When and How to Correct Atmospheric Effects?. *Remote Sensing of Environment, 4257*(2), 230-244.

Spatial Planning and Urban Design Department. (2009). *Cape Town - Spatial Development Framework - Technical Report* (pp. 34-43).

Stocking, M., & Murnaghan, N. (2001). *Handbook for the field assessment of land degradation* (pp. 9-25). Margate: Earthscan Publications Ltd.

Strand, H., Höft, R., Stritthold, J., Miles, L., Horning, N., Fosnight, E., et al. (2007). *Sourcebook on remote sensing and biodiversity indicators* (Technical ., p. 203). Montreal: Secretariat of the Convention on Biological Diversity.

Symeonakis, E., & Drake, N. (2004). Monitoring desertification and land degradation over sub-Saharan Africa. *International Journal of Remote Sensing, 25*(3), 573-592.

UNESCO. (2010). Cape Floral Region Protected Areas. Retrieved from http://whc.unesco.org/en/list/1007/.

USGS. (2010). Global Visualization Viewer. Retrieved from http://glovis.usgs.gov/.

Van Der Wal, R., Truscott, A.-M., Pearce, I. S. K., Cole, L., Harris, M. P., & Wanless, S. (2008). Multiple anthropogenic changes cause biodiversity loss through plant invasion. *Global Change Biology, 14*(6), 1428-1436.

Wessels, K., Prince, S., Malherbe, J., Small, J., Frost, P., & Vanzyl, D. (2007). Can human-induced land degradation be distinguished from the effects of rainfall variability? A case study in South Africa. *Journal of Arid Environments*, *68*(2), 271-297.

Wilkinson, P. (2000). City profile Cape Town. *Cities*, *17*(3), 195-205.

Wood, A. R., & Morris, M. J. (2007). Impact of the gall-forming rust fungus Uromycladium tepperianum on the invasive tree Acacia saligna in South Africa : 15 years of monitoring. *Biological Control*, *41*, 68-77.

Yelenik, S. G., Stock, W. D., & Richardson, D. M. (2004). Ecosystem Level Impacts of Invasive Acacia saligna in the South African Fynbos. *Restoration Ecology*, *12*(1), 44-51.

A Appendix

A.1 Sections of the Study Area

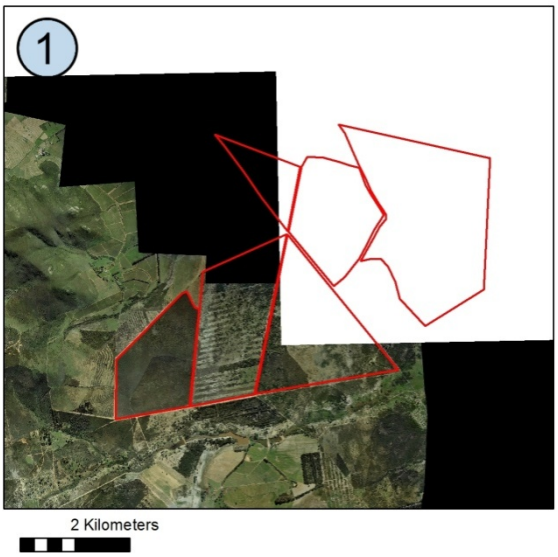

Figure A.1: Section 1 showing Riverlands Nature Reserve.

Figure A.2: Section 2 showing Mamre.

Figure A.3: Section 3 showing Schoongezicht Farm.

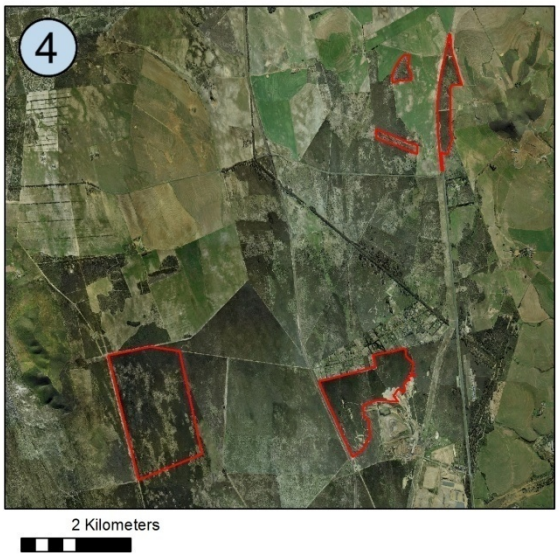

Figure A.4: Section 4 showing Baasariesfontein (north), East Blaauwberg Conservation Area (west), Kohler Bricks (east).

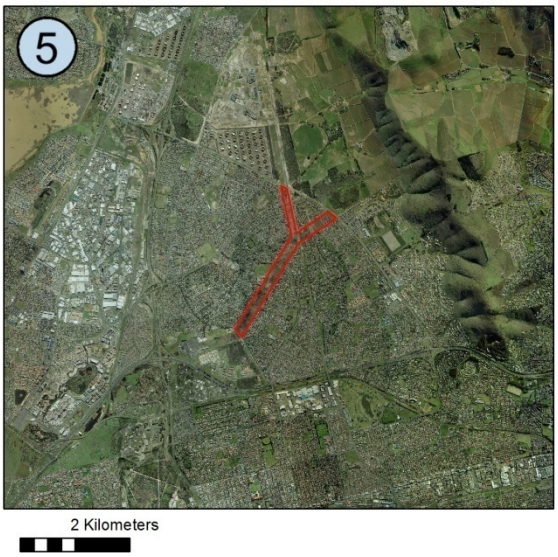

Figure A.5: Section 5 showing Plattekloof.

Figure A.6: Section 6 showing Haasendal.

Figure A.7: Section 7 showing Rondebosch Common (north) and Kenilworth Race Course (south).

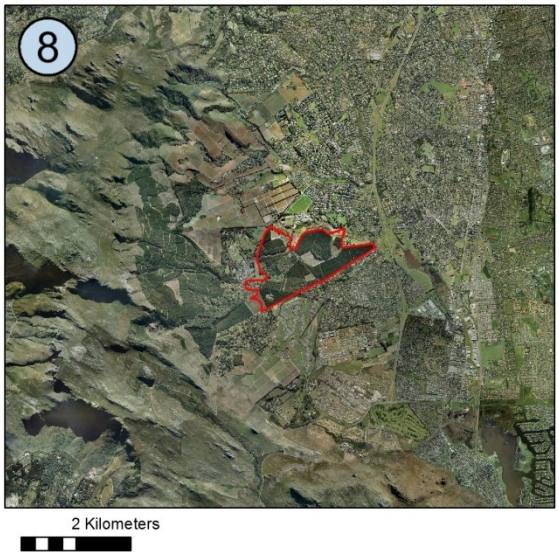

Figure A.8: Section 8 showing Tokai Forest.

A.2 IDL Script: Reformatting of Precipitation Data

```
; Programm zum Einlesen, Umformatieren und Aufsummieren spezieller
; Niederschlagsdaten aus SA bereitgestellt durch den SAWS.
; Diese werden zunächst aus einer Textdatei eingelesen, von Jahres-Blattdaten in Listen
; für  jede Station umgewandelt,
; dann 16-Tage-weise und Jahres-weise aufsummiert und in eine Text-Datei ausgegeben.
; Output:  Textdatei mit Klimastationen in Spalten
;          Textdatei mit 16-Tagessummen
;          Textdatei mit Jahresummen
; Autor: Kim Knauer
; Datum 6.11.2009
; Modifikation zu kim_klima:
; Mod: Aufstocken auf 19 Klimastationen

pro kim_klima_all, pfad, rain
; record length
      dummy=''
      anz=0l
      openr,1,pfad
       while not EOF(1) do begin
          readf,1,dummy
          anz=anz+1
       endwhile
      close,1

print,' Anzahl der Tage im Regendatensatz:  ',anz

;definition of arrays
   rain=fltarr(12, anz)
   rains=fltarr(12, 1)            ; Das ist der Schluessel
```

```
; Read in data
openr,1,pfad

  for i=0,anz-1 do begin
      readf,1, rains      ;, FORMAT='(12F0)'
       rain(*, i)=rains
  endfor

close, 1
free_lun, 1

end

; HAUPTPROGRAMM
;-------------------------

;Variablen

pfad= 'F:\Diplomarbeit\IDL_scripts\Rainfall_short3_2_ohne_minus_update08.txt'

; genau definierte Jahre
monate=    [31, 28, 31, 30, 31, 30, 31, 31, 30, 31, 30, 31, $     ; 1999
          31, 29, 31, 30, 31, 30, 31, 31, 30, 31, 30, 31, $     ; 2000
          31, 28, 31, 30, 31, 30, 31, 31, 30, 31, 30, 31, $     ; 2001
          31, 28, 31, 30, 31, 30, 31, 31, 30, 31, 30, 31, $     ; 2002
          31, 28, 31, 30, 31, 30, 31, 31, 30, 31, 30, 31, $     ; 2003
          31, 29, 31, 30, 31, 30, 31, 31, 30, 31, 30, 31, $     ; 2004
          31, 28, 31, 30, 31, 30, 31, 31, 30, 31, 30, 31, $     ; 2005
          31, 28, 31, 30, 31, 30, 31, 31, 30, 31, 30, 31, $     ; 2006
          31, 28, 31, 30, 31, 30, 31, 31, 30, 31, 30, 31, $     ; 2007
          31, 29, 31, 30, 31, 30, 31, 31, 30, 31, 30, 31]       ; 2008
```

```
 jahre= [365, 366, 365, 365, 365, 366, 365, 365, 365, 366]

; Anzahl der Klimastationen
anz_stat= 19

; Länge des Outputarrays
length= total(monate)

; Outputarray
output= fltarr(anz_stat, length)

; Einlesen der Regendaten
kim_klima_all, pfad, rain

; _____UMFORMATIEREN DER DATEN VON BLAETTERN IN SPALTEN _____

; Einlesen aller Jahre aller Stationen
for k=0, 18 do begin

anf_o= 0
ende_o= -1

; Einlesen aller Jahre einer Station
  for j=0, 9 do begin

; Einlesen von einem Jahr
    for i=0, 11 do begin

;      print, 'Anfang ', anf_o
     anf_in= j*31 + k*310            ; 31 = Länge eines Jahresblatts, 310= Länge von 10 Jahren
einer Station
     ende_in= j*31 + monate(i+(12*j))-1 + k*310
```

```
    ende_o= ende_o+monate(i+(12*j))
    output(k,anf_o:ende_o)=rain(i,anf_in:ende_in)
    anf_o= anf_o+monate(i+(12*j))
;     print, 'Ende   ', ende_in

   endfor
  endfor
endfor



;Rausschreiben des Ergebnisses in eine Textdatei

result=fix(output)
   OPENW, 2, 'F:\Diplomarbeit\IDL_scripts\output_3_all.txt'
   PRINTF, 2, output  ,FORMAT = '(19F10.2)'
   CLOSE, 2
;_____________JAHRESSUMMEN_____________________________________________________

jahr_sum = fltarr(anz_stat, 10)

for k=0, 18 do begin
anf_sum=0
ende_sum=-1
  for i=0, 9 do begin

    ende_sum= ende_sum + jahre(i)
    jahr_sum(k, i)= total(output(k, anf_sum:ende_sum))
    anf_sum= anf_sum + jahre(i)

  endfor
endfor
```

```
result=fix(jahr_sum)
  OPENW, 2, 'F:\Diplomarbeit\IDL_scripts\jahressummen4_all.txt'
  PRINTF, 2, jahr_sum  ,FORMAT = '(19F10.2)'
  CLOSE, 2



; _____16er-SUMMEN_____

no_sedecad= 23*10 ; Zahl der Zeitschnitte in einem Jahr * Jahre

 no_daydec=(intarr(no_sedecad)+1)*16   ; Array fuer die Anzahl der Tage innerhalb einer
Dekade
 output_sum=fltarr(anz_stat, no_sedecad)         ; Ergebnisarray

; Schleife zum Erstellen der Anzahl an Tagen, die in die 23. Dekade kommen
j=-1
for i= 0, 9 do begin
  j=j+23
  no_daydec(j)=jahre(i)-352
endfor

; Daten in Sedekadensummen umwandeln
   anf=0
   ende=-1
   for i=0,no_sedecad-1 do begin
;    print, 'anf', i, '=' ,anf
         ende=ende+no_daydec(i)
;    print, 'end', i, '=' ,ende
       output_sum(*,i)= total(output(*,anf:ende), 2)
         anf=anf+no_daydec(i)
```

```
  endfor


;Rausschreiben des Ergebnisses in eine Textdatei
result=fix(output_sum)
  OPENW, 2, 'F:\Diplomarbeit\IDL_scripts\output_sum2_all.txt'
  PRINTF, 2, output_sum  ,FORMAT = '(19F10.2)'
  CLOSE, 2

end
```

A.3 IDL Script: Calculation of the RUE

```
; Programm zur Erstellung der RUE aus interpolierten Niederschlags-Daten und EVI-Daten
; Input: Jahres-Tiffs mit jährlicher Summe des ND und jährlicher Summe des EVI
;   data type: zwei Ordner mit TIFFs (EVI, ND)
;   specifications:
; Output: Stack der RUE
;   data type: TIFF
;   specifications:
; ; Comment: Extent der Datensätze muss im Skript angepasst werden!
;          Extent und Pixelgröße der Datensätze muss übereinstimmen!
; Date: 10.11.2009
; Author: K.Knauer

;_PROCEDURES ZUM EINLESEN, ÖFFNEN UND STACKEN DES NIEDERSCHLAGS & DES EVI _

pro read_rain, rain, rainarray, header  ; ACHTUNG: Übergabe des Headers aus dieser Pro
an den Output

 such_str=strmid(rain, 0,strpos(rain,'\',/reverse_search)+1)      ; extrahiert den Pfad aus
"rain"
```

```
  File_Specification=such_str+'*.tif'             ; Filter, welche Dateien beruecksichtigt werden
  dateiliste = FINDFILE( File_Specification , COUNT=anzahl)
; Schreiben aller Dateien die im "File_Specification" Pfad angegeben sind und die Endung
.tif ; besitzen in result
  ;print, dateiliste

  rainarray=FINDGEN(anzahl, 240, 376)

  for i=0, anzahl-1 do begin                      ; Stack der Nd-Daten
    daten_rain=read_tiff(dateiliste(i), geotiff=header)
    ;help, daten_rain
    ;print, daten_rain
    rainarray(i,*,*)=daten_rain
  endfor

end

pro read_EVI, EVI, eviarray

  such_str_evi=strmid(EVI, 0,strpos(EVI,'\',/reverse_search)+1)  ; gleiches Einlesen der EVI-
;Daten wie bei ND
  File_Specification=such_str_evi+'*.tif'
  dateiliste_evi = FINDFILE( File_Specification , COUNT=anzahl_evi)

  ;print, dateiliste_evi

  eviarray=FINDGEN(anzahl_evi, 240, 376)

  for i=0, anzahl_evi-1 do begin                  ; Stack der EVI-Daten
    daten_evi=read_tiff(dateiliste_evi(i), geotiff=header2)
    ;help, daten_evi
    ;print, daten_evi
```

```
  eviarray(i,*,*)=daten_evi
 endfor

 ; NoData-Value des EVI wird auf 0 gesetzt:
 EVI_null= where(eviarray lt 0)
 eviarray(EVI_null)= 0

end


;_____________________________HAUPTPROGRAMM _____________________________

;Definition der ND-Pfads:
rain_pfad= envi_pickfile(title= 'Please choose first Rain-.tif')
;Definition des EVI-Pfads:
EVI_pfad= envi_pickfile(title= 'Please choose first EVI-.tif')
;Definition des Output-RUE-Stacks:
RUE_stack= 'F:\Diplomarbeit\RUE\RUE_rainy_season_00-08_stack.tif'

output_nd= 'F:\Diplomarbeit\RUE\ND_rainy_season_00-08_stack.tif'
output_evi= 'F:\Diplomarbeit\RUE\EVI9years-stack.tif'

read_rain, rain_pfad, rainarray, header

read_EVI, EVI_pfad, eviarray

; --------- RUE bilden ------------------

;eviarray2 = eviarray * 0.0001
; Multiplikation der EVI-Daten wie auf Homepage beschrieben!
https://lpdaac.usgs.gov/lpdaac/products/modis_products_table/vegetation_indices/16_day_l3_global_250m/mod13q1
```

```
RUE = eviarray/rainarray

; Die Stellen des NoData-Values der Nd-Daten werden im Output auf 0 gesetzt:
ND_null= where(rainarray le 0)
RUE(ND_null)= 0

; Die Stellen des NoData-Values der Nd-Daten werden im stack auf 0 gesetzt:
ND_null= where(rainarray lt 0)
rainarray(ND_null)= 0



; ------ Rausschreiben des Stacks --------

WRITE_TIFF, RUE_stack, RUE, geotiff=header, /float
WRITE_TIFF, output_nd, rainarray, geotiff=header, /float
;WRITE_TIFF, output_evi, eviarray2, geotiff=header, /float

print, 'Done!'
end
```

A.4 Email Interview with Ismail Ebrahim

The following email interview about the Mamre fragment with Ismail Ebrahim, employee of the CREW programme at SANBI, was conducted by Dr. Nicky Allsopp on the 10th May, 2010.

Date of becoming part of city reserve system?
Ebrahim: *Not part of the City reserve network. Long history of struggle with getting the land to the community. Process is currently underway to transfer the land to a community trust. I'm not 100% sure but I think there is a small part (14ha) that is proclaimed as the Mamre Nature Garden. I will have to double check.*

What did people use the area for in the past, and present?
Ebrahim: *Most of the Mamre Commange area has been been used as grazing at some stage. They use to plant crops on the slopes of the dassenberg but currently the main lasduse is livestock farming. Huge areas of the commnage is densely infested with aliens mainly Port Jackson. In the new plan for the commange area I think the community is planning to recultivate the old lands. There is talk of fodder crops for the livestock, vineyards, compost farms, etc. They do however plan to have about 400-500ha of conservation land.*

Has the area been grazed? By what? When? Any estimate of how many animals or if there are periods with and without animals.
Ebrahim: *Last estimate I heard from the community is that there are approx 2000 big livestock units, which is hell of lot more than the carrying capacity of the land. The granite slopes have been very heavily overgrazed the Atlantis sands not so much. More pig, goat and sheep farmers tucked away in the atlantis sands area.*

Are you aware of any fires, if so when and did they burn the whole area or not. Has the area historically been burnt for grazing?

Ebrahim: *The area burnt last year. A big part of the Mamre commange on the sands. Also a burn on the top of Dassenberg on the granites. Not intentional burns for grazing. Not sure what they have done in the past.*

Have there been any alien clearing projects? If so when and which areas were cleared?
Ebrahim: *Small scale alien projects only. Funding for alien clearing very limited. City has cleared some areas but there has not been a big initiative by WFW or Landcare to clear the area. This area is in desperate need of large alien clearing initiatives.*

Do people collect firewood on the common and if so do you know what species?
Ebrahim: *Yes the firewood trade is quite a expansive business in Mamre and Atlantis. They do collect mainly port jackson and rooikrans. Much more port jackson collected.*

A.5 Email Interview with Joanne Eastman

The following summary of an email interview about the Rondebosch Common with Joanne Eastman, a member of the Friends of the Rondebosch Common, was conducted by Dr. Nicky Allsopp on the 27th July, 2010.

Friends of Rondebosch common became active in clearing Eragrostis from 1995. They have also removed Echium, vetch and lupins. These have all been removed by hand and they think they've been quite successful at getting rid of them. Echium, vetch and lupin are all herbaceous and have their main growth period around August. Echium reached high levels in 2000 but is under control now.
The removal of Eragrostis was suggested after input from scientists and is part of the Friends management plan for the Common. It appears to have spread from an area near the car park on the west side as a consequence of dumping. They've had to clear about half of rondebsoch common of Eragrostis.
Prior to 1995 there were a few people who removed aliens as they found them. For example removing 500 Acacia seedlings in 1990, but since the friends have been involved there has not been any obvious Acacias. (see letter from Dr Cullis)
[...]

The last big fire was in 1999 – but it didn't burn the whole common (maybe the centre???). Other parts haven't burnt since 1991.

The common has been used for several purposes in the past: army camp with horses, sports fields, golf course and there are even a couple of graves on the common (on Park road side near some pines).

A.6 List of the Ground Truth Polygons

Table A.1: Percentage vegetation cover of the ground truth polygons and classes assigned. Determined during the field trip in January 2010.

Classified As	GTP Name	Acacia Saligna (%)	Grass (%)	Fynbos (%)
Acacia	baB07	76.8	2.0	0.6
	bbE02	72.5	8.8	0.0
	maC01	93.5	0.0	0.3
	koB03	81.8	0.0	0.3
	koD08	74.5	18.0	0.3
Fynbos	peE03	0.0	0.0	64.3
	peE05	0.0	0.0	75.1
	peE07	0.0	0.0	52.0
	RLpix01	0.0	0.8	49.3
	RLpix02	0.0	1.0	48.8
	RLpix03	0.5	10.0	34.3
Grass	roC05	0.0	70.0	10.3
	roC04	0.0	86.3	1.0
	roC03	0.0	80.0	0.0
	baA08	3.0	39.5	0.0
	RLpl08	0.0	87.5	2.5
	RLpl09	0.0	82.5	6.3
Mixed	bbF07	33.5	42.7	3.3
	RivSouth	36.3	0.0	33.2
	maA03	23.3	0.0	40.1
	maC04	18.0	0.0	49.1
	maE04	0.0	0.0	18.5
	maD04	14.5	0.0	21.1
	maC06	24.0	0.0	39.3
	RLpl01	0.0	28.8	17.6
	RLpl02	0.0	50.0	32.5
	RLpl03	10.0	58.8	31.3
	RLpl04	0.0	5.0	0.0
	RLpl05	0.0	33.8	43.8
	RLpl06	3.8	13.8	16.3
	RLpl07	8.8	35.0	5.0

A.7 Rain-use Efficiency

Table A.2: Rain-use Efficiency of the ground truth polygons (period 2000-2008).

Classified As	GTP Name	2000	2001	2002	2003	2004	2005	2006	2007	2008
Acacia	baB07	0.95	0.55	0.86	1.16	1.11	1.18	1.01	0.77	0.69
	bbE02	0.63	0.56	0.89	1.06	0.84	0.94	0.82	0.68	0.61
	maC01	1.75	0.91	1.18	0.72	1.02	1.11	1.21	0.83	0.85
	koB03	0.64	0.59	0.83	1	0.83	1.01	0.95	0.68	0.7
	koD08	0.95	0.6	0.94	1.07	0.9	1.11	0.84	0.7	0.78
Fynbos	peE07	1.18	0.67	0.94	1.2	1.02	0.75	0.96	0.54	0.48
	peE05	1	0.56	0.7	0.83	0.76	0.69	0.77	0.6	0.53
	peE03	1.07	0.59	0.7	0.93	0.8	0.69	0.82	0.64	0.58
	RLpix01	0.96	0.5	0.67	0.74	0.65	0.61	0.64	0.57	0.53
	RLpix02	0.96	0.51	0.68	0.75	0.67	0.63	0.69	0.58	0.53
	RLpix03	1.21	0.55	0.76	0.81	0.81	0.72	0.73	0.59	0.57
Grass	roC05	0.44	0.27	0.43	0.59	0.41	0.36	0.39	0.33	0.34
	roC04	0.44	0.32	0.47	0.62	0.47	0.41	0.48	0.38	0.4
	roC03	0.44	0.31	0.53	0.62	0.48	0.46	0.48	0.4	0.41
	baA08	1.07	0.58	0.86	1.14	1.17	1.16	1.16	0.77	0.68
	RLpl08	1.17	0.69	0.83	0.96	0.98	0.89	1.24	0.8	0.73
	RLpl09	1.18	0.72	0.83	0.96	0.87	0.89	1.12	0.79	0.7
Mixed	bbF07	0.67	0.6	0.97	1.04	0.87	1	0.86	0.7	0.68
	RivSouth	1.14	0.58	0.87	0.98	0.94	0.78	0.88	0.53	0.75
	maA03	1.24	0.66	0.96	1.08	0.93	0.79	0.94	0.65	0.63
	maC04	1.21	0.65	0.84	0.9	0.94	0.81	0.91	0.62	0.61
	maE04	1.19	0.55	0.76	0.77	1.02	0.86	0.9	0.65	0.59
	maD04	1.21	0.59	0.77	0.77	1	0.88	0.92	0.66	0.6
	maC06	1.47	0.74	1	1.2	0.94	0.86	0.96	0.67	0.71
	RLpl01	1.19	0.64	0.83	0.63	0.77	0.83	0.76	0.81	0.62
	RLpl02	0.99	0.55	0.72	0.69	0.75	0.82	0.7	0.7	0.6
	RLpl03	1.01	0.56	0.76	0.68	0.75	0.76	0.69	0.75	0.59
	RLpl04	1.04	0.56	0.77	0.69	0.84	0.84	0.72	0.72	0.56
	RLpl05	1.09	0.62	0.76	0.76	0.89	0.93	0.68	0.71	0.58
	RLpl06	1.2	0.63	0.81	0.75	0.91	0.97	0.77	0.7	0.63
	RLpl07	1.22	0.64	0.86	0.77	0.88	0.91	0.93	0.72	0.64